An Investigation on Neural Network based Controller for Hybrid Active Power Filter

THESIS

Submitted in partial fulfilment
of the requirements for the degree of
DOCTOR OF PHILOSOPHY

By

Satya Prakash Dubey

Under the Supervision of

Prof. H.V. Manjunath

BIRLA INSTITUTE OF TECHNOLOGY & SCIENCE
PILANI (RAJASTHAN) INDIA

2005

DEDICATED
TO
MY WIFE
REENU

BIRLA INSTITUTE OF TECHNOLOGY & SCIENCE

PILANI (RAJASTHAN)

CERTIFICATE

This is to certify that the thesis entitled **"An Investigation on Neural Network based Controller for Hybrid Active Power Filter"** and submitted by **Satya Prakash Dubey** ID.No. **2001PHXF019** for award of Ph.D. Degree of the Institute, embodies original work done by him under my supervision.

Signature in full of the Supervisor _____

Name in capital block letters: **H.V.MANJUNATH**

Designation: Associate Professor of Electrical & Electronics Engineering Group

Date: 7/12/2005

ACKNOWLEDGEMENTS

I wish to express deep sense of gratitude and sincere thanks to my thesis supervisor Dr. H.V. Manjunath, Associate Prof., Electrical & Electronics Group for his valuable guidance, encouragement and suggestions throughout the period of this research work. It has been a privilege for me to work under his guidance.

Gratitude is also accorded to B.I.T.S., Pilani for providing all the necessary facilities to complete the research work. My special thanks go to Prof. S. Venkateswaran, Vice-Chancellor, B.I.T.S., Pilani for giving me an opportunity to do research at the Institute. I also thank Prof. L. K. Maheshwari, Pro Vice Chanceller and Director, B.I.T.S.-Pilani, Prof. K. E. Raman Deputy Director (Administration), Prof. V. S. Rao, Deputy Director (Off-Campus), Prof. G Raghurama, Chief Admissions and Placement Unit & Dean FD II, and Prof. A. K. Sarkar, Dean Instruction Division and Faculty Division-I of the institute for providing the necessary infrastructure and other facilities.

I also express my heartfelt gratitude to Prof. Ravi Prakash, Dean, Research and Consultancy Division for his kind and affectionate enquiries about the work and continuous encouragement for making this work as a success.

Much appreciation is expressed to Dr. Pukhraj Singh Sr. Scientist Power Electronic Group, CEERI, Pilani for his valuable suggestions, moral support and assistance. I am deeply indebted to Prof. Surekha Bhanot and Prof. Vimal Bhanot who are the members of Doctoral Advisory Committee, for their valuable suggestions and moral support.

I also express my gratitude for the kind and affectionate enquiries about the work and the encouragement given by Research and Consultancy Division staff and my colleagues.

Special thanks are also extended to all of senior faculties of EEE Group and my colleagues for their kind inspiration.

Finally a very special expression of appreciation is extended to my parents without their encouragement, patience, and understanding this endeavor would not have been possible. I would like to record my special affection and thanks to my wife Reenu, whose constant persuasion and moral support has been a source of inspiration to me.

ABSTRACT

The problem of harmonic pollution has been increasingly serious owing to the wide use of nonlinear loads. Conventionally, using passive filters, whose main components are inductors and capacitors, can solve this problem. However, the poor flexibility of passive filters to adapt to variable load compensation requirements constitutes a major disadvantage. Active filters were developed to mitigate the problems of passive filters. The active filters are very powerful tool for the harmonic compensation due to their superior performance as compared to traditional compensation equipments. However, the power rating of the PWM converters employed in the active power filters and its cost is the cornerstone to make these a reality in high power applications. Further, these active power filters are installed in power networks with highly contaminated electrical power, where compensation of harmonic is a challenging problem.

The research work carried out in this Ph.D. thesis has been made to develop active power filters with low power rated PWM converters and schemes for effective control of these active filters under non-sinusoidal, balance/unbalance, load and source conditions. In this direction, novel power circuit topology of Active Filters with neural network control scheme has been proposed, developed and validated through simulation results. This thesis has been mainly divided into three parts.

In the first part, a novel power circuit topology named Hybrid Active Power Filter has been proposed to compensate the harmonic currents. It composed of passive LC filters connected in series to an active power filter through a

coupling transformer. The active filter generates a voltage at the terminal of the coupling transformer winding, changing the passive filter frequency response, and therefore increasing the harmonic compensation performance. Moreover, compensation characteristics of already installed passive filters can be significantly improved by connecting a series active power filter at its terminals giving more flexibility to the compensation scheme. The hybrid topology significantly improves the compensation characteristics of simple passive filters, making the active power filter available for high power applications.

In the second part, a simplified neural network control algorithm has been proposed. Mathematical and simulation models of the algorithm have been developed and presented. Further, the training detail of the control algorithm has also been reported. To evaluate the performance, the controller has been simulated under various load and source conditions. The proposed control algorithm has also been implemented in real time using digital signal processor (DSP). The simulation results have been demonstrated the proposed control algorithm can be effectively used to compensate undesired harmonic components under symmetrical as well as asymmetrical load and non-sinusoidal source conditions.

In the third part, a complete computational model (power circuit and controller) of hybrid active power filters developed in MATLAB/SIMULINK to study its behavior under various operating conditions. Details of various blocks of computational model and the method used to develop these blocks have been

presented. Simulation results obtained in steady state as well as in dynamic conditions have also been presented and analyzed.

In the end of thesis, the conclusions and future scope of this research work has been discussed. It is hoped that the investigations as reported in this thesis will help in establishing new topological designs and control schemes for harmonic compensators in an attempt to improve the power quality. It is further hoped that application engineers will be able to utilize the results as reported in this thesis for further enhancement of compensator performance under adverse conditions of load as well as source.

TABLE OF CONTENTS

LIST OF TABLES

LIST OF FIGURES

LIST OF SYMBOLS

i	: rms current
i_s	: source current
i_L	: load current
v	: rms voltage
v_s	: source voltage
i_{as}	: phase-a source current
i_{bs}	: phase-b source current
i_{cs}	: phase-c source current
i_{La}	: phase-a load current
i_{Lb}	: phase-b load current
i_{Lc}	: phase-c load current
v_a	: phase-a source voltage
v_b	: phase-b source voltage
v_c	: phase-b source voltage
S	: apparent power
P	: active power
Q	: reactive power
H	: harmonic power
ϕ	: power factor angle
L	: inductor
C	: capacitor
i_r	: reference current
i_f	: fundamental component of current

i_{sh}	: harmonic component of source current
$i_{L.h}$	: harmonic component of load current
v_{sh}	: harmonic component of source voltage
Z_S	: impedance of source
Z_{pf}	: impedance of passive filter
i_α, i_β	: two phase transformed currents
i^*_α, i^*_β	: two phase transformed reference currents
i_d, i_q	: d-axis and q-axis currents
i^*_d, i^*_q	: d-axis and q-axis reference currents
v_α, v_β	: two phase transformed voltages
p	: instantaneous active power
q	: instantaneous reactive power
i(t)	: current in stationary reference frame
I_{DC}	: dc component of current
G_n	: transfer function evaluated at the n^{th} harmonic of notch filter
ω	: fundamental angular frequency
ω_c	: cut-off angular frequency
t	: time in seconds
m	: momentum at the iteration for training the neural network
j	: sum of squired error
MSE	: mean squired error
PCC	: Point of Common Coupling
V_{dc}	: dc capacitore voltage
V_{ch}	: harmonic voltage of active filter

V^{*}_{dc}	: refernce dc voltage
K_h	: gain of hybrid filter
K_{dc}	: dc voltage gain
i_p	: passive filter branch current
i_{pf}	: fundamental component of passive filter branch current
i_{ph}	: harmonic component of passive filter branch current
$i_{\alpha f}$, $i_{\beta f}$	: fundamental components of two phase transformed currents
$i_{\alpha h}$, $i_{\beta h}$	: harmonic components of two phase transformed currents
i_{pa}, i_{pb}, i_{pc}	: three phase passive filter currents
i_{paf}, i_{pbf}, i_{pcf}	: fundamental component of three phase passive filter currents
i_{pah}, i_{pbh}, i_{pch}	: harmonic component of three phase passive filter currents
$i_{p\alpha}$, $i_{p\beta}$	: phase transformed currents passive filter current
$i_{p\alpha,f}$, $i_{p\beta,f}$	: dc component of phase transformed currents passive filter current
$i_{p\alpha h}$, $i_{p\beta h}$	: harmonic component of phase transformed currents passive filter current
i_o	: two phase transformed current (α-β-0)
i_{of}	: fundamental component of two phase transformed current (α-β-0)
i_{oh}	: harmonic component of two phase transformed current (α-β-0)
w	: weight of neural network
b	: bias value of neural network

CHAPTER 1

INTRODUCTION TO POWER QUALITY PROBLEMS AND SOLUTIONS

1.1 INTRODUCTION

Electric power generated by the utilities is distributed to the consumers in the form of 50 Hz ac voltages. The utilities have a tight control on the design and operation of the equipment used for transmission and distribution, and can therefore keep frequency and voltage delivered to their customers within close limits. Unfortunately, an increasing portion of loads connected to the power system comprises of power electronic converters. These loads are non linear and inject harmonic currents in the network and consequently, through line drops, they generate harmonic voltage waveforms. Power converters such as rectifiers, power supplies and arc furnaces are all sources of distortion. The distortion, whether it is produced by a large single source or by the cumulative effect of many small loads, often propagates for miles along distribution feeders.

As the use of non-linear equipment is spreading, the degradation of the power quality in the utility networks is increasing and is becoming a major problem. Limiting the voltage distortion is therefore a concern for both utilities and consumers. For these reasons international agencies like IEEE and IEC (International Electrical Commission) are proposing or enforcing distortion limits

[1-3]. The simple block diagram of Fig.1.1 illustrates the distortion problem due to harmonic at low and medium power levels.

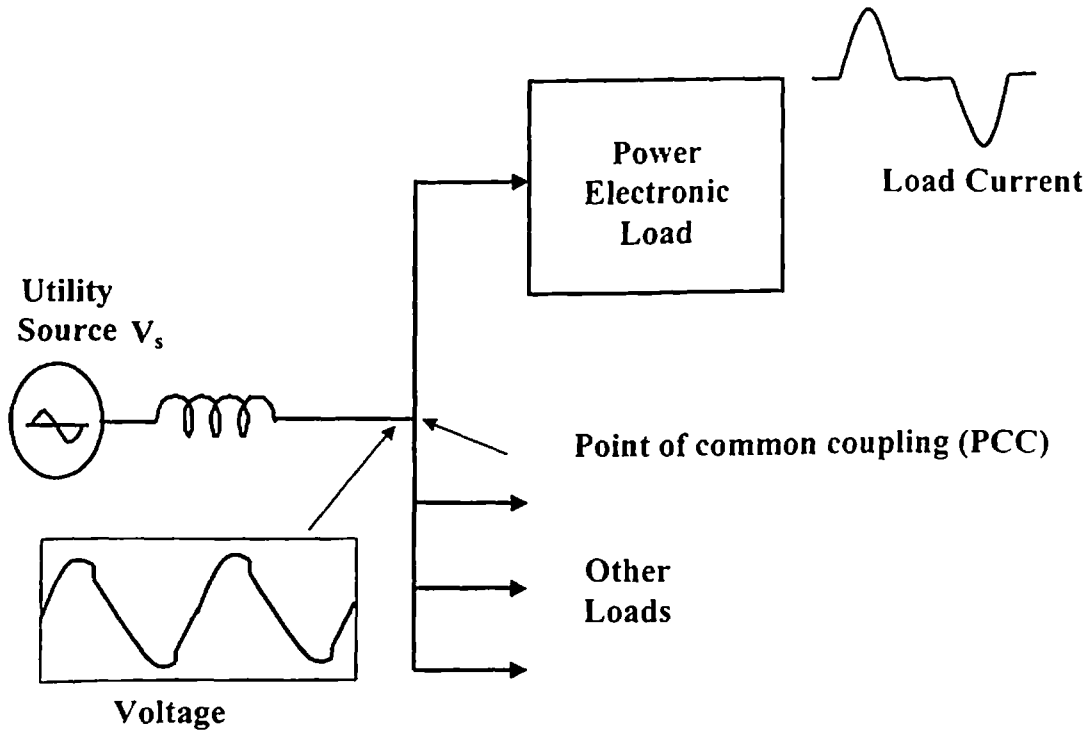

Fig. 1.1: Harmonic distortion at PCC

The utility is represented by an AC voltage source in series with lumped impedance representing lines and transformers. The voltage waveform at the point of common coupling is distorted due to harmonic current generated by the power electronic load or the non-linear load. Further, the AC source because of its non-linear characteristics also contributes to this distortion and thus aggravates the problem. The distorted supply voltages that adversely affect the performance of other equipments connected to same network. Table 1.1 summaries some of the adverse effects of harmonics on the consumer equipments and power system components [4-6].

Table 1.1: Effect of Harmonics on Power System Equipments

Equipment	Effects
Transformers	Overheating
Motors	Overheating, Increased noise level, Additional vibrations
Capacitor banks	Overheating, Insulation breakdown
Reactors	Overheating
Protection equipments	False tripping, No tripping when required
Lines	Overheating
Incandescent lamps	Reduced life time, Flicker
Electronic devices	Wrong pulses on data transmission, Flickering of screen
Measuring devices	Wrong measurement
Telephones	Noise at respective frequency

The harmonic currents result in the malfunctioning of various power system equipments and must be fully compensated. Some kind of filters is often required to eliminate the distortion from the supply voltages. The classical solution has always been to install passive filters, but these have significant

inherent problem e.g., tuning to specific load and frequency, in conjunction with its bulky size. As such, new solutions need to be developed to overcome the detrimental effects of harmonics as mentioned above.

1.2 POWER QUALITY

Electrical power is perhaps the most essential raw material used by commerce and industry today. It is an unusual commodity because it is required as a continuous flow, it cannot be conveniently stored in quantity and it cannot be subject to quality assurance checks before it is used. It is, in fact, the epitome of the ' Just in Time' philosophy in which components are delivered to a production line at the point and time of use by a trusted and approved supplier with no requirement for 'goods in' inspection. For 'Just in Time' to be successful it is necessary to have good control of the component specification, a high confidence that the supplier can produce and deliver to specification and on time, and a knowledge of the overall product behavior with 'on limit' components [7,8].

It is expected that the supply voltages at each point in any power system (distribution as well as transmission), should be sinusoidal and should have constant and equal magnitudes, fixed frequency, equal phase displacement of 120^0 among the three phases and above all the three should be no zero sequence voltage. However, because of nonlinear loads connected to the distribution system, the supply voltages no longer are found to exhibit these characteristics. It may be pointed out that the good quality of power supply voltages implies voltage quality and supply reliability [9, 10].

1.3 DISTORTIONS IN POWER NETWORKS

As shown in Fig. 1.2, the different sources of distortion in power networks conveniently can be divided into three classes according to the power level of the equipment and frequency range [11,12]: (a) sub-cycle distortion give rise to flicker and occur generally at the highest power level, they are caused by dynamic loads, such as arc furnaces, mill drives, mine winders, (b) high frequency distortion is caused by modern power electronic equipment, due to high rate of rise of current and voltage, and (c) intra-cycle distortion which covers a very wide range of power, and results from the power processing technique. The distortion generated by these last sources is usually termed "harmonics". This work focuses on distortion caused by harmonics.

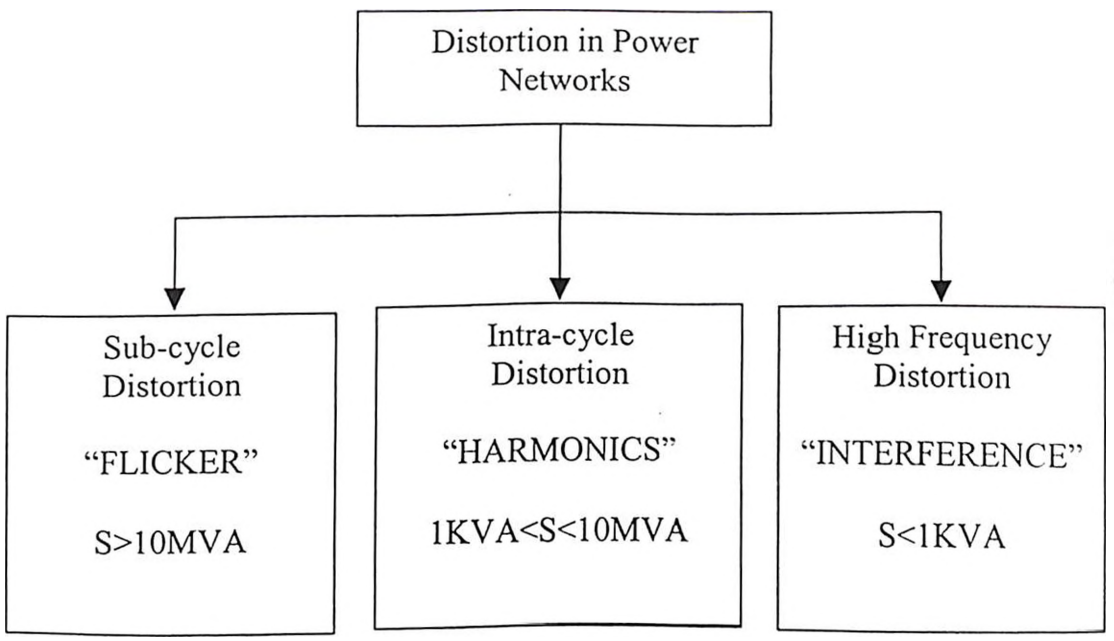

Fig. 1.2: Classification of distortion types in power networks

1.4 HARMONIC STANDARDS AND RECOMMENDED PRACTICES

In view of the proliferation of the power electronic equipment connected to the utility distribution system, various international agencies have proposed limits on the magnitude of harmonic current injected into the supply to maintain acceptable power quality. The resulting guidelines and standards specify limits on the magnitudes of harmonic currents and harmonic voltage distortion at various harmonic frequencies. The most widely known are the IEEE-519 guidelines [1] in North America and the IEC-1000 Standard (formerly IEC 555 [2] prepared by the International Electrical Commission (in effect since 1996). However, the approach taken in these documents is drastically different. The IEC Standard imposes limits on individual equipment (up to 15 A, 220 V) connected to the supply, whereas the IEEE Recommended Practice addresses the issue of harmonic distortion at the point of common of coupling (PCC). Complying with the IEC Standard usually requires special design of the equipment itself [13,14]. However, meeting the IEEE guidelines can be achieved by means of filters, particularly active filters. Therefore, reference in this work will only be made to the IEEE guideline.

IEEE 519 proposes to designers of industrial plants harmonic limits as given in Table 1.2 and 1.3. For existing installations, harmonic mitigation techniques may have to be used to reduce distortion to the specified limits.

Table 1.2: IEEE-519 Maximum Odd-Harmonic Current Distortion.

I_{SC}/I_l	H < 11	11<H<17	17<H<23	23<H<35	35<H	THD
< 20	4.0	2.0	1.5	0.3	0.3	5.0
20-50	7.0	3.5	2.5	1.0	0.5	8.0
50-100	10.0	4.5	4.0	1.5	0.7	12.0
100-1000	12.0	5.5	5.0	2.0	1.0	15.0
>1000	15.0	7.0	6.0	2.5	1.4	20.0

Notes: 1. % Limits of Harmonic Currents (Bus voltage @ PCC<69 KV)

2. I_{SC} is the maximum short-circuit current @ PCC.

3. I_l is the maximum fundamental frequency load current @PCC.

Table 1.3: IEEE-519 Voltage Distortions Limits

Bus Voltage @PCC	HDv(%)	THDv(%)
69 KV and below	3.0	5.0

HDv = Individual harmonic voltage distortion

1.5 POWER IN DISTORTED AC NETWORKS

The active and reactive power components for electric circuits with sinusoidal and linear loads are well established. In the case of non-linear loads, however the use of the reactive and the harmonic power is an actual necessity for accomplishing

reactive power compensation and/or harmonic filtering. The components of the electric power are showing in Fig. 1.3 assuming a sinusoidal voltage supply and a non-linear load. In this case, the power factor ($\cos\phi$) is the product of the Distortion factor and Displacement factor:

Power Factor = Distortion factor x Displacement factor

The displacement factor corresponds to the power factor of systems without harmonics. This factor may be called fundamental power factor, as it depends only on the current fundamental component. On the other hand, the power factor, as defined above, may be called total power factor, as it depends on fundamental and all harmonic components. Hence, harmonics cause lower power factor. The power components in distorted networks are represented in power tetrahedron, instead of the triangle as in the linear case, is shown in Fig. 1.4.

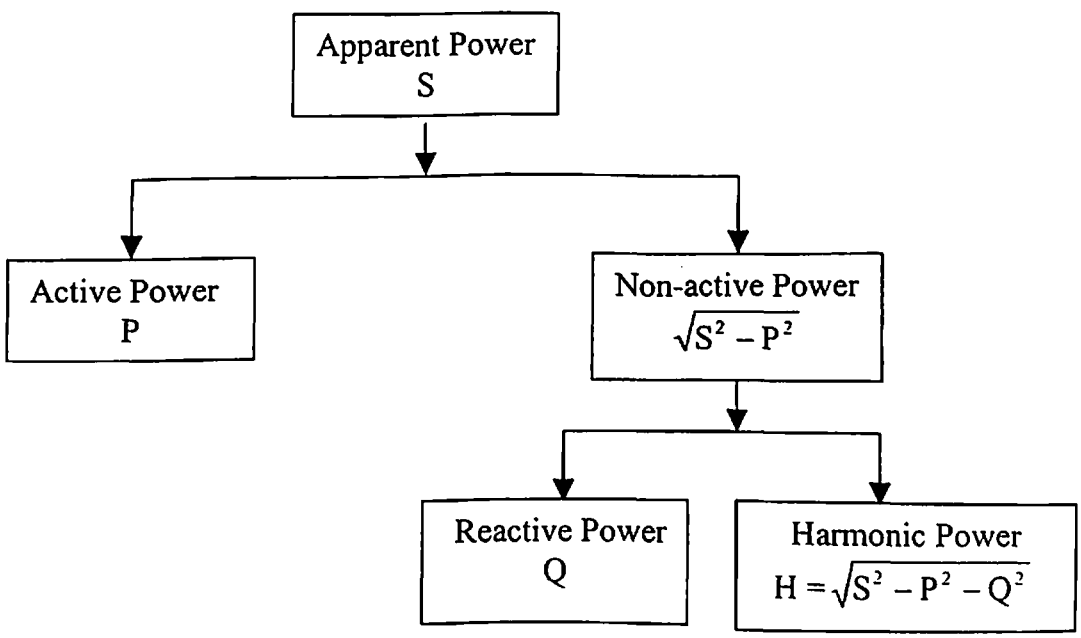

Fig. 1.3: Components of electric power

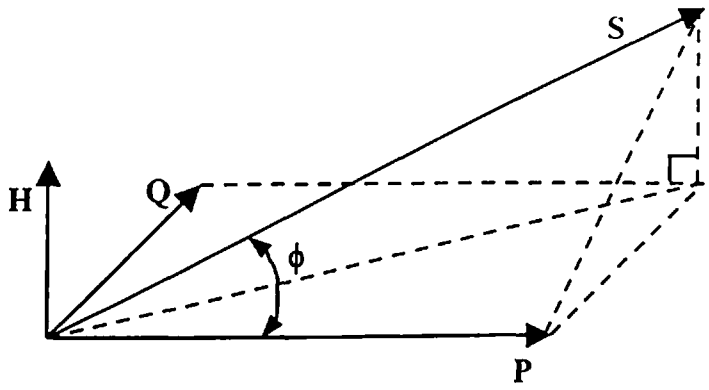

Fig. 1.4: Power tetrahedron

From Fig. 1.3 and 1.4, various important factors are determined on the use of reactive power and harmonic compensation:

(i) The reactive component is dependent only on the current component at fundamental frequency. The reactive component can be eliminated by using a conveniently chosen capacitor or inductor. The connection of an inductor or a capacitor component in parallel with load allows the generation of a current at fundamental frequency that absorbs or generates the reactive power required by the load;

(ii) The distorting power is dependent on the current components with frequencies different from fundamental frequency (harmonics) and cannot be eliminated by a single capacitor or inductor. The elimination of harmonic power depends on filters that work as short-circuit for the harmonic current generated by the load.

1.6 COMPENSATION TECHNIQUES: A REVIEW

The problem of harmonic pollution has become increasingly serious owing to the wide use of nonlinear loads. Conventionally, this problem can be solved by using passive filters whose main components are inductors and capacitors. This kind of filter has the advantage of low hardware cost, but the problems including large volume, parallel resonance and series resonance may offset the benefit of this method. Some special designs for performance improvement have been suggested for the passive filters. However, their circuits are often complicated due to consideration of the varied power system impedance and load characteristics. With the emergence of power electronics, an active power filter that helps to suppress the harmonics and upgrade the power quality was developed. In recent years, there has been considerable interest in the development and application of active power filters because of their superior filtering performance over passive filters [15]. The active filters have been extensively researched and developed for the effective control of reactive power, harmonic compensation and to improve voltage quality under various operating conditions [16-18]. Ever since the active power filters have been introduced [19], various power circuit topologies and control algorithms for the active power filters have been suggested and explored, with a view to improve the compensation effectiveness and also to make the active filtering cost effective solution [20].

In this section, various power circuit topologies and control techniques of three-phase active power filters as available in the published literature have been

investigated and explored, with a view to suggest more practical and effective solutions.

1.6.1 Passive Filters

Passive filters in power systems as shown in Fig. 1.5, are usually shunt connected, the accepted practice being to connect a number of separate shunt branches across the terminals of the load or the plant. Each of these branches is tuned to one of the dominant harmonics; with a low pass branch added that exhibits low impedance for the remaining higher order harmonics.

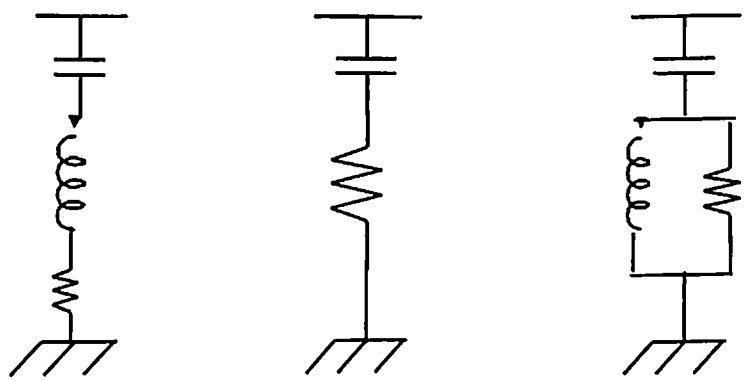

Fig. 1.5 Types of passive filters (a) single tuned filter (b) first order high-pass filter (c) second order high-pass filter

Conventionally, passive LC filters have been used to eliminate the line current harmonics and to increase the load power factor because of its low cost, simplicity and high operating efficiency. However, in practical applications these filters having many disadvantages, such as:

- The source impedance strongly affects filtering characteristics.

- As both the harmonic and the fundamental current components flow into the filter, the capacity of the filter must be rated by taking into account both the currents.
- When the harmonic current components increase, the filter can be overloaded.
- Parallel resonance between the power system and the passive filter causes amplification of harmonic currents on the source side at a specific frequency.
- The passive filter may fall into series resonance with the power system, so that voltage distortion produces excessive harmonic currents flowing into the passive filter.
- Lastly, these filters are not suitable for fast varying loads, because of their inherent sluggish response time.

The classical solution of tuned passive filters therefore has serious limitations. Furthermore, with the widespread use of variable distorting electronic loads, harmonic tracking is not adequately achieved. Also the probability of encountering resonant conditions increases with the number of installed filtering units. To overcome the limitations of these passive filters, active compensation approach has been researched and being developed. The following section presents review of active filtering technique [21-24].

1.6.2 Active Filters

The first attempt to reduce harmonics without the use of conventional passive filters was made by B. Bird, et al. [25]. Their design proposed changing the waveform of the current drawn by the load by injecting a third harmonic current, displaced in phase, into the converter itself. With this method however it is impossible to fully eliminate more than one harmonic.

It was Ametani's idea to expand the current injection method by proposing a technique to eliminate multiple harmonics [26,27]. According to this theory, an active control circuit could be used to precisely shape the injected current. Ideally, this current would contain harmonic components of opposing phase, thus the harmonics would be neutralized, and only the fundamental component would remain. Despite the promising theoretical concept, Ametani was not successful in producing a practical circuit capable of creating a precise current. The total harmonic distortion was reduced, but single harmonics were not completely eliminated.

One the other hand, Sasakli and Machida theorized that harmonics can be eliminated by using the principle of magnetic flux compensation [28]. In principle this is the use of current to produce a flux to counteract the flux produced by the harmonics. Once again, theoretically, any number of harmonics could be directly eliminated. The current that would be required to eliminate waveform distortion caused by harmonics was calculated mathematically, but again, a practical control circuit was not realized.

Over the last ten to twenty years the remarkable progress in capacity and switching performance of devices such as Bipolar Transistors (BJT), Gate Turn-Off Thyristors (GTO) and Insulated Gate Bipolar Transistors (IGBT), has spurred in the study of active power filters for harmonic compensation. In addition, advances in topologies and controls schemes for static PWM converters have enabled active power filter using these converters to generate specified harmonic currents, such as created by non-linear loads.

Active filtering method was developed to mitigate the problems of conventional equipment such as passive filters. This technique involves deriving a signal corresponding to the undesired (harmonic, reactive etc.) component of load current, invert and amplify this signal for adding back to the supply current, so as to cancel this undesired component of the supply currents from AC mains. To achieve effective active filtering, various power circuit topologies of active power filters have been proposed [28]. The following subsections review the most popular topologies of the active power filters.

1.6.2.1 Shunt active power filter

Shunt active filters are developed to suppress the harmonic current and compensate reactive power simultaneously. Figure 1.6 shows the system configuration of a shunt active filter, which is one of the most basic system configurations [29]. It mainly consists of a reference current generator, PWM controller and a PWM converter with a capacitor on its DC side. The shunt active filters operated as a current source parallel with the nonlinear load. The PWM converter of the active filter is controlled to generate a compensation current that

is equal-but-opposite the harmonic and reactive current generated from the nonlinear load. In this situation, the source current becomes sinusoidal and in phase with the source voltage [30]. As shown in Fig. 1.6, the reference current generator calculates the reference current i_r^*, from load current i_L for a given compensation requirement and the PWM converter inject this current after amplification and inversion into the supply system, so as to cancel the undesired component from source current 'i_s'.

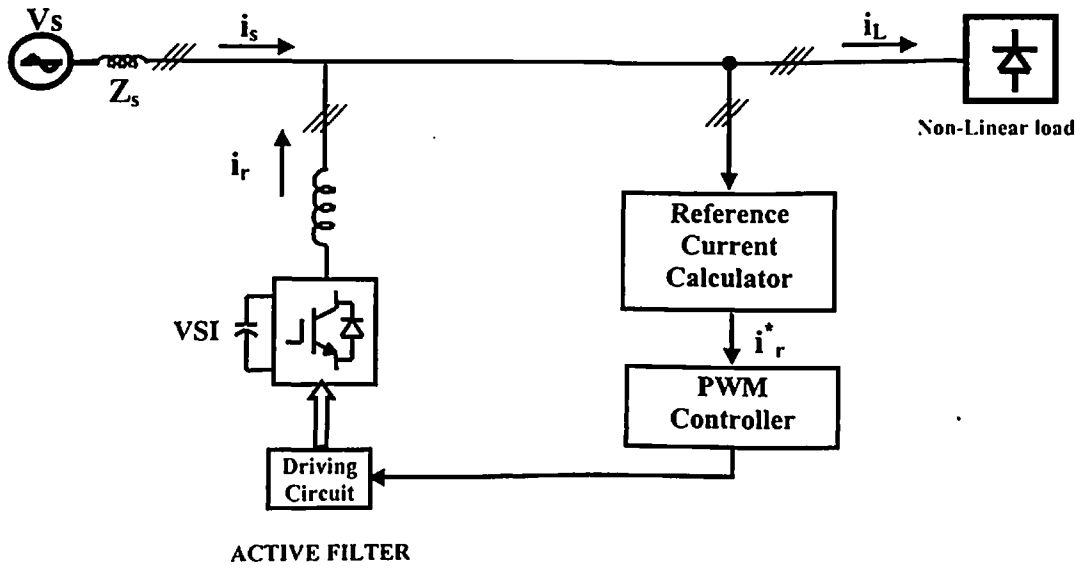

Fig. 1.6: Block diagram of shunt active power filter

A shunt active filter solves the resonance problem. It consists of a three-phase converter operating as a current source, its equivalent impedance is very high, and so the filter-line resonance does not occur. The shunt filter has the capability of load/source harmonic current filtering, displacement power factor improvement, damping of power oscillation and load voltage regulation [31]. All these functions of active filter can be implemented individually or simultaneously.

Moreover, the Shunt Active Filter does not create any displacement power factor and utility loading related problems. Further, for low power industrial applications, one PWM converter using presently available power semiconductor devices can realize a shunt active filter. However, there are some issues, which remain to be resolved, mentioned as under, if this active filter is to be applied for high power applications.

- It is still difficult to realize a high power PWM inverter with low energy losses, high switching frequency, and rapid dynamic current response.
- The capital cost of active filtering is very high as compared with conventional passive filtering solution [32].
- The compensation effect is completely lost in case of fault in the active filter.

In order to overcome the above-mentioned limitations several alternatives such as multilevel inverter [33], series parallel combination of inverters [34-36], have been suggested as main power circuit of shunt active filter. However, these configurations require complex control and large number of power components resulting in higher cost and poor output efficiency. A more effective and economical solution as compared to Shunt Active Filter proposed in literature and known as Hybrid Active Filter is discussed in the following sub-section.

1.6.2.2 Hybrid active power filters (HAF)

As an alternative to mitigate the problems of passive and stand alone shunt filter, hybrid filter have been proposed. The hybrid Active power filter

topologies consist of both Active Filters and passive tuned filters. By improving the compensation characteristics of the passive filters, hybrid active filters get a reduction in the rating of the active filter. Figure 1.7(a) and (b) show the configurations of parallel [37] and series hybrid active power filters [38] respectively. In parallel hybrid active power filter system, passive and active filters are connected in series. These HAF improve the compensation characteristics of passive filters by inserting a voltage v_c proportional to harmonics of supply current 'i_s' in series with passive filter as shown in Fig. 1.7(a). These hybrid active power filters have been shown to effectively overcome most of the problems of using either passive filters or Shunt Active Filter alone.

For the hybrid active filter as shown in Fig. 1.7(a), equation (1.1) gives the following relationship among the harmonics of source current, load current and source voltage as derived in [37].

$$i_{Sh} = \frac{Z_{pf}}{Z_{pf} + Z_s + K_h} * i_{Lh} + \frac{1}{Z_{pf} + Z_s + K_h} * v_{Sh} \qquad (1.1)$$

where K_h is the gain of hybrid active filter and i_{sh}, i_{Lh} and v_{sh} are the harmonic components of source current 'i_s' load current 'i_L' and source voltage 'v_s' respectively. Further, Z_S and Z_{pf} are the impedance of source and passive filter as shown in Fig. 1.7.

If $K_h >> |Z_{pf} + Z_S|$, then harmonic components of source currents $i_{sh} \approx 0$ and v_{sh} would be applied to the Active Filter. This prevents the harmonic currents caused by v_{sh} from flowing into the passive filter. The filtering performance up to a great extent is not influenced by source impedance. In the hybrid series active filter, active filter is connected in series of line while the passive filter in parallel of load. The goal of this combination is to operate the active filter as short-circuit for the line (power) frequency and as an open-circuit for harmonic currents. With this scheme, harmonics are forced to flow through the passive filters achieving harmonic isolation between source and load. Therefore, series active filter is sized only to a fraction of the total compensating power and the overall cost is limited. The equation (1.1) is also valid for series hybrid active filter shown in Fig. 1.7(b). The hybrid parallel active filter having advantage compared to the hybrid series active filter is the easy protection and that possible failure in active filter.

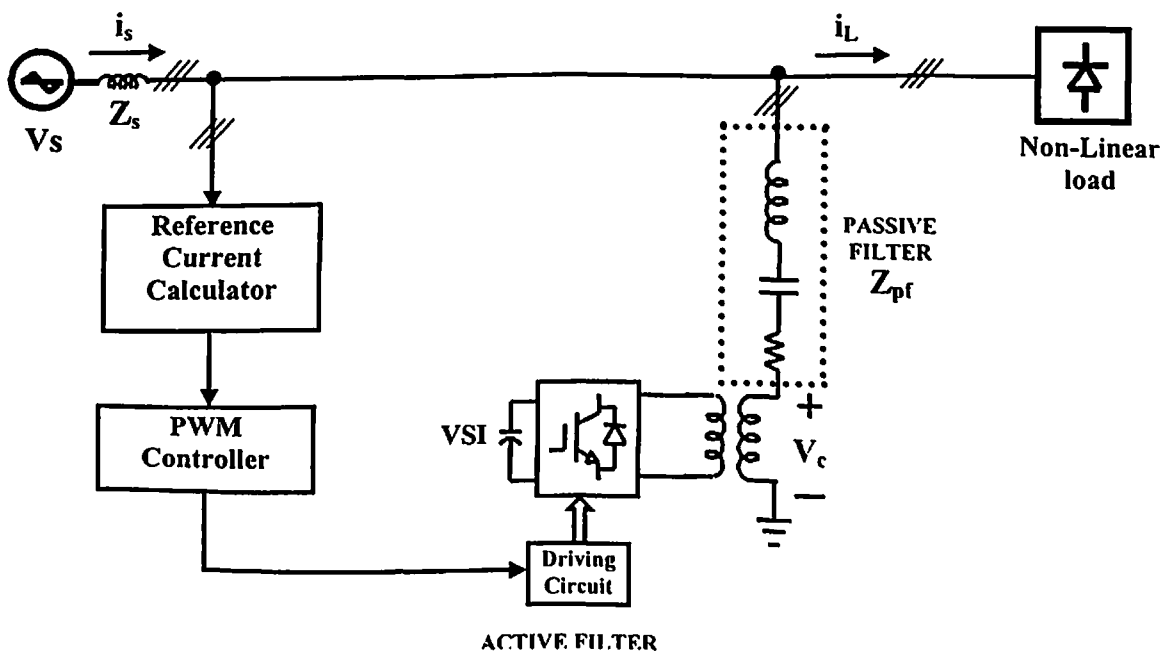

(a)

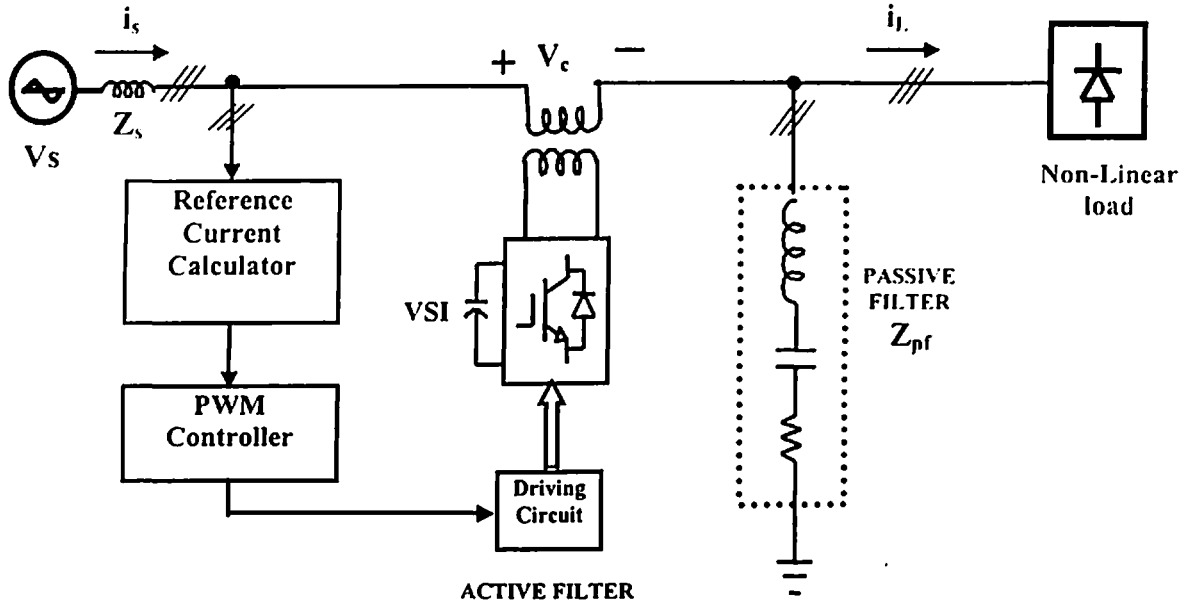

(b)

Fig.1.7 Configuration of hybrid active power filter. (a) Parallel hybrid active power filter (b) Series hybrid active power filter.

The hybrid active filters retain the advantages of active filters and have not the drawbacks of passive and active filters. The hybrid active filters are cost-effective and become more practical in industry applications. Various other topologies, combining the passive filters and active filters in different ways, in an attempt to overcome the limitations of shunt active filter have also been suggested and reported [39-44].

The hybrid active filters, not only compensates the harmonics, but also generate fundamental frequency capacitive reactive power. Under light load conditions, excess reactive power generated by these hybrid active filters makes the displacement power factor poor. If the displacement power factor is not a constraint, then hybrid active filter is the most attractive solution for harmonic

current compensation. However, it is always desirable that the power factor should be maintained close to unity.

1.6.2.3 Active power filter control methods

The reference current generation defines the compensation characteristics and accuracy of the active power filter. Various popular control schemes for the calculation of reference current have been proposed in the published literature [45]. The existing approaches to compute the reference current for active power filter can be divided into time-domain and frequency-domain methods, the former being usually preferred because the compensating signal is calculated almost instantaneously without the application of any DFT. Indeed, the need for a fast response and simplicity in this kind of application, where the ability to quickly track sudden load changes is crucial, has motivated the development of neural network based methods to detriment of those techniques formulated in the frequency-domain and time-domain. Some of the popular control techniques available in the published literature have been investigated in the following paragraphs.

In early 30's Fryze proposed new power definitions in time domain [46]. According to this, if 'v' is the source voltage and 'V' is its RMS value, then the source current 'i' can be decomposed in the time domain into an active current 'i_A' and non-active current 'i_q' which are defined as:

$$i_A(t) = \frac{P}{V^2} \times v(t) \qquad (1.2)$$

$$i_q(t) = i(t) - \frac{P}{V^2} \times v(t) \tag{1.3}$$

$$\text{Where } P = \frac{1}{T}\int_0^T (v \times i)dt \text{ and } V = \sqrt{\frac{1}{T}\int_0^T v^2 dt} \tag{1.4}$$

The *active current component* 'i_A' *has the same waveform and phase as the source voltage* 'v'. The average power transfer from source to load is associated only with active current component 'i_A' which the non-active current 'i_q' increases the RMS value of source current and causes an increase in undesired losses and voltage distortion. The non-active current i_q can be used as reference signal for the control of Active Filters. It is to be noted from (1.3) that a full period of voltage has to elapse to calculate the new value of current i_q.

Depenbrock [47], decomposed the reactive current 'i_q' further into two current components, namely a reactive component 'i_R' and distortion component 'i_D' such that:

$$i_q = i_R + i_D \tag{1.5}$$

The *reactive current component 'i_R' has the same waveform and phase as that of the current in an inductor or capacitor with the same voltage across it.* This current does not contribute to the energy flow and only increases the system losses and makes voltage regulation poor. The *distortion component or the harmonic component 'i_D' is the component, which remains out of the total current 'i' after the active 'i_A' and reactive current 'i_R' have been extracted.* The current component 'i_D' is mainly responsible for voltage distortions in power system and

EMI & RFI related problems. All the three current components are mutually orthogonal and they are related to source current as per the following expression:

$$I^2 = I_A^2 + I_R^2 + I_D^2 \qquad (1.6)$$

where I_A, I_R, I_D are the RMS values of active, reactive and harmonic current components respectively. The instantaneous current components i_R and i_D can be individually used as reference signal to achieve compensation objectives such as reactive power compensation, harmonic filtering etc. Further, this decomposition method can be applied to three-phase system as well as for a system consisting of 'm' number of conductors. However, the calculation of reactive current i_R and i_H under asymmetrical and non-sinusoidal conditions is quite involved due to the use of complicated definition of reactive power [48, 49].

Czarnecki [50, 51] proposed yet another schemes for the decomposition of current in three-phase non-linear asymmetrical circuit, under non-sinusoidal voltage source into five orthogonal current components. However, the procedure of decomposition presented here is very complex and therefore it is not suitable for application in active filtering.

Enslin et al [52] proposed the calculation of reference currents by decomposing the conventional apparent power into real and fictitious power. The fictitious power has been further sub-divided into reactive and deactive power using a complicate correlation technique.

It may be summed that the approaches used in the above methods for the current decomposition under non-ideal conditions are quite complicated in nature and

require large computational efforts, when used in three-phase system. Some more efficient and simple algorithms proposed in the published literature are discussed in the next sub-section.

Akagi [53] introduced the Instantaneous Reactive Power Theory (IRPT) to obtain the reference currents of active filters instantaneously. This method is based on the transformation of current and voltages to the α-β axes, where the instantaneous active and reactive powers p-q are defined. Basically, assuming sinusoidal voltages, both 'p' and 'q' can be divided into a constant and fluctuating terms. The fluctuating term being produced by the harmonic current demanded by the nonlinear load. Then, the reference current can be easily obtained by isolating these fluctuating power components through a high pass filter. Assuming sinusoidal voltages and ideal filter behavior the reference current can be extracted without error. However, an error on the computed reference current is expected when those conditions do not hold. In order to obtain the reference currents according to this theory, three-phase voltages (v_a, v_b, v_c) and currents (i_a, i_b, i_c) are first transformed from three-phase to two-phase α-β system, using (1.7) and (1.8).

$$\begin{bmatrix} v_\alpha \\ v_\beta \end{bmatrix} = \sqrt{\frac{2}{3}} \begin{bmatrix} 1 & -\frac{1}{2} & -\frac{1}{2} \\ 0 & \frac{\sqrt{3}}{2} & -\frac{\sqrt{3}}{2} \end{bmatrix} \begin{bmatrix} v_a \\ v_b \\ v_c \end{bmatrix} \tag{1.7}$$

$$\begin{bmatrix} i_\alpha \\ i_\beta \end{bmatrix} = \sqrt{\frac{2}{3}} \begin{bmatrix} 1 & -\frac{1}{2} & -\frac{1}{2} \\ 0 & \frac{\sqrt{3}}{2} & -\frac{\sqrt{3}}{2} \end{bmatrix} \begin{bmatrix} i_a \\ i_b \\ i_c \end{bmatrix} \tag{1.8}$$

Then instantaneous active power 'p' and instantaneous reactive powers 'q' are defined as:

$$\begin{bmatrix} p \\ q \end{bmatrix} = \begin{bmatrix} v_\alpha & v_\beta \\ -v_\beta & v_\alpha \end{bmatrix} \begin{bmatrix} i_\alpha \\ i_\beta \end{bmatrix} \tag{1.9}$$

The α-β axes are equivalent to the stationary reference frame where the Park domain is defined. Furthermore, it can be demonstrated that instantaneous active and reactive powers correspond to the real and imaginary components of the complex Park power [54]. This complex Park power can be split into a constant and a fluctuating term, equivalent to the p-q decomposition carried out below.

$$p = v_\alpha . i_\alpha + v_\beta . i_\beta = \bar{p} + \tilde{p} \tag{1.10}$$

$$q = v_\alpha . i_\beta - v_\beta . i_\alpha = \bar{q} + \tilde{q} \tag{1.11}$$

$$\begin{bmatrix} i^*_\alpha \\ i^*_\beta \end{bmatrix} = \begin{bmatrix} v_\alpha & -v_\beta \\ v_\beta & v_\alpha \end{bmatrix}^{-1} \begin{bmatrix} \tilde{p} \\ \tilde{q} \end{bmatrix} \tag{1.12}$$

The currents of equation (1.12) are next transformed back to three-phase system by two-phase to three-phase transformation as under:

$$\begin{bmatrix} i^*_a \\ i^*_b \\ i^*_c \end{bmatrix} = \sqrt{\frac{2}{3}} \begin{bmatrix} 1 & 0 \\ -\frac{1}{2} & \frac{\sqrt{3}}{2} \\ -\frac{1}{2} & -\frac{\sqrt{3}}{2} \end{bmatrix} \begin{bmatrix} i^*_\alpha \\ i^*_\beta \end{bmatrix} \tag{1.13}$$

The block diagram of the instantaneous reactive power theory for the calculation of harmonic currents is shown in Fig.1.8. The compensation algorithms based on the powers defined in this algorithm are very flexible [55]. For instance, the undesirable powers to be compensated can be conveniently selected. Further, the instantaneous reactive power is calculated without time delay. This scheme has been most widely used in literature because of its flexibility and fast dynamic response as compared to conventional methods discussed in preceding section [56-63]. However, IRPT method is quite complex and yields incorrect reference currents under unbalance load condition and also under distorted and unbalance source condition.

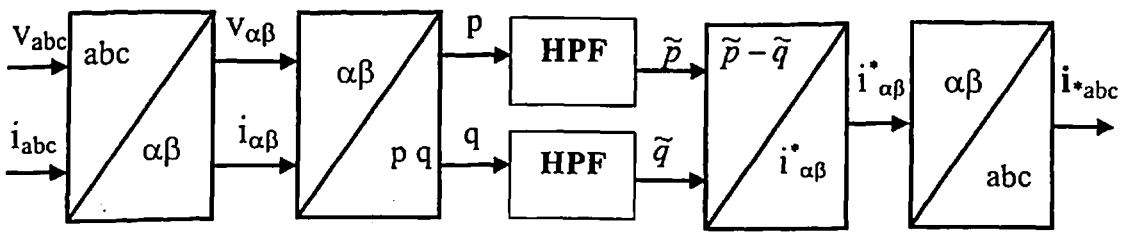

Fig. 1.8: Block diagram of IRPT scheme for harmonic current calculation

In order to improve the performance of IRPT under the distorted and unbalanced source voltage conditions, new definition of 'q' has been proposed in [56]. However, the reference current calculation under unbalanced load conditions still remains unresolved.

Further, i_d-i_q method has been proposed to improve the IRPT under distorted mains voltage conditions [57]. However, as concluded by the authors themselves that its performance under unbalanced and non-sinusoidal conditions

are not very satisfactory. Decomposition of current under unbalanced load conditions using a new technique of power decomposition based on IRPT, assuming symmetrical voltage system has been presented in [57]. This scheme has been applied for the analysis of stator faults in induction machines. However, it can also be used for different compensation objectives.

Divan et al [64] have proposed the calculation of reference currents in Synchronous Reference Frame (SRF). This method relies on the transformation of currents to a synchronous rotating reference frame as shown in the block diagram of Fig. 1.9.

In such a framework, the fundamental current component turns into a dc quantity, which can be obtained by applying a low-pass filter. In order to perform the transformation, synchronization with the system voltage is needed to extract the phase information, which is usually achieved through a phase-locked loop (PLL), although other methods can be used as well.

Two error sources can be identified when computing the reference current by this procedure, namely: (a) response of the low-pass filter used to extract the dc current in the synchronous reference frame and (b) influence of voltage distortion on the synchronization system employed to estimate the voltage phase. As explained in the previous subsection, filtering errors can be considered negligible compared to errors originating in the voltage distortion.

The general formulation of the reference current computation method is quite simple. The current in the stationary frame can be expressed as

$$i(t) = \sum_k I_{lk} e^{jk\omega t} = \sum_k I_{lk} e^{jk\theta} = i(\theta) \tag{1.14}$$

The change from this stationary to a synchronous rotating reference frame is performed by means of the rotation factor $e^{-j\hat{\theta}}$, where $\hat{\theta}$ is the phase estimation given by the synchronization system

$$i_s = ie^{-j\hat{\theta}} = \sum_k I_{lk} e^{j(k\theta - \hat{\theta})} \tag{1.15}$$

The reference current is obtained by subtracting from this current its dc component and transforming back to the stationary reference frame, as shown in Fig. 1.9. An estimation of that dc component, I_{DC}^{est}, is provided by a low-pass filter.

Assuming again an ideal filter behavior the following simplification applies:

$$I_{DC}^{est} \simeq I_{DC} = \frac{1}{2\pi} \int_0^{2\pi} i_s(\theta) d\theta \tag{1.16}$$

Once the dc component I_{DC} is computed, the reference current is obtained from

$$i^* = (i_s - I_{dc}) e^{j\hat{\theta}} \tag{1.17}$$

Then, the error, as defined in equation (1.17), is the difference between the reference signal and the load current harmonics

$$e_r = I_{11} e^{j\theta} - I_{dc} e^{j\hat{\theta}} \tag{1.18}$$

Note that, when the system voltage phase is perfectly estimated (i.e., $\hat{\theta} = \theta$), assuming ideal filter behavior, the dc current exactly corresponds to

the fundamental component of the load current, and the reference current perfectly matches the load current harmonics. Therefore, it is necessary to obtain a phase estimate in order to compute e_r, which clearly depends on the synchronization method adopted.

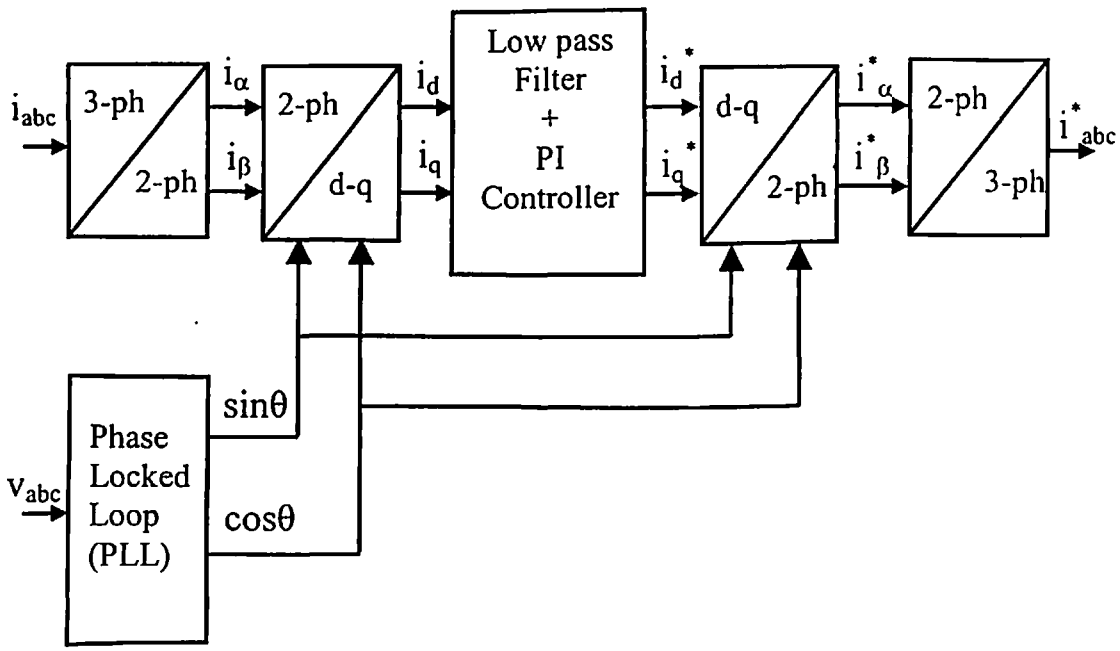

Fig. 1.9: Block diagram of synchronous rotating reference frame method for harmonic current calculation

The SRF method becomes quite complicated when it is applied under asymmetrical source and load conditions. Recently, few more control schemes, which, deal with collective compensation of reactive power under unbalanced and non-sinusoidal source conditions have also been proposed [65-74].

Pukhraj Singh [75] modeled and verified the decomposition scheme in his thesis work. The currents in a three-phase system are mainly composed of fundamental frequency positive sequence component, fundamental frequency

negative sequence component and the harmonics. The positive and negative sequence components can be further divided into active and reactive currents. The general definition of these active, reactive and harmonic currents as defined in FBD method.

In order to decompose an unbalanced and non-sinusoidal current under asymmetrical and distorted AC mains, two reference signals of unity magnitude are used in the proposed algorithm. These signals are of the same frequency and have the same phase as that of the fundamental frequency positive sequence active component of AC mains voltages. These reference signals in α, β coordinates are defined as under:

$$V_{\alpha ref} = \sin(\omega t)$$

$$V_{\beta ref} = -\cos(\omega t) \tag{1.19}$$

Further, the reference signal $V_{\alpha ref}$ is in synchronism with the phase 'a' of source voltage.

Let us assume that the three-phase line currents namely i_{La}, i_{Lb} and i_{Lc} drawn by a nonlinear load are to be decomposed using the newly proposed algorithm. As such, these currents are first transformed from three-phase system to a two phase α-β system using standard Part transformation as under:

$$\begin{bmatrix} i_{L\alpha} \\ I_{L\beta} \end{bmatrix} = \sqrt{\frac{2}{3}} \begin{bmatrix} 1 & -\frac{1}{2} & -\frac{1}{2} \\ 0 & \frac{\sqrt{3}}{2} & -\frac{\sqrt{3}}{2} \end{bmatrix} \begin{bmatrix} i_{La} \\ i_{Lb} \\ i_{Lc} \end{bmatrix} \tag{1.20}$$

These transformed currents named as $i_{L\alpha}$ and $i_{L\beta}$ can be written as a sum of fundamental positive sequence current (i_{kp}), fundamental negative sequence current (i_{kn}) and harmonic currents of both sequences (i_{kH}), as per the following equation:

$$i_{Lk} = ikp + ikn + ikH \tag{1.21}$$

where k represents either α or β phase. The current i_{kp}, can be further subdivided into fundamental positive active and reactive currents of magnitude I_{pmA} and I_{pmR} respectively. Similarly the current i_{kn}, can also be subdivided into negative sequence active and reactive currents of magnitude I_{nmA} and I_{nmR} respectively. It may be pointed out that zero sequence current does not exist because the power system considered for development of the proposed mathematical model has no neutral connection between load and source. The α-β axis currents of (1.20) are next multiplied by a matrix of reference signals in such a way that the fundamental frequency positive sequence currents on α-β axis become the DC quantities. The modified currents in α-β axis are thus expressed in the following equation as:

$$\begin{bmatrix} i'_{Lp} \\ i''_{Lp} \end{bmatrix} = \begin{bmatrix} \sin(\omega t) & -\cos(\omega t) \\ -\cos(\omega t) & -\sin(\omega t) \end{bmatrix} \begin{bmatrix} i_{L\alpha} \\ i_{L\beta} \end{bmatrix} \tag{1.22}$$

The fictious currents i_{Lp}' and i_{Lp}" thus obtained have no physical meaning and have only been defined for convenience of expression, in order to decompose the currents. These fictitious currents consist of DC components, representing the magnitude of fundamental positive sequence active and reactive currents, and

high frequency AC components. The DC components are then extracted by applying a moving window algorithm to these individual currents.

Magnitude of positive sequence active current is computed as:

$$\frac{1}{T}\int_{t-T}^{T} i_{Lp}'\,dt = \frac{1}{T}\int_{t-T}^{T} i_{L\alpha} * \sin(\omega t)\,dt + \frac{1}{T}\int_{t-T}^{T} i_{L\beta} * (-\cos(\omega t))\,dt \qquad (1.23)$$

$$= I_{pmA}$$

Similarly, the magnitude of positive sequence reactive current is computed as:

$$\frac{1}{T}\int_{t-T}^{T} i_{Lp}''\,dt = \frac{1}{T}\int_{t-T}^{T} i_{L\alpha} * (-\cos(\omega t))\,dt + \frac{1}{T}\int_{t-T}^{T} i_{L\beta} * (-\sin(\omega t))\,dt \qquad (1.24)$$

The α-β axis currents of equation (1.20) are now multiplied again by a new matrix of reference signals in such a way that the fundamental frequency negative sequence currents on α-β axis become the DC quantities. The new load currents in α-β axis are written as:

$$\begin{bmatrix} i_{Ln}' \\ i_{Ln}'' \end{bmatrix} = \begin{bmatrix} \sin(\omega t) & \cos(\omega t) \\ \cos(\omega t) & -\sin(\omega t) \end{bmatrix} \begin{bmatrix} i_{L\alpha} \\ i_{L\beta} \end{bmatrix} \qquad (1.25)$$

The magnitude of negative sequence active and reactive currents are estimated in the same manner as the applied for the positive sequence currents. Thus, the magnitude of negative sequence active current is written as:

$$\frac{1}{T}\int_{t-T}^{T} i_{Ln}'\,dt = \frac{1}{T}\int_{t-T}^{T} i_{L\alpha} * \sin(\omega t)\,dt + \frac{1}{T}\int_{t-T}^{T} i_{L\beta} * \cos(\omega t)\,dt \qquad (1.26)$$

$$= I_{nmA}$$

$$\frac{1}{T}\int_{t-T}^{t} i_{L\beta}\,dt = \frac{1}{T}\int_{t-T}^{t} i_{L\alpha} * \cos(\omega t)dt + \frac{1}{T}\int_{t-T}^{t} i_{L\beta} * (-\sin(\omega t))dt \qquad (1.27)$$

$$= I_{nmR}$$

Equations (1.23) – (1.27) give the analytical expressions for the magnitudes of positive and negative sequence currents in α-β axis. The instantaneous currents in α-β axis are obtained by multiplying the magnitudes depicted in (1.23) – (1.27) by reference signals of (1.19). The instantaneous currents thus obtained are then transformed back to the three-phase system by using standard two-phase to three-phase transformation.

Further, instantaneous fundamental positive sequence active components (i_{apA}, i_{bpA}, i_{cpA}) of line currents (i_{La}, i_{Lb}, i_{Lc}) in three-phase system are calculated as,

$$\begin{bmatrix} i_{apA} \\ i_{bpA} \\ i_{cpA} \end{bmatrix} = \sqrt{\frac{2}{3}} \begin{bmatrix} 1 & 0 \\ -\frac{1}{2} & \frac{\sqrt{3}}{2} \\ -\frac{1}{2} & -\frac{\sqrt{3}}{2} \end{bmatrix} \begin{bmatrix} I_{pmR} * & \sin(\omega t) \\ I_{pmR} * & (-\cos(\omega t)) \end{bmatrix} \qquad (1.28)$$

similarly, the instantaneous fundamental positive sequence reactive currents (i_{apR}, i_{bpR}, i_{cpR}) are obtained as:

$$\begin{bmatrix} i_{apR} \\ i_{bpR} \\ i_{cpR} \end{bmatrix} = \sqrt{\frac{2}{3}} \begin{bmatrix} 1 & 0 \\ -\frac{1}{2} & \frac{\sqrt{3}}{2} \\ -\frac{1}{2} & -\frac{\sqrt{3}}{2} \end{bmatrix} \begin{bmatrix} I_{pmR} * & (-\cos(\omega t)) \\ I_{pmR} * & (-\sin(\omega t)) \end{bmatrix} \qquad (1.29)$$

The instantaneous fundamental negative sequence currents (i_{an}, i_{bn}, i_{cn}) in three-phase system are also computed as follows:

$$\begin{bmatrix} i_{\alpha n} \\ i_{\beta n} \end{bmatrix} = \begin{bmatrix} \sin(\omega t) & \cos(\omega t) \\ \cos(\omega t) & -\sin(\omega t) \end{bmatrix} \begin{bmatrix} I_{nmA} \\ I_{nmR} \end{bmatrix} \tag{1.30}$$

$$\begin{bmatrix} i_{an} \\ i_{bn} \\ i_{cn} \end{bmatrix} = \sqrt{\frac{2}{3}} \begin{bmatrix} 1 & 0 \\ -\frac{1}{2} & \frac{\sqrt{3}}{2} \\ -\frac{1}{2} & -\frac{\sqrt{3}}{2} \end{bmatrix} \begin{bmatrix} i_{\alpha n} \\ i_{\beta n} \end{bmatrix} \tag{1.31}$$

Further, it may be pointed out that the harmonic current components in three-phase system are computed by subtracting the decomposed instantaneous active, reactive and negative sequence current components from their respective instantaneous line currents as:

$$\begin{aligned} i_{aH} &= i_{aL} - (i_{apA} + i_{apR} + i_{an}) \\ i_{bH} &= i_{bL} - (i_{bpA} + i_{bpR} + i_{bn}) \\ i_{cH} &= i_{cL} - (i_{cpA} + i_{cpR} + i_{cn}) \end{aligned} \tag{1.32}$$

It is observed from the mathematical expressions developed so far that supply voltages are not used in the proposed algorithm. Therefore, this newly proposed methodology is almost insensitive to voltage unbalance and voltage distortion of AC mains supply, but this algorithm require many complicated mathematical operations such as, division, square root, inversion, integration, differentiation etc., to decompose the current. This makes the proposed method very complex.

M. A. Perales et. al [76] has reported the filter based technique, this method is based on the application of transfer function to extract the load current harmonic components. The main difference between these techniques and those analyzed previously lies in the fact that the system voltage is not used to compute the harmonic components. Therefore, the voltage distortion does not play a role in the computation of the reference current, the main error source arising in the particular formulation adopted for the transfer function. This method eliminates the fundamental component of the load current by applying the transfer function to each phase as shown in block diagram of Fig. 1.10.

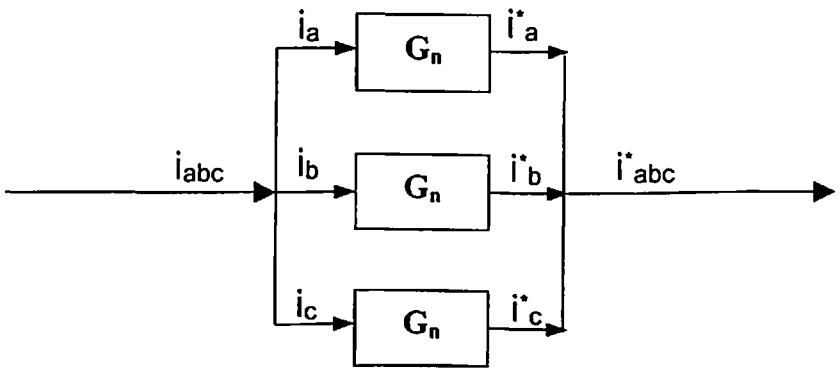

Fig. 1.10: Notch filter technique

The reference current in the Park domain can be written as:

$$i^* = \sum_n G_n I_{ln} e^{jnwt} \tag{1.33}$$

where G_n is the transfer function evaluated at the n^{th} harmonic. For a narrow-band notch filter around the fundamental frequency ω and cutoff frequency ω_c, is given by,

$$G_n = \frac{\omega^2(1-n^2)}{\omega^2(1-n^2)+2jn\omega\omega_c} \tag{1.34}$$

Then the computed error signal can be expressed as

$$e_r(t) = G_1 I_{1l} e^{jwt} + \sum_{k>1}(G_n - 1)I_{lk} e^{jn\omega t} \tag{1.35}$$

Because of the independent application of the notch filter to each phase, it is not possible to compensate for the negative sequence of the load current fundamental component. This method is quite complicated and difficult to implement.

A variety of methods are used for instantaneous current harmonics detection of an APF such as the FFT (fast Fourier transform). Instantaneous p-q theory, synchronous d-q reference frame theory, or using suitable analogue or digital electronics filters to separate successive harmonic components. In the FFT technique, the harmonic current determination is delayed by more than two cycles of the operating waveform, one cycle for the data and another cycle for analysis of the data, to determine the harmonic components. In the case of harmonic current determination by a digital filter, a cascade structure of a biquadratic notch filter is necessary, which makes the method complicated and the implementation difficult. Other harmonic current detection methods mentioned above have their own advantages and drawbacks. The disadvantage of synchronous reference frame theory is that it cannot compensate for reactive power. Instantaneous p-q theory can only determine the harmonic current components under balanced load conditions.

Nowadays, artificial neural networks (ANNs) have been systematically applied to electrical engineering [77, 78]. This technique is considered as a new tool for designing APF control circuits. The ANNs present two principal characteristics. It is not necessary to establish specific input-output relationships, but they are formulated through a learning process or through an adaptive algorithm. Moreover, parallel computing architecture increases the system speed and reliability [79-83].

Pecharanin N. et al [84] have presented a methodology of harmonic detection scheme in active power filter from the power line by using neural network. Harmonic detection by using Fourier transformation is an advantageous method to compensate a specific harmonic component. However, it needs input data for one cycle of the current waveform and needs time for the analysis in next coming cycle. Therefore, the harmonic compensation will be delayed for more than two cycles.

In this proposed scheme a multi-layer neural network is used to detect harmonics from a distorted waveform. In order to detect each harmonic component without the restriction of range and number of input data. It is a pattern recognition ability of neural network for harmonic detection. Neural network presented in this scheme for a harmonic component detection consists of 3-layer network in which input layer = 100 units, middle layer = 10 units and output layer = 1 unit. In the case that 3^{rd} and 5^{th} harmonics are required to be detected, 2 sets of the mentioned network structure will be consisting of the same

input layer. Here a 3-phase bridge circuit is assumed as the harmonic load. This load current can be expressed as:

$$i_L = I_1 \cos(\omega t) - I_3 \cos(3\omega t) + I_5 \cos(5\omega t) \quad (1.36)$$

The variation of each component (I_1, I_3, I_5) is shown in Table 1.3. The harmonics over 11^{th} order are omitted because it is possible to cancel them by high pass filter anyway. Moreover, this scheme assumes the harmonic compensation for a specific load, and the fluctuation of harmonic phase is not considered.

Table 1.4: Content of Harmonics in Distorted Wave

Components	Content [A]	Phase [degree]
1st	20 to 100	0
3rd	10 to 30	– 180
5th	6 to 18	0

In this scheme, a half cycle of distorted wave is used for the harmonic detection by neural network. Fig. 1.11 shows the concept of input and output patterns. The amplitudes of from a distorted wave are sequentially input to the neural network. When a amplitude signal (i_n) is provided, the network calculation $i_n \cdot w_{m,n}$ (for m = 1 to 20) is conducted within the period of sampling data. Therefore when the last amplitude signal (i_{100}) is provided, the processing from

input layer to middle layer is almost conducted. So the proposed algorithm can realize the processing of data input and network calculation by parallel processing.

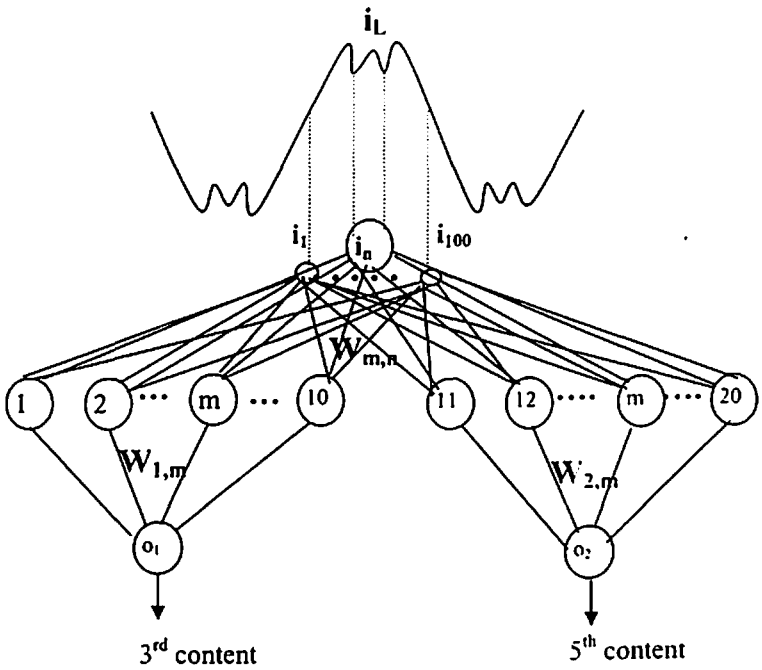

Fig. 1.11: Structure of neural network for harmonic detection

In learning process, the harmonic wave which each component is defined as shown in Table 1.5 are used as input data and the content of each harmonic is used as the supervisors. Neural network repeats learning until each unit signal in output layer (0.0 to 1.0) satisfies the setting learning error by back propagation law [85]. After the learning, it is desired that neural network enables the 3rd and 5th harmonics detection not only from the learning waveforms but also the other waveforms, which are never used for learning.

Table 1.5: Content of Each Components in Learning Waves

Components	Content for learning [A]
I_{h1}	20, 40, 60, 80, 100 [A]
I_{h3}	10, 15, 20, 25, 30 [A]
I_{h5}	6, 9, 12, 15, 18 [A]

The value of each output unit means the detected results of the corresponding harmonic component, which is included in the given distorted wave. These detected results will be used to control the compensative component by inverter. This proposed method is able to analyze each order of harmonic for active power filter as same as Fourier transformation. However, the procedure of extraction of reference current presented in this scheme is complex and requires too much data for training the network.

Rukonuzzaman M. et al [86] have proposed a magnitude and phase determination of harmonic currents by adaptive learning back-propagation neural network. This approach introduces adaptive learning multi-layer back propagation neural network, which converge faster than simple back-propagation neural network. This method is four times faster than conventional method and this makes possible the on-line determination of instantaneous harmonic current components.

Let us assume that the power system of the given fundamental angular frequency ω is distorted by the presence of the higher order harmonics of unknown magnitudes and phases. The general form of the line current, y(t) is predicted as follows;

$$y(t) = \sum_{n=1}^{N} X_n \sin(n\omega t + \varphi_n) \tag{1.37}$$

where n is any integer 1, 2, 3, ... N, X_n is the magnitude and φ_n is the phase of n-th harmonic component.

In normal operating conditions, only odd harmonics are present in electrical equipment and electronic appliance [87]. Considering only odd harmonics, the equation (1.37) may be written as;

$$y(t) = \sum_{n=1,3,5}^{N} X_n \sin(n\omega t + \varphi_n) \tag{1.38}$$

$$y(t) = (a_n \sin n\omega t + b_n \cos n\omega t) \tag{1.39}$$

where

$$a_n = X_n \cos \varphi_n \tag{1.40}$$

and $$b_n = X_n \sin \varphi_n \tag{1.41}$$

By estimating the values of a_n and b_n, the magnitude and phase of n-th harmonic component can be determined from equations (1.42) and (1.43).

$$X_n = \sqrt{\left(a_n^2 + b_n^2\right)}X \tag{1.42}$$

$$\varphi_n = \arctan \frac{b_n}{a_n} \tag{1.43}$$

The process of magnitude and phase determination of each harmonic component by neutral network from the distorted line current is illustrated in Fig. 1.12. The half cycle of the line currents is sampled at different points with regular interval of time axis and these normalized sampled values are the inputs of the three-layer back-propagation neural network. The output layer of the network consists of two units with one for the detection of sine-wave components and another unit for the cosine-wave component detection. The partial connecting neural network with adaptive learning back-propagation algorithm is introduced therein where each output-unit is connected with its own hidden-unit only. The hidden layer is divided into two units. Both the units in the hidden layer contain the same number of hidden nodes. From the sine-wave and cosine-wave component of the output nodes of the two output units, the magnitude and phase of each harmonic current component can be determined in accordance with the equations (1.42) and (1.43). Neural network evolves a nonlinear mapping between the input and output in the learning phase and this is accomplished by selecting appropriate training patterns during the learning phase. In harmonic component prediction process, the training patterns are constructed by varying the magnitude and phases of the fundamental and different harmonic components. The magnitude of the fundamental component is varied at 20%, 40%, 60%, 80% and 100% while the magnitudes of the 3rd, 5th and 7th harmonic components are varied

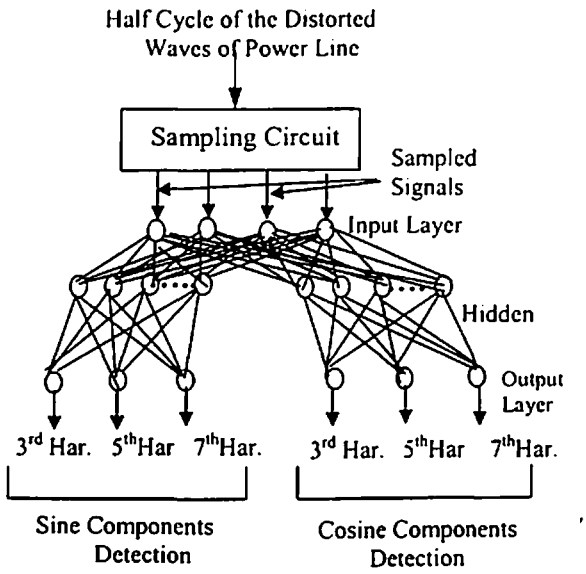

Fig. 1.12: Neural network based harmonic component determination

-varied at 33.33%, 20%, and 14.28% respectively for each value of the fundamental magnitude. The phases of fundamental and different current harmonic components are varied from–180 degree to +180 degree with an interval of 45 degree.

Unlike conventional back-propagation algorithm [88] in which both the learning rate and momentum rate are kept constant, but in this scheme the momentum rate is also updated after each iteration using the following rule to coerce the learning process converge more rapidly:

$$m(i+1) = 1.01m(i); \Delta J_t \leq 0 \qquad (1.44)$$

$$= 0.99m(i); otherwise$$

where m(i) is the momentum at iteration i, and $\Delta J_t = J(i-1) - J(i)$ with J(i) being

the sum of squared error at the end of i-th iteration. Here, the basic idea is to decrease m when ΔJ_t is positive when the error is decreasing, which implies that the connection weights are updated to the correct direction. In this case it is reasonable to maintain this update direction in next iteration. This is achieved by decreasing the momentum in next iteration. This scheme has demonstrated the effective performance of the network in determining the magnitude and phase of the harmonic current. However, in this scheme the learning procedure is complicated.

Marks H. John et al [89] have presented a Predictive Harmonic Identifier for generation of a contemporary estimate of the fundamental component of the distorted input current or voltage waveform. The proposed identifier is shown in Fig. 1.13. A feed forward ANN is used to estimate the mean d-q axis rectifier input currents (voltages), using the instantaneous dc link current and voltage. Information relating to the fundamental and sixth harmonic reference angles is also provided so that the fluctuation of dc current (voltage), can be accounted for. These estimated mean values are then subtracted from the instantaneous values to yield a cancellation reference.

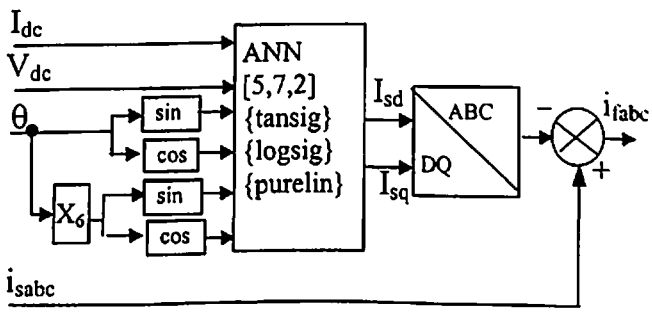

Fig. 1.13: Predictive harmonic identifier

The dc link current (voltage) is used as a basis for the prediction as it exhibits much less distortion than the dq-axis rectifier input currents. The *sine* and *cosine* functions of the sixth harmonic reference angles are included to give a continuous signal representing the periodicity of the dc link distortion. Similar information for the fundamental harmonic reference angle is included to allow the ANN to deal with unbalanced supply conditions.

The ANN used has the following configuration.

- A hidden layer with five neurons with hyperbolic tangent sigmoid transfer function.
- A second hidden layer with seven neurons with log sigmoid transfer function.
- An output layer with two output neurons with liner transfer function.

A two hidden layer ANN is used as it is proven to be able to adapt any arbitrary function. No delays or feedback were used within the ANN.

The network is trained by presenting it with a large set of steady-state input and target output data. The training is accomplished using Levenberg-marqurdt (LM) back-propagation method, in conjunction with the gradient descent with momentum (GDM) learning method to update the ANN weights and bias values. The ANN performance is judged according to the mean squared error (MSE) between the actual ANN output and the target outputs.

To generate the target output data for training the contemporary mean of the d-q axis rectifier distorted input current (voltage) is calculated using a non-causal moving average filter. Equation (1.45) is the linear differential equation representing the filter. This method can, therefore, only be used on data processed off-line.

$$\overline{X}(n) = \frac{1}{m} \sum_{k=-m/2}^{m/2-1} x(n-k) \qquad (1.45)$$

where, n index of the present sample;

m period of the input, in number of samples;

$\overline{X}(n)$ mean value of the input at a specific sample index n;

x(n-k) input at sample index (n-k);

k sample index offset.

The presented neural network scheme can determine the current harmonic components effectively and can be implemented in real time also. This technique is based on back-propagation learning rule for training the network to estimate the harmonic components. However, this approach requires too much data for training the network and leads to inaccurate results in the presence of random noise.

1.7 SUMMARY

A survey of various power circuit configurations and control strategies of Active Filters has been carried out and presented in this Chapter. The important points noted from this survey are summarized as under:

The power circuit configuration plays very important role in the active filtering approach, because it decides the compensation performance and cost. The most popular configuration i.e., Shunt active Filter has been found to have several limitations. The Hybrid Active Filter configurations offer very effective alternative to shunt active filters. Study of various configurations indicated that efficient and cost effective filtering solutions, at the moment, couldn't be realized without the use of passive filters. It is thus felt that research efforts are still needed to develop more effective, multifunctional and efficient power circuit configurations of the Active Filters.

Most of the schemes of reference calculation studied in this chapter have been derived based on the assumptions of a balanced sinusoidal voltage supply feeding a balanced non-linear load. However, there are several schemes, which assume unbalanced and non-sinusoidal conditions either in load or in source only. As it is known, that the Active Filters are generally installed in power system where neither the source nor the load exhibits the above-assumed conditions. Therefore, the control of Active Filters implemented based on these schemes will provide ineffective compensation under real conditions. It is worth mentioning that some of the schemes considered are more general cases of unbalanced and distortions both in source and load. However, this resulted in complicated expressions and has been found difficult for implementation. Further, technical literature on the aspects of more practical conditions is limited.

1.8 OBJECTIVES OF THE RESEARCH WORK

The research work in this doctoral thesis is aimed to develop more effective and efficient harmonic power compensation system for application on three phase three wire and three phase four wire system to develop mathematical models, to do simulation studies using standard packages e.g. MATLAB/SIMULINK.

The following objectives have been laid down for this research work:

- To carry out investigations and research on the existing approaches of harmonic compensation methodologies.
- To design and develop a simplified neural network algorithm for the extraction of harmonic component from non-sinusoidal currents.
    - ❖ Develop neural network model.
    - ❖ Training of the proposed model.
    - ❖ Implement the algorithm using Digital Signal Processor (DSP).
    - ❖ Evaluate the performance of the algorithm by means of simulation investigations under nonlinear, balanced/unbalanced source and load conditions.
- To develop a hybrid power circuit topology having low rated Active Filters for the compensation of current harmonics.
    - ❖ Develop the mathematical model.
    - ❖ Evaluate its performance under different power system conditions (linear/nonlinear, balanced/unbalanced source and load conditions) by means of simulation.

1.9 PREVIEW OF THESIS

The research work reported in this thesis has been focused on the hybrid harmonic power compensation mechanism for use in three-phase, three-wire and three-phase, four-wire power system. The work reported in this thesis has been organized into six Chapters. The contents of each Chapter are presented in brief in the following paragraphs

In Chapter 2, mathematical modeling of the parallel hybrid active power filter is presented. The basic principle of the proposed system is also described in detail. This chapter also covers the control strategy of the proposed hybrid filter.

In Chapter 3, complete modeling of proposed neural network algorithm for the extraction of fundamental current from the highly distorted current waveform has been reported. This Chapter also presents the details of training of proposed neural network. After training the network, the final weight values of the neuron have also been given in tabular form.

Chapter 4 presents the simulation results of the proposed neural network controller under non-linear, unbalance load/source conditions. After getting the satisfactory results of proposed neural network through simulation, it is implemented in real time system using Digital Signal Processor (DSP) to verify the obtained simulated results.

In Chapter 5, the simulation model of the proposed Parallel Hybrid Active Power Filter configuration using SIMULINK has been reported. The simulation

results under various load and source conditions are also investigated and presented to show the excellent steady state and dynamic performance in conjunction with their good agreement with the proposed topological design.

Chapter 6 concludes the research study and also brings out some significant and important contributions of this Ph. D. thesis.

CHAPTER 2

HYBRID ACTIVE POWER FILTER

2.1 INTRODUCTION

Current harmonics generated by nonlinear loads are causing widespread concern to power system engineers and have attracted special interest. Harmonics can cause interference as well as undesired power losses within sensitive electrical equipment. These harmonics cause an array of problems such as equipment overheating, machine vibration, motor failures, capacitor fuse blowing, excessive neutral currents and inaccurate power metering etc. To obtain clean power and avoid unwanted losses, it is a prerequisite to compensate the harmonic components and active filters have an effective way for compensating harmonic components in nonlinear loads. Shunt topology have already been discussed in the literature survey. Hybrid topologies composed of passive LC filter connected in series with an active power filter have already been discussed. Hybrid active filter significantly improves the compensation characteristics of simple passive filters, making the active power filter available for high power applications [90], at a relative lower cost Moreover, compensation characteristics of already installed passive filters can be significantly improved by connecting a series active power filter at its terminals, giving more flexibility to the compensation scheme [91-98].

This Chapter deals with a Parallel Hybrid Active Power Filter (HAPF) topology with Neural Network (NN) controller. This HAPF is capable of reducing the harmonic current distortion below a specified standard level for a given

application. In this Chapter, the concept of proposed HAPF, description of its power circuit configuration and the principle of compensation of HAPF have been presented.

The investigation reported in this Chapter starts with description of operation of HAPF with the help of equivalent circuits and mathematical model. Simplified control scheme for the control of HAPF has also been proposed.

2.2 SYSTEM DESCRIPTION

Fig. 2.1 shows circuit configuration of the adoptive hybrid active filter, which consists of an active filter and a passive filter connected in series. The inverter is connected to the passive filters through a power transformer. The hybrid active filter is connected in parallel with the nonlinear load. The nonlinear load consists of a diode rectifier followed by a capacitor. The tuned passive filters are used to filter the dominant harmonic currents and to reduce the power capacity of active converter. The voltage source inverter (VSI) with an L – C filter is used to generate the equivalent voltage which is related to the source harmonic current by using the impedance variation method. The source harmonic current is suppressed by increasing the ratio of effective source impedance to the harmonic components. To achieve a constant dc-bus voltage of the active filter, a PI voltage controller is employed. The gating signals are obtained from a carrier-based PWM generator.

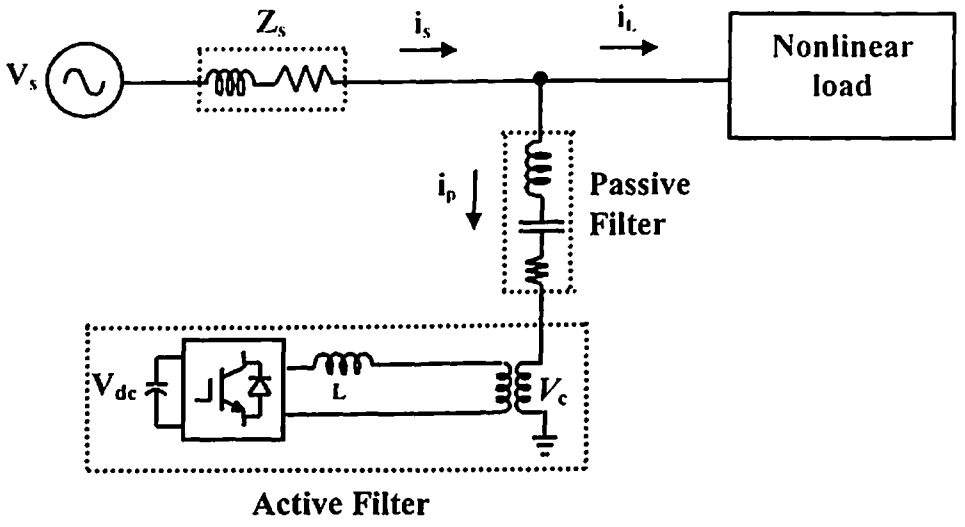

Fig. 2.1 Circuit configuration of HAPF

2.3 SYSTEM ANALYSIS

A three phase Voltage Source Inverter (VSI) is employed in the hybrid active filter to perform harmonic suppression and dc voltage regulation. For harmonic suppression, the power converter of active filter is represented as a harmonic resistor to reduce the source harmonic current.

$$v_{ch}(t) = K_h i_{sh}(t) \tag{2.1}$$

where $i_{sh}(t)$ is the harmonic component of source current, and K_h is the equivalent harmonic resistor at the harmonic frequency. The active converter is operated as a harmonic resistor at the harmonic frequency. The equivalent mains impedance at the harmonic frequency is increased such that the harmonic current flowing into the source is decreased. Because the VSI is operated as a harmonic resistor, a harmonic real power will be consumed in the VSI. The dc-bus voltage of active filter will be fluctuated by this real power. To achieve a constant dc-link voltage of VSI, this energy must be sent to the source by the inverter. At this condition,

the dc capacitor of VSI is operated as a buffer to transfer the absorbed harmonic real power into the fundamental real power to the source. A fundamental voltage component of VSI must be generated and in phase with the fundamental current of hybrid active filter in order to send a real power to the source. This fundamental voltage is illustrated as

$$v_{dc}(t) = K_{dc} i_{pf}(t) \tag{2.2}$$

where $i_{pf}(t)$ is the fundamental current of hybrid active filter. Combining the harmonic suppression and dc voltage regulation, the output voltage of active filter is given by

$$v_c(t) = v_{ch}(t) + v_{dc}(t) = K_h i_{sh}(t) + K_{dc} i_{pf}(t) \tag{2.3}$$

The equivalent circuit of adopted system is shown in Fig. 2.2. The VSI is operated as a variable voltage source, which is controlled by the ac source harmonic current. The nonlinear load is represented by a current source i_L. The impedance of the passive filter is Z_p. The output voltage of active filter is v_c which is related to the source current i_s. According to the equivalent circuit shown in Fig. 2.2, the overall equations in the steady state are obtained as:

$$V_s = Z_s i_s + Z_p i_p + v_c \tag{2.4}$$

$$i_s = i_p + i_L \tag{2.5}$$

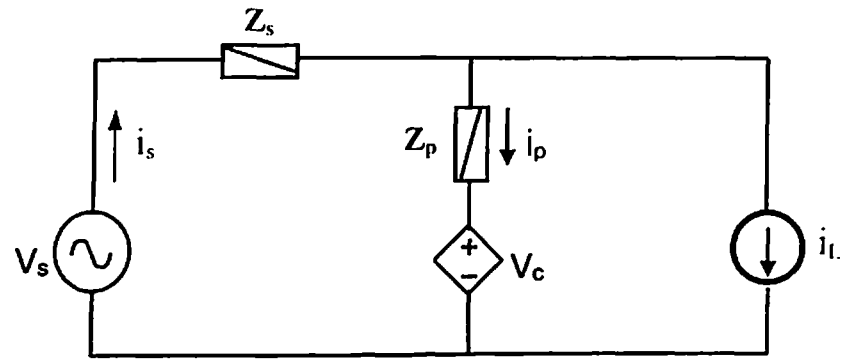

(a)

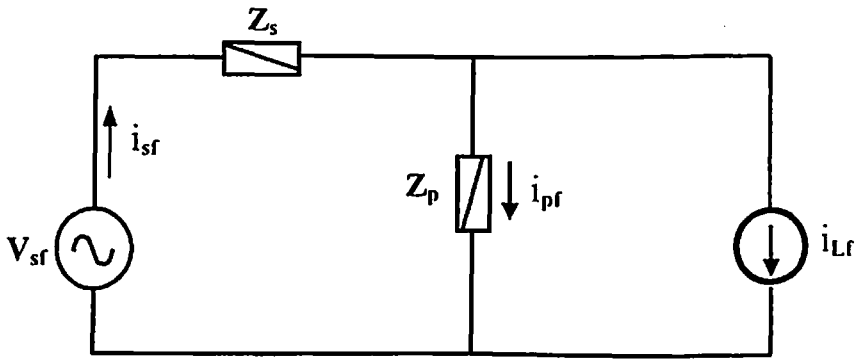

(b)

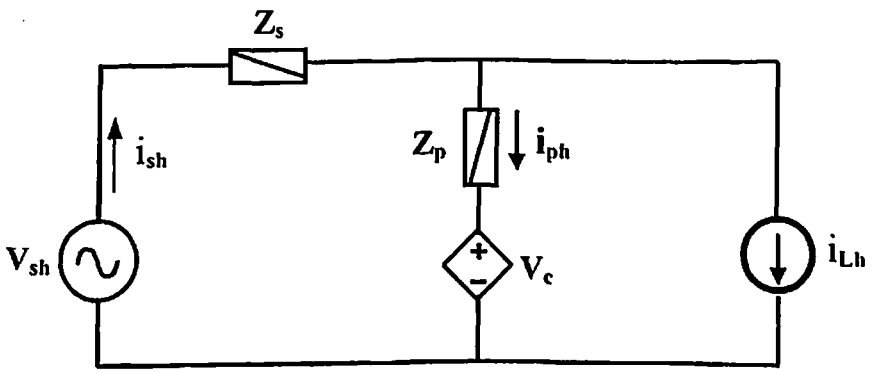

(c)

Fig. 2.2 (a)-(c): Equivalent circuit of HAPF

where $i_s(t)$, $i_p(t)$ and $i_L(t)$ are the source current, the filter current and the nonlinear load current respectively. According to the function of harmonic current suppression, the output voltage of active filter is controlled as

$$v_c(t) = K\, i_s(t). \tag{2.6}$$

Substituting equations (2.5) and (2.6) into equation (2.4), the source current can be expressed as

$$i_s(t) = \frac{v_s(t)}{Z_s + K + Z_p} + \frac{Z_p i_L(t)}{Z_s + K + Z_p}. \tag{2.7}$$

It is assumed that the mains voltage and nonlinear load current contain the fundamental and harmonic components. The source voltage and nonlinear load current are expressed as

$$v_s(t) = v_{sf}(t) + v_{sh}(t), \tag{2.8}$$

$$i_L(t) = i_{Lf}(t) + i_{Lh}(t) \tag{2.9}$$

where $i_{sf}(t)$ and $i_{Lf}(t)$ are the fundamental components of line current and nonlinear load current respectively, $i_{sh}(t)$ and $i_{Lh}(t)$ are the source harmonic current and the load harmonic current respectively. To analysie the operation principle of the hybrid active filter, the circuit in Fig. 2.2(a) is redrawn as Fig. 2.2(b) and (c). The equivalent circuit of the adopted system at the fundamental frequency is shown in Fig. 2.2(b). Fig. 2.2(c) gives the equivalent circuit at the

harmonic frequency. For the fundamental component of source current, the equivalent output voltage $v_{cf}(t)$ of active filter is controlled to zero, i.e. $K_h = 0$.

The fundamental source current as shown in Fig. 2.2(b) is illustrated as

$$i_s(t) = \frac{V_{sf}(t)}{Z_s + Z_p} + \frac{Z_p i_{Lf}(t)}{Z_s + Z_p} \tag{2.10}$$

If the passive filter impedance $Z_p >> Z_s$, the source fundamental current is approximately equal to

$$i_{sf}(t) \approx i_{Lf}(t) + \frac{V_{sf}(t)}{Z_s + Z_p} \tag{2.11}$$

The fundamental current flow into the hybrid active filter is derived as:

$$i_{pf}(t) = \frac{V_{sf}(t)}{Z_s + Z_p} - \frac{Z_s i_{Lf}(t)}{Z_s + Z_p}. \tag{2.12}$$

Fig. 2.2(c) shows the equivalent circuit of the adopted system for the harmonic component. The output voltage of active filter is related to source harmonic current and expressed as equation (2.1). The filter is controlled to provide the load harmonic current such that it does not flow into the source. However, the source harmonic current is not zero due to the finite harmonic resistor. The source harmonic current $i_{sh}(t)$ and filter harmonic current $i_{ph}(t)$ are expressed as

$$i_{sh}(t) = \frac{V_{sh}(t)}{Z_s + Z_p + K_h} + \frac{Z_p i_{Lh}(t)}{Z_s + Z_p + K_h} \tag{2.13}$$

$$i_{ph}(t) = \frac{V_{sh}(t)}{Z_s + Z_p + K_h} - \frac{(Z_s + K_h) i_{l,h}(t)}{Z_s + Z_p + K_h}. \qquad (2.14)$$

If the supply voltage is a pure sine wave, then $v_{sh}(t)$ equals zero. For the harmonic components, the impedance K_h is controlled such that $K_h >> Z_p + Z_s$. The source harmonic current is approximately equal to zero and filter harmonic current is equal-but-opposite the harmonic current of nonlinear load. This means that the most of harmonic currents generated from the nonlinear load are blocked by the equivalent harmonic resistor K_h and flow into the passive filter. Only a small part of nonlinear harmonic current flows into the ac source. The total harmonic distortion (THD) of source current is reduced. The nonlinear load current suppression can be performed by controlling the equivalent harmonic resistor K_h.

2.4 CONTROL STRATAGY

Because the equivalent output voltage of the converter $v_c(t)$ is controlled by the source harmonic current, the harmonic current detected method is presented. The source current is given as:

$$i_s(t) = \sum_{n=1}^{\infty} I_{sn} \sin(n\omega t - \phi_n)$$

$$= I_{sf} \sin(\omega t - \phi_f) + \sum_{n=2}^{\infty} I_{sn} \sin(n\omega t - \phi_n)$$

$$= i_{sf}(t) + i_{sh}(t) \qquad (2.15)$$

where $i_{sf}(t)$ and $i_{sh}(t)$ are source fundamental and harmonic currents respectively. A neural network block is used to filter the source fundamental current and a

subtractor is employed to obtain the source harmonic current. Multiplication of measured harmonics and the harmonic resistor K_h is done to obtain the equivalent voltage command for harmonic current suppression.

$$v_{ch}(t) = K_h i_{sh}(t) = K_h[i_s(t) - i_{sf}(t)] \tag{2.16}$$

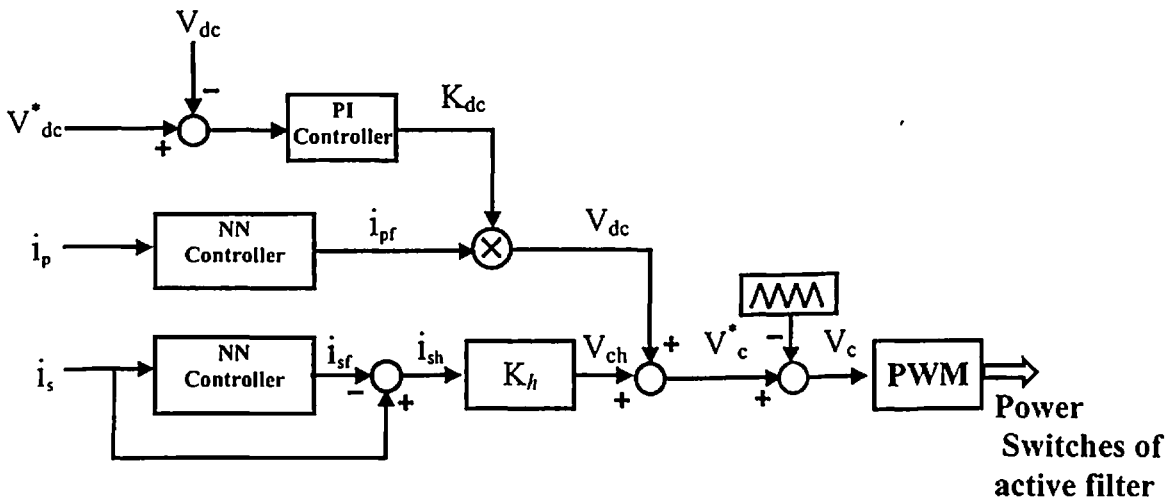

Fig. 2.3 Control strategy of the proposed system

Fig. 2.3 shows the control block diagram of the hybrid active power filter. There are two control blocks in this figure, one is the harmonic suppression block to eliminate the nonlinear harmonic current, and the other is the dc voltage control block to maintain a constant dc-bus voltage. In the harmonic suppression loop, a neural network filter is used to obtain the source fundamental current. The source harmonic current is obtained by subtracting the source fundamental current from the measured. The output voltage of converter for harmonic current suppression is obtained from the multiplication of the calculated source harmonic current and the equivalent harmonic resistor K_h. In the dc voltage control loop, a constant dc-bus

voltage of the converter is generally required. The voltage error between the measured and reference dc-link voltage is sent to the PI voltage controller. To prevent dc-bus voltage variation due to the absorbed harmonic real power, the converter should provide the fundamental real power to the source. To achieve this goal, a filter fundamental current must be generated. A neural network filter is used to obtain filter fundamental current $i_{pf}(t)$. The output of voltage controller is multiplied by the detected filter fundamental current $i_{pf}(t)$ to obtain the dc-link compensated voltage $v_{dc}(t)$ which is used to compensate the switching losses of power switches and to generate a fundamental real power to the source for balancing the absorbed harmonic real power.

$$v_{dc}(t) = \left[PI\left(v_{dc}^{*} - v_{dc}\right)\right] i_{pf}(t) = K_{dc} i_{pf}(t) \tag{2.17}$$

where PI denotes a proportional integral controller and K_{dc} is a equivalent resistor at the fundamental frequency. Finally the required output voltage of converter is the summation of signals $v_{ch}(t)$ and $v_{dc}(t)$ to perform harmonic current suppression and dc voltage regulation. A PWM generates waveform to trigger the power switches of converter. Then the converter can generate the desired voltage $v_c^{*}(t)$.

2.5 THREE-PHASE HYBRID ACTIVE POWER FILTER SYSTEM

The proposed control scheme can be applied in the three-phase hybrid filter system. Fig. 2.4 gives the adopted three-phase hybrid filter system. The three-phase source voltages and currents are v_a, v_b, v_c, i_a, i_b and i_c. The nonlinear load currents are given as i_{La}, i_{Lb} and i_{Lc}. The filter currents are i_{pa}, i_{pb} and i_{pc}. The

output voltages of the active filter based on impedance variation method are controlled to reduce the harmonics of source currents. To maintain a constant dc-link voltage of inverter, a fundamental voltage in phase with fundamental current of active filter is generated to transfer the absorbed harmonic real power into the fundamental real power to the source.

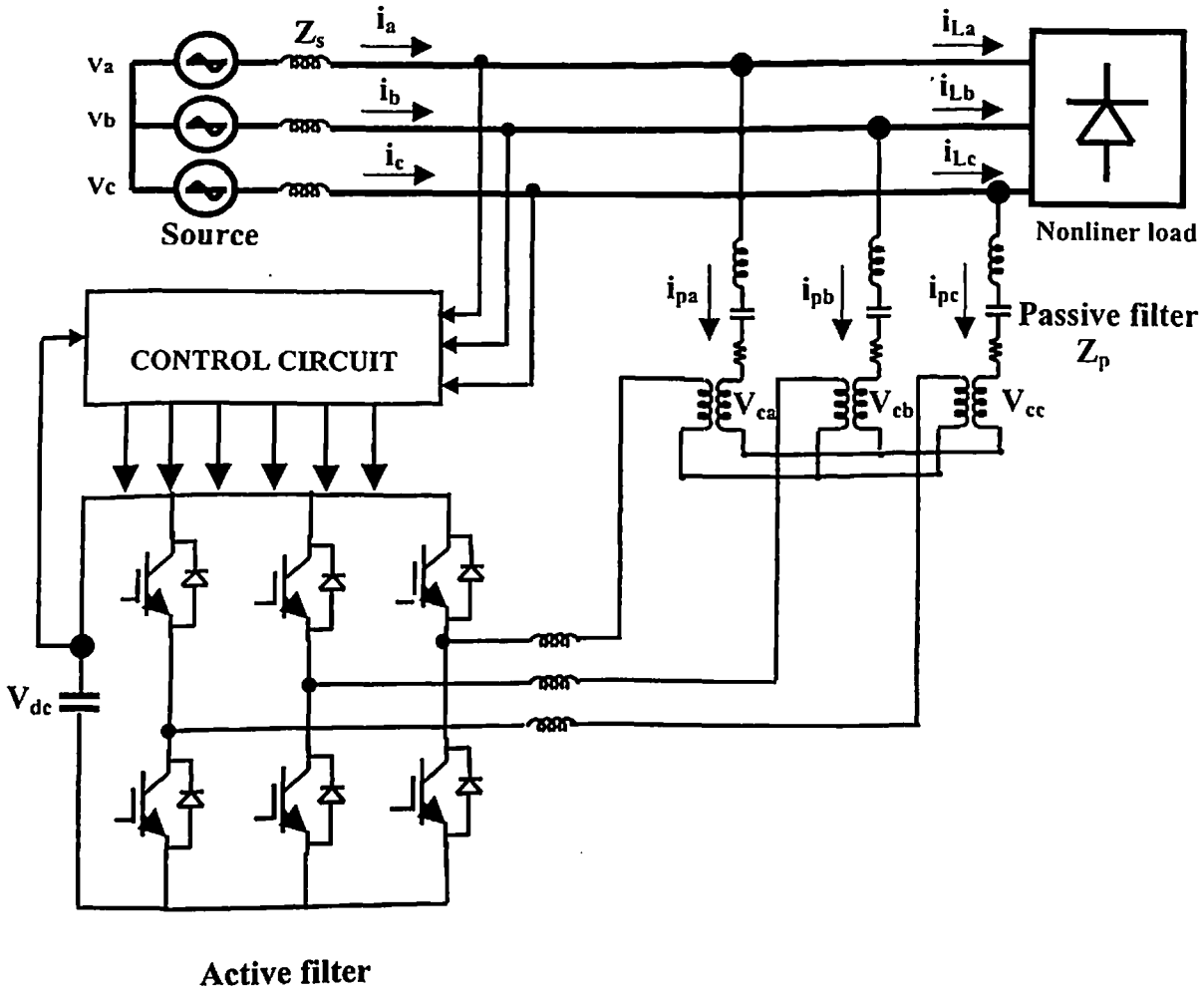

Fig. 2.4: Three-phase three-wire HAPF

The control scheme is based on the synchronous reference frame to obtain the source harmonic currents. The source current between a-b-c and α-β synchronous reference frame is given as

$$\begin{bmatrix} i_\alpha \\ i_\beta \end{bmatrix} = \begin{bmatrix} i_{\alpha f} + i_{\alpha h} \\ i_{\beta f} + i_{\beta h} \end{bmatrix}$$

$$= \sqrt{\frac{2}{3}} \begin{bmatrix} \cos(\theta) & \cos\left(\theta - \frac{2\pi}{3}\right) & \cos\left(\theta + \frac{2\pi}{3}\right) \\ \sin(\theta) & -\sin\left(\theta - \frac{2\pi}{3}\right) & -\sin\left(\theta + \frac{2\pi}{3}\right) \end{bmatrix} \begin{bmatrix} i_a \\ i_b \\ i_c \end{bmatrix} \qquad (2.18)$$

where $\theta = \omega t$.

The source current in the synchronous reference frame can be decomposed into fundamental and harmonic components.

$$i_\alpha = i_{\alpha f} + i_{\alpha h} \qquad (2.19)$$

$$i_\beta = i_{\beta f} + i_{\beta h} \qquad (2.20)$$

The harmonic components $i_{\alpha h}$ and $i_{\beta h}$ are obtained by using a neural network filter that gives the fundamental component, and subtracted from the two-phase currents i_α and i_β. The coordinate transformation between the synchronous frame and a-b-c coordinate is used to obtain the harmonic components of the source current.

$$\begin{bmatrix} i_{ah} \\ i_{bh} \\ i_{ch} \end{bmatrix} = \sqrt{\frac{2}{3}} \begin{bmatrix} \cos(\theta) & -\sin(\theta) \\ \cos\left(\theta - \frac{2\pi}{3}\right) & -\sin\left(\theta - \frac{2\pi}{3}\right) \\ \cos\left(\theta + \frac{2\pi}{3}\right) & -\sin\left(\theta + \frac{2\pi}{3}\right) \end{bmatrix} \begin{bmatrix} i_{\alpha h} \\ i_{\beta h} \end{bmatrix}. \tag{2.21}$$

The equivalent output voltage commands for harmonic current suppression are obtained by multiplication of the measured source harmonic currents and the equivalent harmonic resistor K_h.

$$\begin{bmatrix} v^{*}_{cah} \\ v^{*}_{cbh} \\ v^{*}_{cch} \end{bmatrix} = K_h \begin{bmatrix} i_{ah} \\ i_{bh} \\ i_{ch} \end{bmatrix} \tag{2.22}$$

A dc-bus voltage controller is used to maintain the constant dc-link. The inverter should provide the fundamental real power to the source in order to prevent dc-bus voltage variation due to the absorbed harmonic real power. The filter currents in the synchronous coordinate are given as

$$\begin{bmatrix} i_{p\alpha} \\ i_{p\beta} \end{bmatrix} = \begin{bmatrix} i_{p\alpha,f} + i_{p\alpha,h} \\ i_{p\beta,f} + i_{p\beta,h} \end{bmatrix}$$

$$= \sqrt{\frac{2}{3}} \begin{bmatrix} \cos(\theta) & \cos\left(\theta - \frac{2\pi}{3}\right) & \cos\left(\theta + \frac{2\pi}{3}\right) \\ \sin(\theta) & -\sin\left(\theta - \frac{2\pi}{3}\right) & -\sin\left(\theta + \frac{2\pi}{3}\right) \end{bmatrix} \begin{bmatrix} i_{pa} \\ i_{pb} \\ i_{pc} \end{bmatrix}. \tag{2.23}$$

The passive filter fundamental currents ($i_{p\alpha,f}$ & $i_{p\beta,f}$) are calculated by using the neural network filter.

The matrix that gives the transformation from two-phase synchronous reference frame to three-phase stationary reference frame is given as:

$$\begin{bmatrix} i_{paf} \\ i_{pbf} \\ i_{pcf} \end{bmatrix} = \sqrt{\frac{2}{3}} \begin{bmatrix} \cos(\theta) & -\sin(\theta) \\ \cos\left(\theta - \frac{2\pi}{3}\right) & -\sin\left(\theta - \frac{2\pi}{3}\right) \\ \cos\left(\theta + \frac{2\pi}{3}\right) & -\sin\left(\theta + \frac{2\pi}{3}\right) \end{bmatrix} \begin{bmatrix} i_{p\alpha f} \\ i_{p\beta f} \end{bmatrix} \quad (2.24)$$

The dc link compensated output voltages of power converter are given by the multiplication of the output of dc-link voltage controller and the calculated filter fundamental currents.

$$\begin{bmatrix} v^*_{ca,dc} \\ v^*_{cb,dc} \\ v^*_{cc,dc} \end{bmatrix} = K_{dc} \begin{bmatrix} i_{paf} \\ i_{pbf} \\ i_{pcf} \end{bmatrix} = PI(\Delta v_{dc}) \begin{bmatrix} i_{paf} \\ i_{pbf} \\ i_{pcf} \end{bmatrix} \quad (2.25)$$

The output voltage commands $v^*_{ca} \sim v^*_{cc}$ of the converter for harmonic current suppression and dc-link voltage compensation are given as

$$\begin{bmatrix} v^*_{ca} \\ v^*_{cb} \\ v^*_{cc} \end{bmatrix} = \begin{bmatrix} v^*_{ca,h} \\ v^*_{cb,h} \\ v^*_{cc,h} \end{bmatrix} + K_h \begin{bmatrix} i_{ah} \\ i_{bh} \\ i_{ch} \end{bmatrix} + K_{dc} \begin{bmatrix} i_{paf} \\ i_{pbf} \\ i_{pcf} \end{bmatrix} \quad (2.26)$$

Finally the reference and the measured output voltages of power converter are compared to generate the proper switching signals through the Pulse Width Modulation.

2.6 THREE-PHASE, FOUR-WIRE HAPF SYSTEM

The proposed control scheme is also applicable for three-phase, four-wire hybrid active filter system. Fig. 2.5 gives the adopted three-phase, four-wire hybrid filter system. The V_a, V_b and V_c are the source phase voltages and i_a, i_b and i_c three phase source currents.

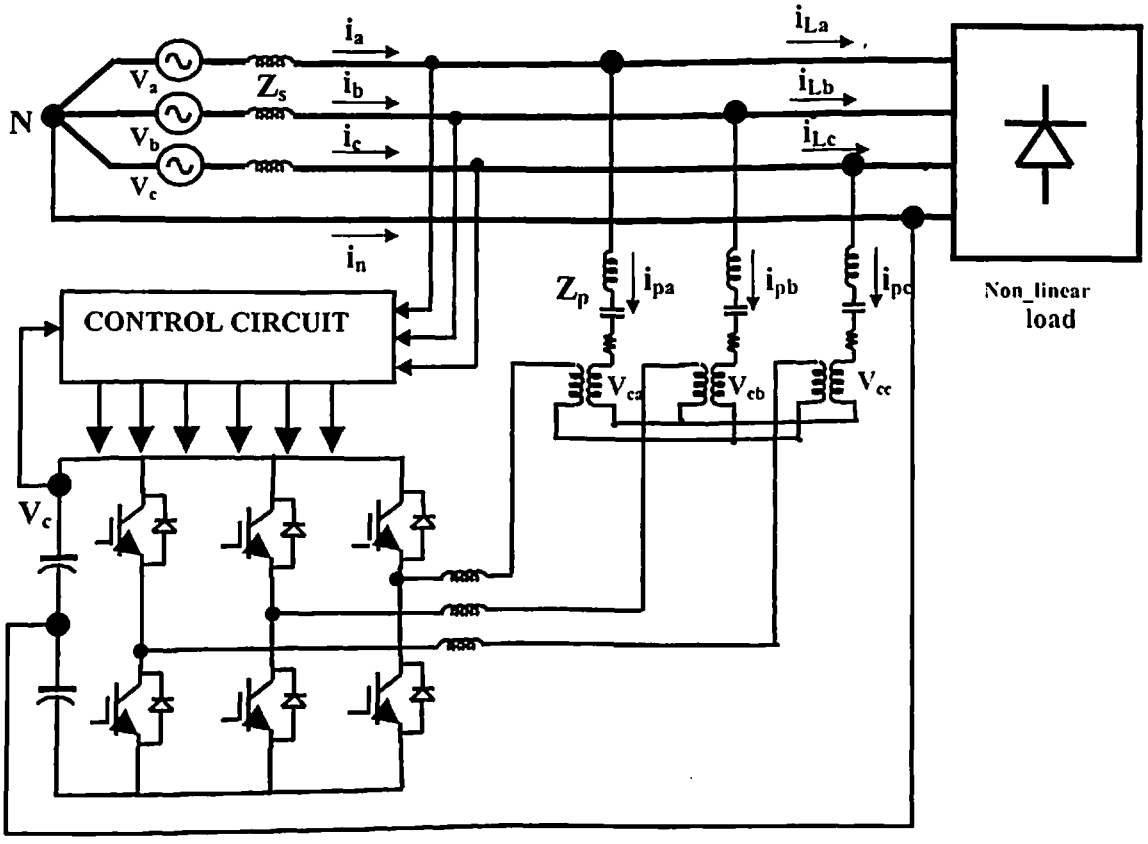

Fig. 2.5: Three-phase, Four-wire HAPF

The i_n is the neutral current flowing in the neutral wire of three-phase four-wire system. The nonlinear load currents are given as i_{La}, i_{Lb} and i_{Lc}. The filter currents are i_{pa}, i_{pb} and i_{pc}. As discussed in section 2.5, the control scheme is

based on the synchronous reference frame to obtain the source harmonic currents. The source current between a-b-c and α-β-0 synchronous reference frame is given as:

$$\begin{bmatrix} i_\alpha \\ i_\beta \\ i_o \end{bmatrix} = \begin{bmatrix} i_{\alpha f} + i_{\alpha h} \\ i_{\beta f} + i_{\beta h} \\ i_{of} + i_{oh} \end{bmatrix}$$

$$= \sqrt{\frac{2}{3}} \begin{bmatrix} \cos(\theta) & \cos\left(\theta - \frac{2\pi}{3}\right) & \cos\left(\theta + \frac{2\pi}{3}\right) \\ \sin(\theta) & -\sin\left(\theta - \frac{2\pi}{3}\right) & -\sin\left(\theta + \frac{2\pi}{3}\right) \\ 0 & 0 & 1 \end{bmatrix} \begin{bmatrix} i_a \\ i_b \\ i_c \end{bmatrix} \quad (2.27)$$

where $\theta = \omega t$.

The source current in the synchronous reference frame can be decomposed into fundamental and harmonic components.

$$i_\alpha = i_{\alpha f} + i_{\alpha h} \quad (2.28)$$

$$i_\beta = i_{\beta f} + i_{\beta h} \quad (2.29)$$

$$i_o = i_{of} + i_{oh} \quad (2.30)$$

The neural network gives the fundamental components of source currents $i_{\alpha f}$, $i_{\beta f}$ and i_{of}, these components are subtracted from source i_α, i_β and i_o currents to achieve the harmonic components $i_{\alpha h}$, $i_{\beta h}$ and i_{oh}.

The coordinate transformation between the synchronous frame and a-b-c coordinate is used to obtain the harmonic components of the source current.

based on the synchronous reference frame to obtain the source harmonic currents. The source current between a-b-c and α-β-0 synchronous reference frame is given as:

$$\begin{bmatrix} i_\alpha \\ i_\beta \\ i_o \end{bmatrix} = \begin{bmatrix} i_{\alpha f} + i_{\alpha h} \\ i_{\beta f} + i_{\beta h} \\ i_{of} + i_{oh} \end{bmatrix}$$

$$= \sqrt{\frac{2}{3}} \begin{bmatrix} \cos(\theta) & \cos\left(\theta - \frac{2\pi}{3}\right) & \cos\left(\theta + \frac{2\pi}{3}\right) \\ \sin(\theta) & -\sin\left(\theta - \frac{2\pi}{3}\right) & -\sin\left(\theta + \frac{2\pi}{3}\right) \\ 0 & 0 & 1 \end{bmatrix} \begin{bmatrix} i_a \\ i_b \\ i_c \end{bmatrix} \quad (2.27)$$

where $\theta = \omega t$.

The source current in the synchronous reference frame can be decomposed into fundamental and harmonic components.

$$i_\alpha = i_{\alpha f} + i_{\alpha h} \quad (2.28)$$

$$i_\beta = i_{\beta f} + i_{\beta h} \quad (2.29)$$

$$i_o = i_{of} + i_{oh} \quad (2.30)$$

The neural network gives the fundamental components of source currents $i_{\alpha f}$, $i_{\beta f}$ and i_{of}, these components are subtracted from source i_α, i_β and i_o currents to achieve the harmonic components $i_{\alpha h}$, $i_{\beta h}$ and i_{oh}.

The coordinate transformation between the synchronous frame and a-b-c coordinate is used to obtain the harmonic components of the source current.

$$\begin{bmatrix} i_{ah} \\ i_{bh} \\ i_{ch} \end{bmatrix} = \sqrt{\frac{2}{3}} \begin{bmatrix} \cos(\theta) & -\sin(\theta) & 0 \\ \cos\left(\theta - \frac{2\pi}{3}\right) & -\sin\left(\theta - \frac{2\pi}{3}\right) & 0 \\ \cos\left(\theta + \frac{2\pi}{3}\right) & -\sin\left(\theta + \frac{2\pi}{3}\right) & 1 \end{bmatrix} \begin{bmatrix} i_{\alpha h} \\ i_{\beta h} \\ i_{oh} \end{bmatrix}. \tag{2.31}$$

The equivalent output voltage commands for harmonic current suppression are obtained by multiplication of the measured source harmonic currents and the equivalent harmonic resistor K_h.

$$\begin{bmatrix} v^{*}_{cah} \\ v^{*}_{cbh} \\ v^{*}_{cch} \end{bmatrix} = K_h \begin{bmatrix} i_{ah} \\ i_{bh} \\ i_{ch} \end{bmatrix} \tag{2.32}$$

A dc-bus voltage controller is used to maintain the constant dc-link. The inverter should provide the fundamental real power to the source in order to prevent dc-bus voltage variation due to the absorbed harmonic real power. The filter currents in the synchronous coordinate are given in equation (2.33).

$$\begin{bmatrix} i_{p\alpha} \\ i_{p\beta} \\ i_{po} \end{bmatrix} = \begin{bmatrix} i_{p\alpha,f} + i_{p\alpha,h} \\ i_{p\beta,f} + i_{p\beta,h} \\ i_{po,f} + i_{po,h} \end{bmatrix} =$$

$$= \sqrt{\frac{2}{3}} \begin{bmatrix} \cos(\theta) & \cos\left(\theta - \frac{2\pi}{3}\right) & \cos\left(\theta + \frac{2\pi}{3}\right) \\ \sin(\theta) & -\sin\left(\theta - \frac{2\pi}{3}\right) & -\sin\left(\theta + \frac{2\pi}{3}\right) \\ 0 & 0 & 1 \end{bmatrix} \begin{bmatrix} i_{pa} \\ i_{pb} \\ i_{pc} \end{bmatrix}. \tag{2.33}$$

The matrix that gives the transformation from two-phase synchronous reference frame to three-phase stationary reference frame is given as:

$$\begin{bmatrix} i_{paf} \\ i_{pbf} \\ i_{pcf} \end{bmatrix} = \sqrt{\frac{2}{3}} \begin{bmatrix} \cos(\theta) & -\sin(\theta) & 0 \\ \cos\left(\theta - \frac{2\pi}{3}\right) & -\sin\left(\theta - \frac{2\pi}{3}\right) & 0 \\ \cos\left(\theta + \frac{2\pi}{3}\right) & -\sin\left(\theta + \frac{2\pi}{3}\right) & 0 \end{bmatrix} \begin{bmatrix} i_{p\alpha.f} \\ i_{p\beta.f} \\ i_{po.f} \end{bmatrix} \tag{2.34}$$

The dc link compensated output voltages of power converter are given by the multiplication of the output of dc-link voltage controller and the calculated filter fundamental currents.

$$\begin{bmatrix} v^*_{ca.dc} \\ v^*_{cb.dc} \\ v^*_{cc.dc} \end{bmatrix} = K_{dc} \begin{bmatrix} i_{paf} \\ i_{pbf} \\ i_{pcf} \end{bmatrix} = PI(\Delta v_{dc}) \begin{bmatrix} i_{paf} \\ i_{pbf} \\ i_{pcf} \end{bmatrix} \tag{2.35}$$

The output voltage commands $v^*_{ca} \sim v^*_{cc}$ of the converter for harmonic current suppression and dc-link voltage compensation are given as

$$\begin{bmatrix} v^*_{ca} \\ v^*_{cb} \\ v^*_{cc} \end{bmatrix} = \begin{bmatrix} v^*_{ca,h} \\ v^*_{cb,h} \\ v^*_{cc,h} \end{bmatrix} + K_h \begin{bmatrix} i_{ah} \\ i_{bh} \\ i_{ch} \end{bmatrix} + K_{dc} \begin{bmatrix} i_{paf} \\ i_{pbf} \\ i_{pcf} \end{bmatrix} \tag{2.36}$$

Finally the reference and the measured output voltages of power converter are compared to generate the proper switching signals through the Pulse Width Modulation.

2.7 SUMMARY

The basic principle and mathematical model of the hybrid active power filter have been presented in this Chapter. The control strategy of the proposed filter has also been described. The mathematical models that are developed in this chapter will be verified by simulation in subsequent chapters.

$$\begin{bmatrix} i_{paf} \\ i_{pbf} \\ i_{pcf} \end{bmatrix} = \sqrt{\frac{2}{3}} \begin{bmatrix} \cos(\theta) & -\sin(\theta) & 0 \\ \cos\left(\theta - \frac{2\pi}{3}\right) & -\sin\left(\theta - \frac{2\pi}{3}\right) & 0 \\ \cos\left(\theta + \frac{2\pi}{3}\right) & -\sin\left(\theta + \frac{2\pi}{3}\right) & 0 \end{bmatrix} \begin{bmatrix} i_{p\alpha.f} \\ i_{p\beta.f} \\ i_{po.f} \end{bmatrix} \tag{2.34}$$

The dc link compensated output voltages of power converter are given by the multiplication of the output of dc-link voltage controller and the calculated filter fundamental currents.

$$\begin{bmatrix} v^{*}_{ca.dc} \\ v^{*}_{cb.dc} \\ v^{*}_{cc.dc} \end{bmatrix} = K_{dc} \begin{bmatrix} i_{paf} \\ i_{pbf} \\ i_{pcf} \end{bmatrix} = PI(\Delta v_{dc}) \begin{bmatrix} i_{paf} \\ i_{pbf} \\ i_{pcf} \end{bmatrix} \tag{2.35}$$

The output voltage commands $v^{*}_{ca} \sim v^{*}_{cc}$ of the converter for harmonic current suppression and dc-link voltage compensation are given as

$$\begin{bmatrix} v^{*}_{ca} \\ v^{*}_{cb} \\ v^{*}_{cc} \end{bmatrix} = \begin{bmatrix} v^{*}_{ca,h} \\ v^{*}_{cb,h} \\ v^{*}_{cc,h} \end{bmatrix} + K_{h} \begin{bmatrix} i_{ah} \\ i_{bh} \\ i_{ch} \end{bmatrix} + K_{dc} \begin{bmatrix} i_{paf} \\ i_{pbf} \\ i_{pcf} \end{bmatrix} \tag{2.36}$$

Finally the reference and the measured output voltages of power converter are compared to generate the proper switching signals through the Pulse Width Modulation.

2.7 SUMMARY

The basic principle and mathematical model of the hybrid active power filter have been presented in this Chapter. The control strategy of the proposed filter has also been described. The mathematical models that are developed in this chapter will be verified by simulation in subsequent chapters.

CHAPTER 3

NEURAL NETWORK CONTOLLER DESIGN

3.1 INTRODUCTION

In previous chapter complete mathematical model of Hybrid Active Power Filter has been discussed. In a HAPF calculation of reference current is an essential task because it directly affects compensator performance parameters such as response, stability and accuracy of control. Various methods proposed in the published literature so far, were discussed in the literature review. These methods lead to very cumbersome and complex mathematical expressions, when applied under asymmetrical nonlinear load and unbalanced source conditions.

In this Chapter, a Neural Network (NN) controller has been proposed for obtaining the reference signals in an effort to produce a simple, more versatile control philosophy for active power filters. The proposed NN algorithm extracts the fundamental waveform from non-sinusoidal waveforms without making any assumptions about unbalance and distortion in either source or load. The extracted components can be used as reference signals for active power filters. A detailed mathematical model of the proposed algorithm is presented in this Chapter.

3.2 ARTIFICIAL NEURAL NETWORKS

Artificial Neural Networks are relatively crude electronic models based on the neural structure of the brain. The brain basically learns from experience. It is natural proof that some problems that are beyond the scope of current computers

are indeed solvable by small energy efficient packages. This brain modeling also promises a less technical way to develop machine solutions. These biologically inspired methods of computing are thought to be the next major advancement in the computing industry. Even simple animal brains are capable of functions that are currently impossible for computers. Computers do those things well, like keeping ledgers or performing complex mathematics. But computers have trouble recognizing even simple patterns much less generalizing those patterns of the past into actions of the future.

Now, advances in biological research promise an initial understanding of the natural thinking mechanism. This research shows that brains store information as patterns. Some of these patterns are very complicated and allow us the ability to recognize individual faces from many different angles. This process of storing information as patterns, utilizing those patterns, and then solving problems encompasses a new field in computing. This field, as mentioned before, does not utilize traditional programming but involves the creation of massively parallel networks and the training of those networks to solve specific problems. This field also utilizes words very different from traditional computing, words like behave, react, self-organize, learn, generalize, and forget [99-101].

3.2.1 Analogy to the Brain

The exact workings of the human brain are still a mystery. Yet, some aspects of this amazing processor are known. In particular, the most basic element of the human brain is a specific type of cell, which unlike the rest of the body,

doesn't appear to regenerate. Because this type of cell is the only part of the body that isn't slowly replaced, it is assumed that these cells are what provide us with our abilities to remember, think, and apply previous experiences to our every action. These cells, all 100 billion of them, are known as neurons. Each of these neurons can connect with up to 200,000 other neurons, although 1,000 to 10,000 are typical, The power of the human mind comes from the sheer numbers of these basic components and the multiple connections between them. It also comes from genetic programming and learning. The individual neurons are complicated. They have a myriad of parts, sub-systems, and control mechanisms. They convey information via a host of electrochemical pathways. There are over one hundred different classes of neurons, depending on the classification method used. Together these neurons and their connections form a process, which is not binary, not stable, and not synchronous. In short, it is nothing like the currently available electronic computers, or even artificial neural networks [102].

These artificial neural networks try to replicate only the most basic elements of this complicated, versatile, and powerful organism. They do it in a primitive way. But for the software engineer who is trying to solve problems, neural computing was never about replicating human brains. It is about machines and a new way to solve problems [103].

3.2.2 Artificial Neurons

The fundamental processing element of a neural network is a neuron. This building block of human awareness encompasses a few general capabilities. Basically, a biological neuron receives inputs from other sources, combines them in some way, performs a generally nonlinear operation on the result, and then outputs the final result. Fig. 3.1 shows the relationship of these four parts.

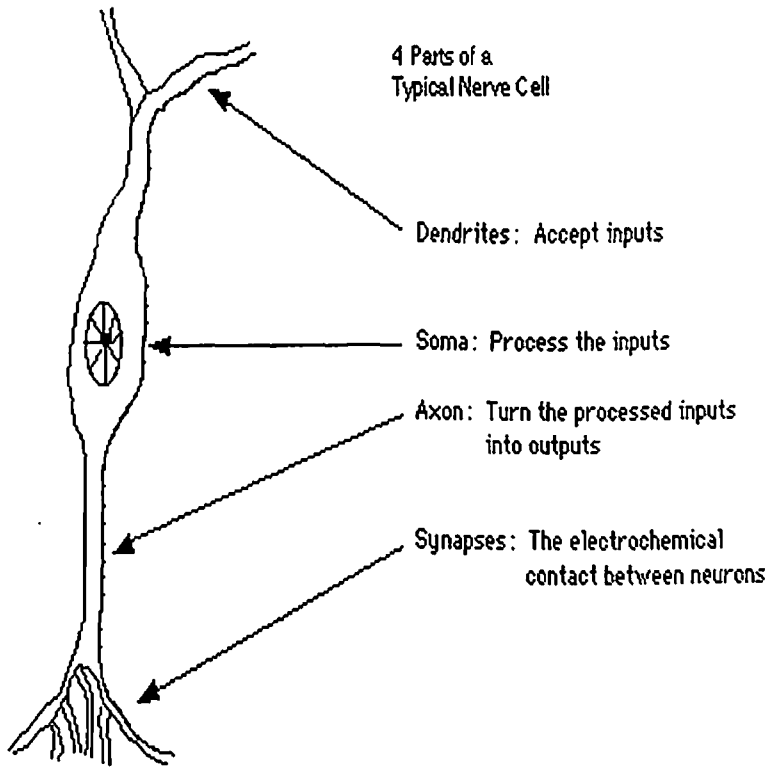

Fig. 3.1: A Simple Neuron.

Within humans there are many variations on this basic type of neuron, further complicating man's attempts at electrically replicating the process of thinking. Yet, all natural neurons have the same four basic components [104]. These components are known by their biological names - dendrites, soma, axon,

and synapses. Dendrites are hair-like extensions of the soma, which act like input channels. These input channels receive their input through the synapses of other neurons. The soma then processes these incoming signals over time. The soma then turns that processed value into an output, which is sent out to other neurons through the axon and the synapses. Recent experimental data has provided further evidence that biological neurons are structurally more complex than the simplistic explanation above. They are significantly more complex than the existing artificial neurons that are built into today's artificial neural networks. As biology provides a better understanding of neurons, and as technology advances, network designers can continue to improve their systems by building upon man's understanding of the biological brain.

But currently, the goal of artificial neural networks is not the grandiose recreation of the brain. On the contrary, neural network researchers are seeking an understanding of nature's capabilities for which people can engineer solutions to problems that have not been solved by traditional computing. To do this, the basic unit of neural networks, the artificial neurons, simulates the four basic functions of natural neurons. Fig. 3.2 shows a fundamental representation of an artificial neuron [105]. In Fig. 3.2 various inputs to the network are represented by the mathematical symbol x(n). Each of these inputs is multiplied by a connection weight. These weights are represented by w(n). In the simplest case, these products are simply summed, fed through a transfer function to generate a result, and then output.

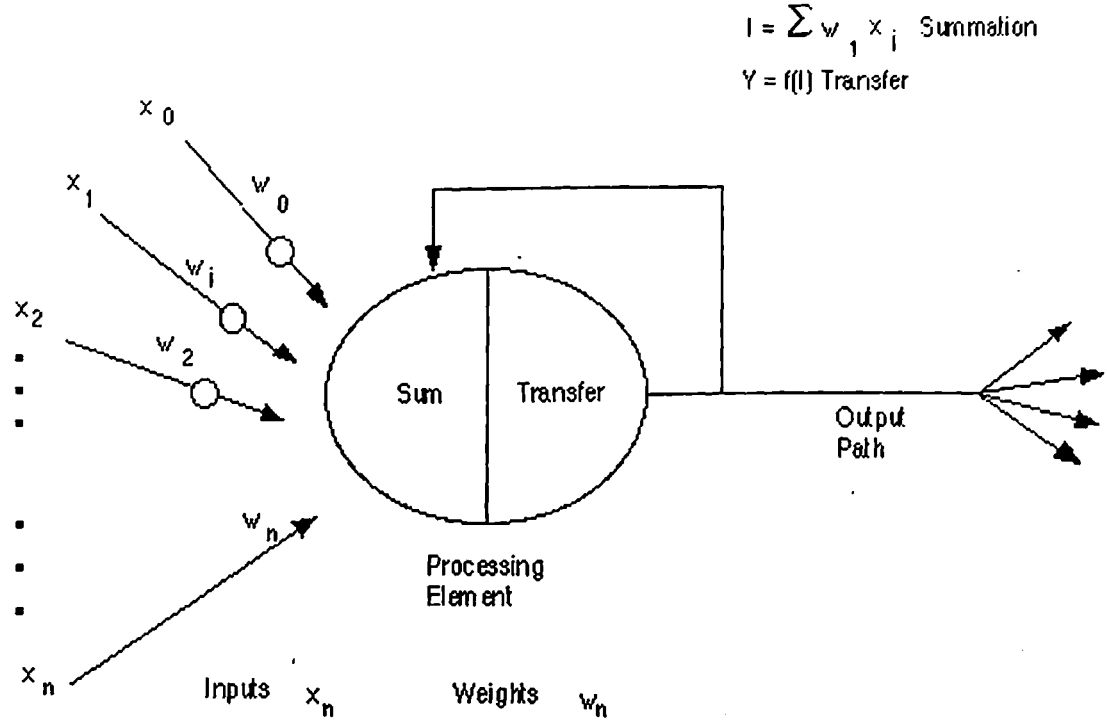

Fig. 3.2: Representation of an artificial neuron

This process lends itself to physical implementation on a large scale in a small package. This electronic implementation is still possible with other network structures, which utilize different summing functions as well as different transfer functions.

3.2.3 Artificial Network Operation

Neural networks are the simple clustering of the primitive artificial neurons. This clustering occurs by creating layers that are then connected to one another. How these layers connect is the other part of the "art" of engineering networks to resolve real world problems.

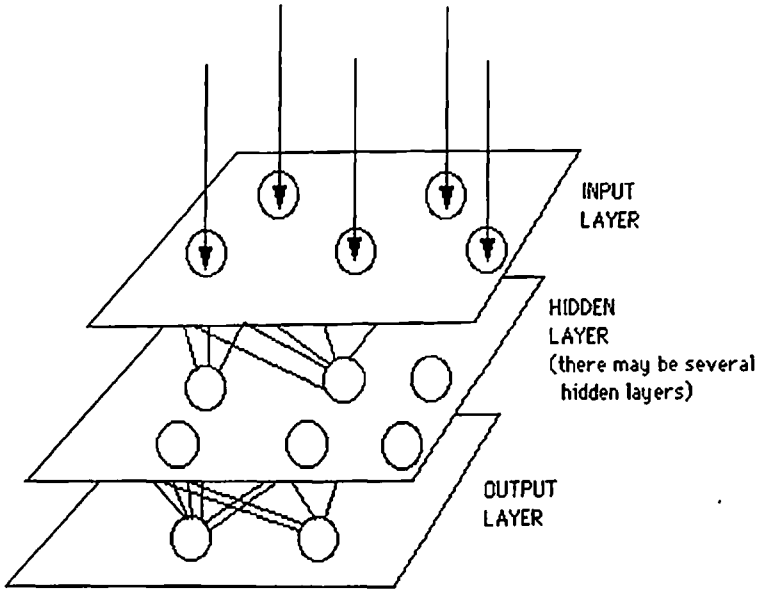

Fig. 3.3: A Simple Neural Network Diagram

Basically, all artificial neural networks have a similar structure or topology as shown in Fig. 3.3 that structure some of the neurons interfaces to the real world to receive its inputs. Other neurons provide the real world with the network's outputs. This output might be the particular character that the network thinks that it has scanned or the particular image it thinks is being viewed. All the rest of the neurons are hidden from view. But a neural network is more than a bunch of neurons. Some early researchers tried to simply connect neurons in a random manner, without much success. Now, it is known that even the brains of snails are structured devices. One of the easiest ways to design a structure is to create layers of elements. It is the grouping of these neurons into layers, the connections between these layers, and the summation and transfer functions that comprises a functioning neural network. The general terms used to describe these characteristics are common to all networks [106].

3.2.4 Major Components of an Artificial Neuron

This section describes the seven major components, which make up an artificial neuron. These components are valid whether the neuron is used for input, output, or is in one of the hidden layers.

(a) Weighting Factors: A neuron usually receives many simultaneous inputs. Each input has its own relative weight, which gives the input the impact that it needs on the processing element's summation function. These weights perform the same type of function, as do the varying synaptic strengths of biological neurons. In both cases, some inputs are made more important than others so that they have a greater effect on the processing element as they combine to produce a neural response.

Weights are adaptive coefficients within the network that determine the intensity of the input signal as registered by the artificial neuron. They are a measure of an input's connection strength. These strengths can be modified in response to various training sets and according to a network's specific topology or through its learning rules [107].

(b) Summation Function: The first step in a processing element's operation is to compute the weighted sum of all of the inputs. Mathematically, the inputs and the corresponding weights are vectors which can be represented as (i1, i2 . . . i*n*) and (w1, w2 . . . w*n*). The total input signal is the dot, or inner, product of these two vectors. This simplistic summation function is found by multiplying each component of the "i" vector by the corresponding component of the "w" vector

and then adding up all the products. Input1 = i1 * w1, input2 = i2 * w2, etc., are added as input1 + input2 + . . . + input*n*. The result is a single number, not a multi-element vector. The summation function can be more complex than just the simple input and weight sum of products. The input and weighting coefficients can be combined in many different ways before passing on to the transfer function. In addition to a simple product summing, the summation function can select the minimum, maximum, majority, product, or several normalizing algorithms. The specific algorithm for combining neural inputs is determined by the chosen network architecture and paradigm [108].

(c) Transfer Function: The result of the summation function, almost always the weighted sum, is transformed to a working output through an algorithmic process known as the transfer function. In the transfer function the summation total can be compared with some threshold to determine the neural output. If the sum is greater than the threshold value, the processing element generates a signal. If the sum of the input and weight products is less than the threshold, no signal (or some inhibitory signal) is generated. Both types of response are significant. The threshold, or transfer function, is generally non-linear. Linear (straight-line) functions are limited because the output is simply proportional to the input. Linear functions are not very useful. That was the problem in the earliest network models as noted in Minsky and Papert's book *Perceptrons*.

The transfer function could be something as simple as depending upon whether the result of the summation function is positive or negative. The network could output zero and one, one and minus one, or other numeric combinations.

The transfer function would then be a "hard limiter" or step function. Sample transfer functions are given in Fig. 3.4[109].

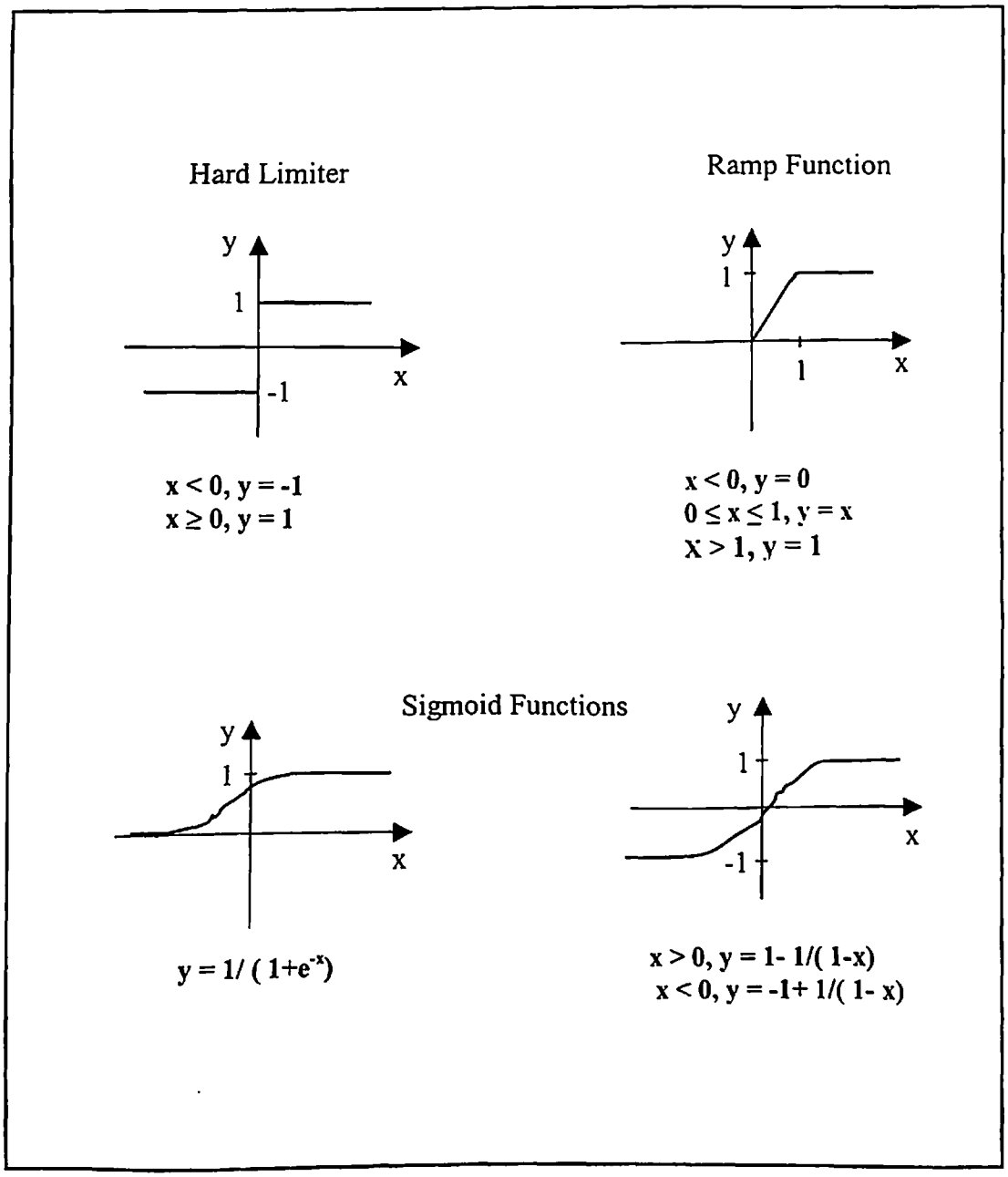

Fig. 3.4: Sample Transfer Functions

(d) Scaling and Limiting: After the processing element's transfer function, the result can pass through additional processes, which scale and limit. This scaling simply multiplies a scale factor times the transfer value, and then adds an offset. Limiting is the mechanism, which insures that the scaled result does not exceed an upper, or lower bound. This limiting is in addition to the hard limits that the original transfer function may have performed.

(e) Output Function (Competition): Each processing element is allowed one output signal, which it may output to hundreds of other neurons. This is just like the biological neuron, where there are many inputs and only one output action. Normally, the output is directly equivalent to the transfer function's result. Some network topologies, however, modify the transfer result to incorporate competition among neighboring processing elements. Neurons are allowed to compete with each other, inhibiting processing elements unless they have great strength. Competition can occur at one or both of two levels. First, competition determines which artificial neuron will be active, or provides an output. Second, competitive inputs help determine which processing element will participate in the learning or adaptation process.

(f) Error Function and Back-Propagated Value: In most learning networks the difference between the current output and the desired output is calculated. This raw error is then transformed by the error function to match particular network architecture. The most basic architectures use this error directly, but some square the error while retaining its sign, some cube the error, other paradigms modify the raw error to fit their specific purposes. The artificial neuron's error is then

typically propagated into the learning function of another processing element. This error term is sometimes called the current error. The current error is typically propagated backwards to a previous layer [110, 111]. Yet, this back-propagated value can be either the current error, the current error scaled in some manner (often by the derivative of the transfer function), or some other desired output depending on the network type. Normally, this back-propagated value, after being scaled by the learning function, is multiplied against each of the incoming connection weights to modify them before the next learning cycle.

(g) Learning Function: The purpose of the learning function is to modify the variable connection weights on the inputs of each processing element according to some neural based algorithm. This process of changing the weights of the input connections to achieve some desired result could also be called the adoption function, as well as the learning mode. There are two types of learning: supervised and unsupervised. Supervised learning requires a teacher. The teacher may be a training set of data or an observer who grades the performance of the network results. Either way, having a teacher is learning by reinforcement. When there is no external teacher, the system must organize itself by some internal criteria designed into the network. This is learning by doing.

3.2.5 Teaching an Artificial Neural Network

Teaching means training or learning of network based on the artificial neuron. Various techniques has been developed to train the network, some very

popular and effective techniques have been presented in the following subsections.

3.2.5.1 Supervised learning

The vast majority of artificial neural network solutions have been trained with supervision [112-114]. In this mode, the actual output of a neural network is compared to the desired output. The network then adjusts weights, which are usually randomly set to begin with, so that the next iteration, or cycle, will produce a closer match between the desired and the actual output. The learning method tries to minimize the current errors of all processing elements. This global error reduction is created over time by continuously modifying the input weights until acceptable network accuracy is reached.

With supervised learning, the artificial neural network must be trained before it becomes useful. Training consists of presenting input and output data to the network. This data is often referred to as the training set. That is, for each input set provided to the system, the corresponding desired output set is provided as well. In most applications, actual data must be used. This training phase can consume a lot of time. In prototype systems, with inadequate processing power, learning can take weeks. This training is considered complete when the neural network reaches a user defined performance level. This level signifies that the network has achieved the desired statistical accuracy as it produces the required outputs for a given sequence of inputs. When no further learning is necessary, the weights are typically frozen for the application. Some network types allow

continual training, at a much slower rate, while in operation. This helps a network to adapt to gradually changing conditions.

Training sets need to be fairly large to contain all the needed information if the network is to learn the features and relationships that are important. Not only do the sets have to be large but also the training sessions must include a wide variety of data. If the network is trained just one example at a time, all the weights set so meticulously for one fact could be drastically altered in learning the next fact. The previous facts could be forgotten in learning something new. As a result, the system has to learn everything together, finding the best weight settings for the total set of facts. For example, in teaching a system to recognize pixel patterns for the ten digits, if there were twenty examples of each digit, all the examples of the digit seven should not be presented at the same time.

How the input and output data is represented, or encoded, is a major component to successfully instructing a network. Artificial networks only deal with numeric input data. Therefore, the raw data must often be converted from the external environment. Additionally, it is usually necessary to scale the data, or normalize it to the network's paradigm. This pre-processing of real-world stimuli, be they cameras or sensors, into machine-readable format is already common for standard computers. Many conditioning techniques, which directly apply to artificial neural network implementations, are readily available. It is then up to the network designer to find the best data format and matching network architecture for a given application.

information about how to organize itself. This information is built into the network topology and learning rules. An unsupervised learning algorithm might emphasize cooperation among clusters of processing elements. In such a scheme, the clusters would work together. If some external input activated any node in the cluster, the cluster's activity as a whole could be increased. Likewise, if external input to nodes in the cluster was decreased, that could have an inhibitory effect on the entire cluster. Competition between processing elements could also form a basis for learning. Training of competitive clusters could amplify the responses of specific groups to specific stimuli. As such, it would associate those groups with each other and with a specific appropriate response. Normally, when competition for learning is in effect, only the weights belonging to the winning processing element will be updated [115, 116].

3.2.5.3 Learning rates

The rate at which ANNs learn depends upon several controllable factors. In selecting the approach there are many trade-offs to consider. Obviously, a slower rate means a lot more time is spent in accomplishing the off-line learning to produce an adequately trained system. With the faster learning rates, however, the network may not be able to make the fine discriminations possible with a system that learns more slowly. Researchers are working on producing the best of both worlds. Most learning functions have some provision for a learning rate, or learning constant [117]. Usually this term is positive and between zero and one. If the learning rate is greater than one, it is easy for the learning algorithm to

overshoot in correcting the weights, and the network will oscillate. Small values of the learning rate will not correct the current error as quickly, but if small steps are taken in correcting errors, there is a good chance of arriving at the best minimum convergence.

3.2.5.4 Learning laws

Many learning laws are in common use. Most of these laws are some sorts of variation of the best-known and oldest learning law, Hebb's Rule [118]. Research into different learning functions continues as new ideas routinely show up in trade publications. Some researchers have the modeling of biological learning as their main objective. Others are experimenting with adaptations of their perceptions of how nature handles learning. Either way, man's understanding of how neural processing actually works is very limited. Learning is certainly more complex than the simplifications represented by the learning laws currently developed. A few of the major laws are presented as examples.

(a) Hebb's Rule: The first, and undoubtedly the best known, learning rule was introduced by Donald Hebb. The description appeared in his book *The Organization of Behavior* in 1949. His basic rule is: If a neuron receives an input from another neuron, and if both are highly active (mathematically have the same sign), the weight between the neurons should be strengthened.

(b) Hopfield Law: It is similar to Hebb's rule with the exception that it specifies the magnitude of the strengthening or weakening. It states, "if the desired output

and the input are both active or both inactive, increment the connection weight by the learning rate, otherwise decrement the weight by the learning rate" [119, 120].

(c) The Delta Rule: This rule is a further variation of Hebb's Rule. It is one of the most commonly used. This rule is based on the simple idea of continuously modifying the strengths of the input connections to reduce the difference (the delta) between the desired output value and the actual output of a processing element. This rule changes the synaptic weights in the way that minimizes the mean squared error of the network. This rule is also referred to as the Widrow-Hoff Learning Rule [121] and the Least Mean Square (LMS) Learning Rule.

The way that the Delta Rule works is that the delta error in the output layer is transformed by the derivative of the transfer function and is then used in the previous neural layer to adjust input connection weights. In other words, this error is back propagated into previous layers one layer at a time. The process of back-propagating the network errors continues until the first layer is reached. The network type called Feed forward, Back-propagation derives its name from this method of computing the error term.

When using the delta rule, it is important to ensure that the input data set is well randomized. Well-ordered or structured presentation of the training set can lead to a network, which cannot converge to the desired accuracy. If that happens, then the network is incapable of learning the problem.

(d) The Gradient Descent Rule: This rule is similar to the Delta Rule in that the derivative of the transfer function is still used to modify the delta error before it is

applied to the connection weights [122]. Here, however, an additional proportional constant tied to the learning rate is appended to the final modifying factor acting upon the weight. This rule is commonly used, even though it converges to a point of stability very slowly.

It has been shown that different learning rates for different layers of network help the learning process converge faster. In these tests, the learning rates for those layers close to the output were set lower than those layers near the input. This is especially important for applications where the input data is not derived from a strong underlying model.

(e) Kohonen's Learning Law: This procedure, developed by Teuvo Kohonen, was inspired by learning in biological systems. In this procedure, the processing elements compete for the opportunity to learn, or update their weights. The processing element with the largest output is declared the winner and has the capability of inhibiting its competitors as well as exciting its neighbors. Only the winner is permitted an output, and only the winner plus its neighbors are allowed to adjust their connection weights.

Further, the size of the neighborhood can vary during the training period. The usual paradigm is to start with a larger definition of the neighborhood, and narrow in as the training process proceeds. Because the winning element is defined as the one that has the closest match to the input pattern, Kohonen networks model the distribution of the inputs. This is good for statistical or

topological modeling of the data and is sometimes referred to as self-organizing maps or self-organizing topologies.

3.3 PROPOSED CONTROL SYSTEM DESCRIPTION

Block diagram of the proposed controller of hybrid active power filter is shown in Fig. 3.5. There are two control blocks in this figure. One is the harmonic suppression block to eliminate the nonlinear harmonic current, and other is the dc voltage control block to maintain a constant dc-bus voltage. In the harmonic suppression loop, Adaptive Liner Neural Network (ADALINE) is used to obtain the fundamental current from load current [123-131]. This fundamental current is subtracted from the load current to obtain the reference (harmonic) currents. The output voltage of converter for harmonic current suppression is obtained from the multiplication of the calculated mains harmonic current and the equivalent harmonic resistor K_h. In the dc voltage control loop, the voltage error between the measured and reference dc link voltage is sent to the PI voltage controller. To prevent dc-bus voltage variation due to the absorbed harmonic real power, the converter should provide the fundamental real power to the mains. To achieve this goal, a filter fundamental current must be generated; the ADALINE is used to obtain the fundamental current. The output of voltage controller is multiplied by the detected fundamental current to obtain the dc-link compensated voltage which is used to compensate the switching losses of power switches and to generate a fundamental real power to the source for balancing the absorbed harmonic real power.

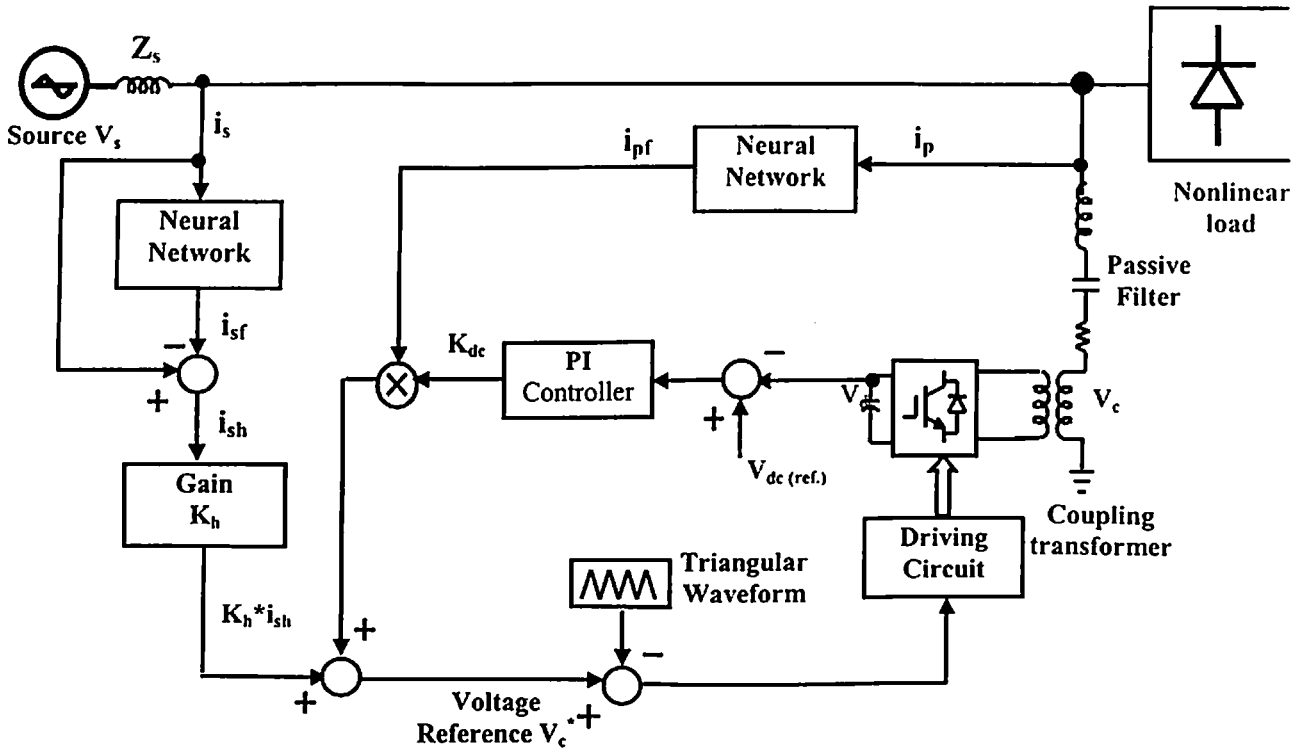

Fig 3.5:Control block diagram of the proposed hybrid active filter

3.4 NN CONTROLLER

In this section, Adaptive Linear Neural Network (ADLINE) controller is modeled and trained to extract the fundamental component from the highly distorted waveform, which is required as a reference current in hybrid active power filters.

3.4.1 Three-Phase, Three-Wire System

The block diagram of proposed NN based controller is shown in Fig. 3.6.

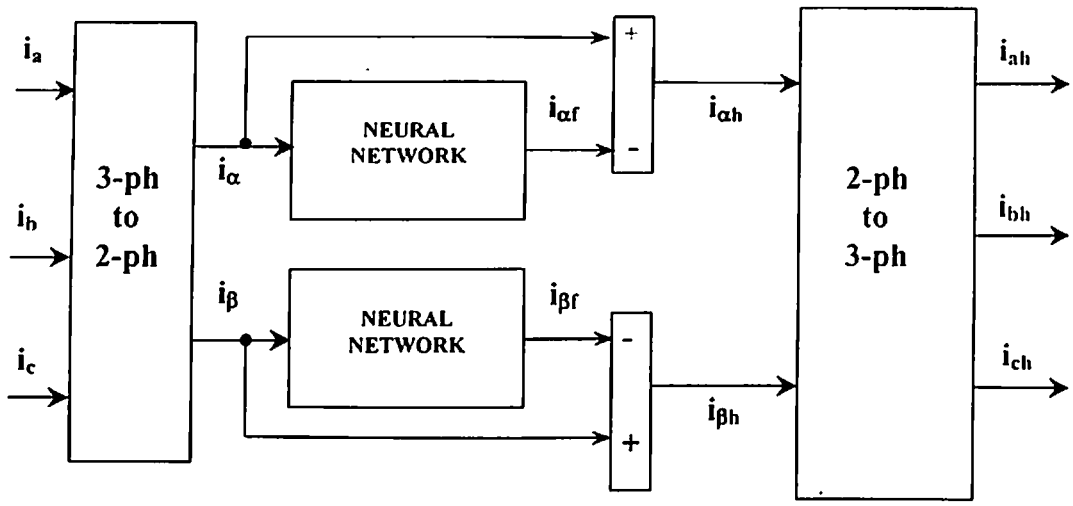

Fig. 3.6: Block diagram of NN based controller of HAPF

The three phase source currents i_a, i_b, and i_c are first transformed into two phase currents i_α and i_β using equation (3.1). The fundamental components of these two phases currents $i_{\alpha f}$ and $i_{\beta f}$ are extracted by proposed Adaptive Linear Neural Network (ADALINE). The two phase harmonic currents $i_{\alpha h}$ and $i_{\beta h}$ are then obtained by subtracting the extracted fundamental currents $i_{\alpha f}$ and $i_{\beta f}$ from the two phase source currents i_α and i_β, respectively. Finally these two phases harmonic components are transformed into three-phase system using equation (3.2). These three phase harmonic currents after being multiplied by a gain K_h are used in generation of switching signals for PWM inverter.

$$\begin{bmatrix} i_\alpha \\ i_\beta \end{bmatrix} = \sqrt{\frac{2}{3}} \begin{bmatrix} 1 & -\frac{1}{2} & -\frac{1}{2} \\ 0 & \frac{\sqrt{3}}{2} & -\frac{\sqrt{3}}{2} \end{bmatrix} \begin{bmatrix} i_a \\ i_b \\ i_c \end{bmatrix} \qquad (3.1)$$

$$\begin{bmatrix} i_{ah} \\ i_{bh} \\ i_{ch} \end{bmatrix} = \sqrt{\frac{2}{3}} \begin{bmatrix} 1 & 0 \\ -\frac{1}{2} & \frac{\sqrt{3}}{2} \\ -\frac{1}{2} & -\frac{\sqrt{3}}{2} \end{bmatrix} \begin{bmatrix} i_{\alpha h} \\ i_{\beta h} \end{bmatrix} \qquad (3.2)$$

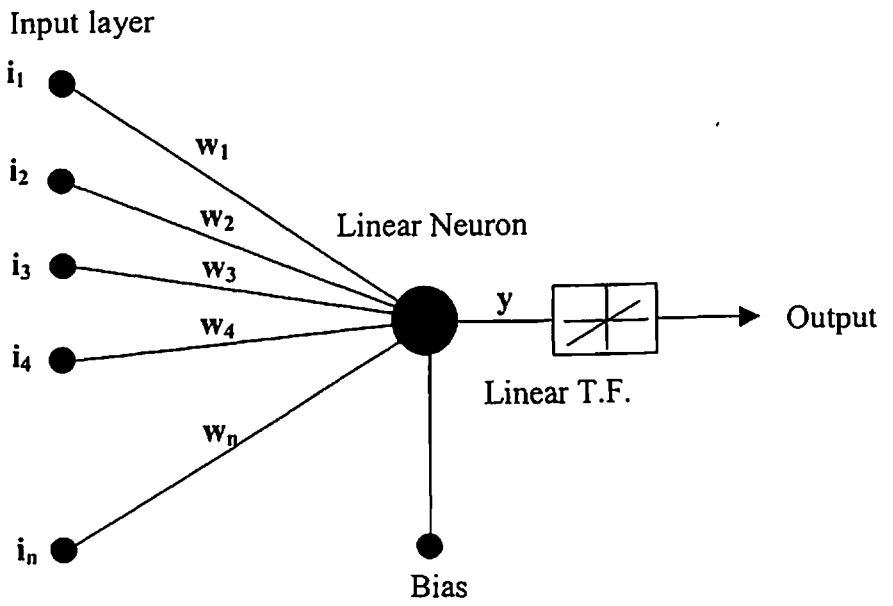

Fig. 3.7 Internal blocks of proposed Neural Network

Fig. 3.7 shows the architecture of proposed ADALINE Neural Network. It is a two layers (input and output) network having n-inputs and a single output. The basic blocks of this network are input signal delay vector, a purelin transfer function, weight matrix and bias. The input output relationship is expressed as:

$$y = \sum_{n=1}^{61} w_n . i_n + b \qquad (3.3)$$

where 'b' is bias, 'w' is weight, and 'i' is the input to the neural network. This output 'y' is fed to the purelin transfer function, whose input output relationship is shown in Fig. 3.8.

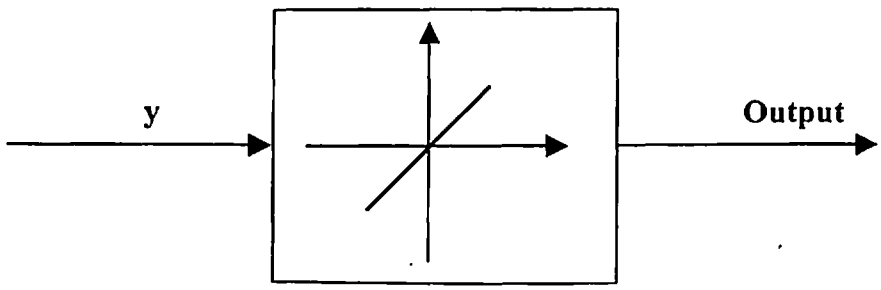

Fig. 3.8. Input/Output relationship of purlin transfer function

The input to the network is a time-delayed series of the signal whose fundamental component is to be extracted. The length of this delay series is 61, which has been decided considering expected maximum distortion and unbalance in 3-phase input signal. Fig. 3.9 shows the internal structure of delay block. The proposed neural network receives 61 samples of input signal at a time and produce single output. The input is sampled at 6KHz i.e. 120 samples per fundamental cycle of voltage. Target data (alpha and beta axis fundamental current) required for training the proposed neural network was generated using current decomposition technique as presented in [111]. The weight adjustment is performed during the training process of the neural network (ADALINE) using Widrow-Hoff delta rule. The Table 3.1 shows the weight values associated with each input. The mean square error between desired output and the actual output was reduced to 3.2×10^{-5} by repetitive training with the learning rate of 0.0006.

The training has also done with many other values of learning rates and with different number of delays but the results was not satisfactory.

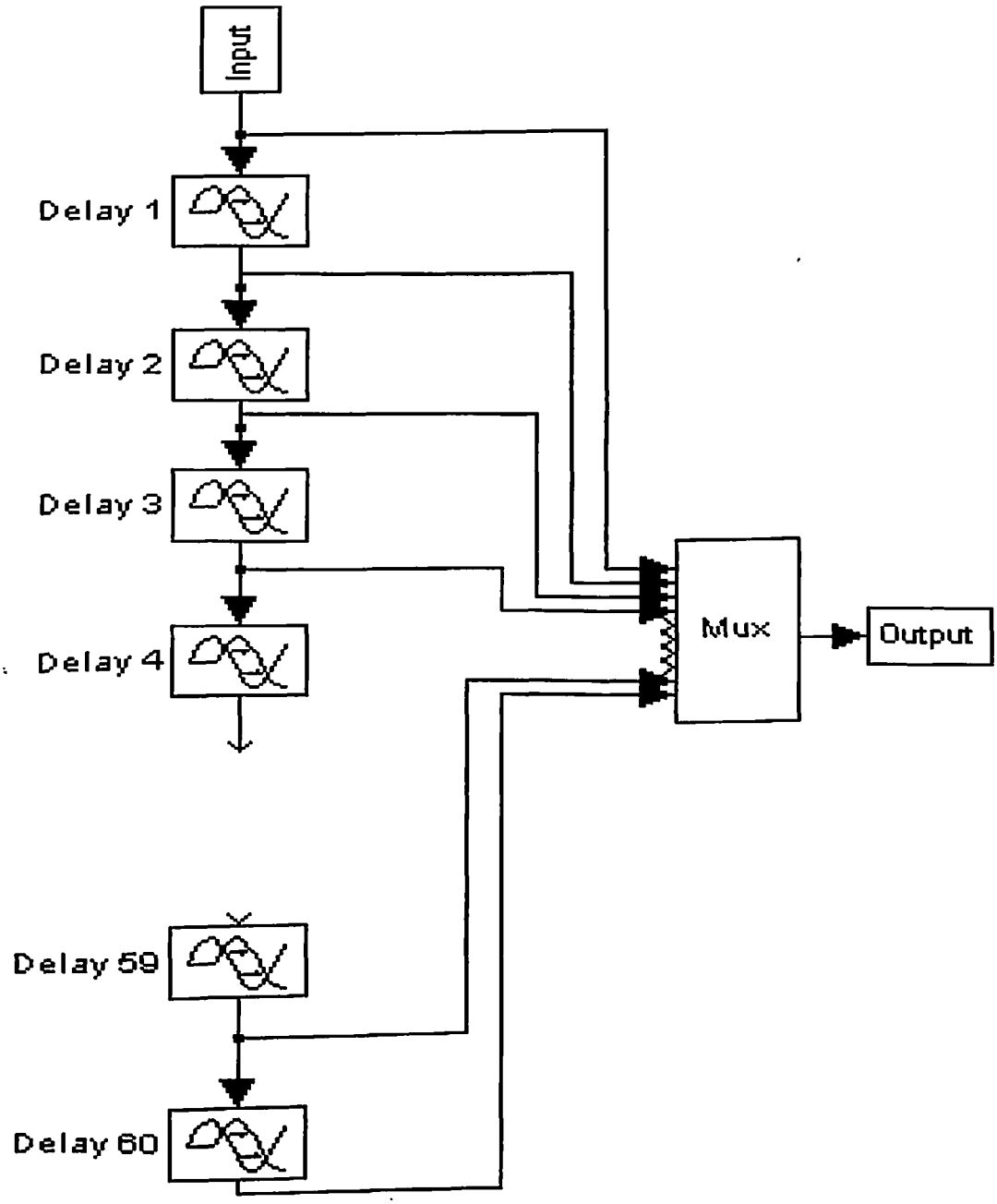

Fig. 3.9. Internal structure of Delays block

Table 3.1: Weights of Trained NN Neurons

W_0	-0.01540	W_{21}	0.02678	W_{42}	-0.03000
W_1	0.01883	W_{22}	0.02437	W_{43}	-0.02812
W_2	0.02403	W_{23}	0.01815	W_{44}	-0.02701
W_3	0.02587	W_{24}	0.01522	W_{45}	-0.02714
W_4	0.02846	W_{25}	0.01165	W_{46}	-0.02717
W_5	0.02928	W_{26}	0.00942	W_{47}	-0.02795
W_6	0.02981	W_{27}	0.00690	W_{48}	-0.02895
W_7	0.02966	W_{28}	0.00515	W_{49}	-0.02837
W_8	0.02985	W_{29}	0.00269	W_{50}	-0.02995
W_9	0.02771	W_{30}	0.00114	W_{51}	-0.02992
W_{10}	0.02866	W_{31}	-0.00163	W_{52}	-0.03042
W_{11}	0.02686	W_{32}	-0.00342	W_{53}	-0.03090
W_{12}	0.02661	W_{33}	-0.00578	W_{54}	-0.03126
W_{13}	0.02552	W_{34}	-0.00780	W_{55}	-0.03162
W_{14}	0.02453	W_{35}	-0.00956	W_{56}	-0.03205
W_{15}	0.02368	W_{36}	-0.01183	W_{57}	-0.03106
W_{16}	0.02239	W_{37}	-0.01331	W_{58}	-0.03116
W_{17}	0.02208	W_{38}	-0.01702	W_{59}	-0.03191
W_{18}	0.02197	W_{39}	-0.01359	W_{60}	-0.05794
W_{19}	0.01654	W_{40}	-0.01105		
W_{20}	0.01006	W_{41}	-0.03093		

3.4.2 Three Phase Four Wire System

Fig. 3.10 shows the block diagram of Neural Network controller applicable for three-phase, four-wire system. In this system the three-phase source currents i_a, i_b, and i_c are first transformed into two phase currents (α-β-o Orthogonal coordinates) i_α, i_β and i_o using equation (3.4). The fundamental components of these two-phase currents $i_{\alpha f}$, $i_{\beta f}$ and i_o are extracted by proposed neural network (ADALINE). The two phase harmonic currents $i_{\alpha h}$, $i_{\beta h}$ and i_{oh} are then obtained by subtracting the extracted fundamental currents $i_{\alpha f}$, $i_{\beta f}$ and i_{of} from the two phase source currents i_α, i_β, and i_o respectively.

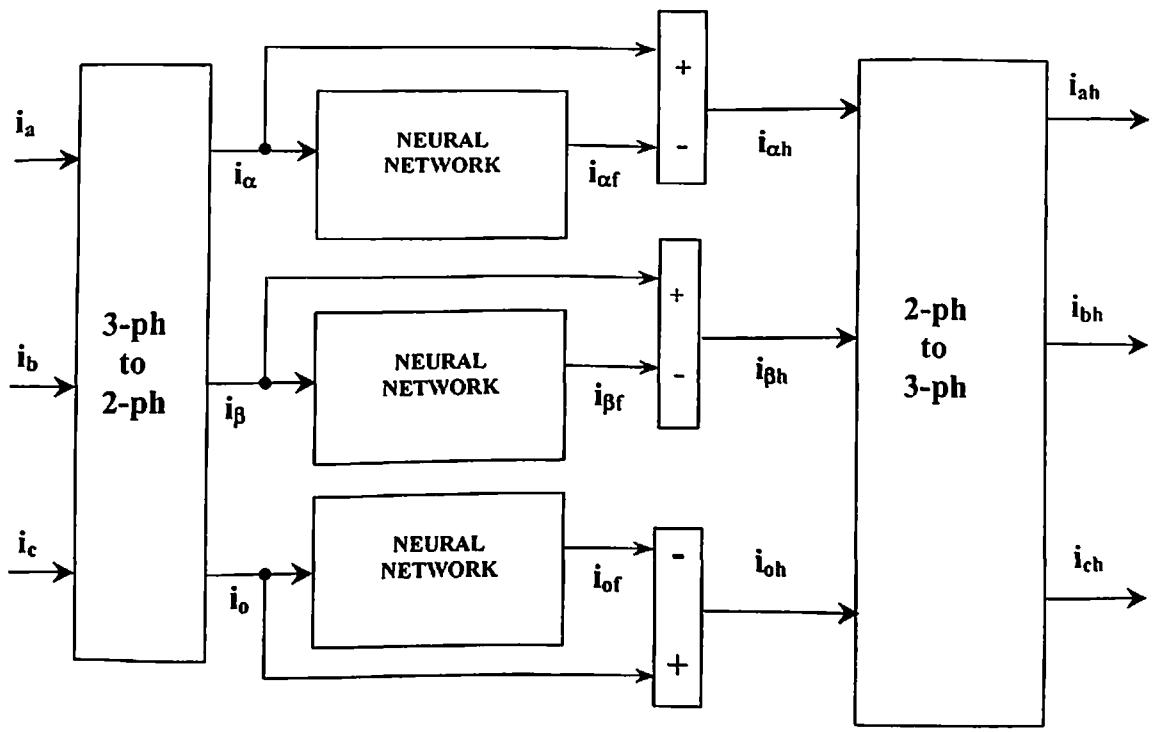

Fig. 3.10: Block diagram of NN based controller of HAPF

Finally these two phases harmonic components are transformed into three-phase system using equation (3.5). These three phase harmonic currents after being multiplied by a gain K_h are used in generation of switching signals for PWM inverter.

$$\begin{bmatrix} i_\alpha \\ i_\beta \\ i_o \end{bmatrix} = \sqrt{\frac{2}{3}} \begin{bmatrix} 1 & -1/2 & -1/2 \\ 0 & \sqrt{3}/2 & -\sqrt{3}/2 \\ 1/\sqrt{2} & 1/\sqrt{2} & 1/\sqrt{2} \end{bmatrix} \begin{bmatrix} i_a \\ i_b \\ i_c \end{bmatrix} \tag{3.4}$$

$$\begin{bmatrix} i_{ah} \\ i_{bh} \\ i_{ch} \end{bmatrix} = \sqrt{\frac{2}{3}} \begin{bmatrix} 1/\sqrt{2} & 1 & 0 \\ 1/\sqrt{2} & -1/2 & \sqrt{3}/2 \\ 1/\sqrt{2} & -1/2 & -\sqrt{3}/2 \end{bmatrix} \begin{bmatrix} i_{\alpha h} \\ i_{\beta h} \\ i_{oh} \end{bmatrix} \tag{3.5}$$

3.5 GATING SIGNAL GENERATOR (PWM)

To track the voltage command V^*_c, a triangular voltage comparator is used to generate a proper PWM waveform to trigger the power switches of converter. The gating signals are generated from the intersection of a triangular waveform superimposed on the reference wave. Then the converter can generate the desired voltage $V_c^*(t)$.

3.6 SUMMARY

The neural network control algorithm for the extraction of fundamental current for three-phase non-sinusoidal current waveforms has been presented in this chapter. The training details of the proposed neural network have also been

reported in this chapter. The simulation results of the proposed neural network controller will be presented in the next chapter. In next chapter the proposed controller has implemented on real time using DSP to verify the simulated results.

CHAPTER 4

NEURAL NETWORK CONTROLLER RESULTS AND ANALYSIS

4.1 INTRODUCTION

In previous Chapter the algorithm and training details for the adaptive liner neural network has been covered. This Chapter deals with the verification of the theory of the proposed Adaptive Neural Network control scheme for the Hybrid Active Power Filter, modeled in the previous Chapter, by means of simulation carried out using MATLAB/SIMULINK 6.1 for three-phase three-wire and three-phase four-wire systems under various load and supply conditions. The proposed Neural Network algorithm has also been implemented in real time using Digital Signal Processor (DSP).

4.2 SIMULATION RESULTS

In this section the simulation results of neural network controller have presented for three-phase three-wire and three-phase four-wire systems under various nonlinear/unbalance load and source conditions. The dynamic performance of the controller has also been investigated.

4.2.1 Three Phase Three Wire System

Simulation results under different operating conditions of three-phase three-wire system have been presented in this section.

4.2.1.1 Steady state performance with balanced load

The NN controller was first simulated in steady state condition with balanced non-linear load (3-phase full bridge diode rectifier followed by load) and sinusoidal & balanced AC voltage source (with source inductance 0.5mH and resistance 0.3Ω) set at 240Vrms (phase voltage) at 50 Hz. The waveforms of Fig. 4.1 show the performance of neural network controller when a resistive load of 100Ω is connected to the rectifier. In Fig. 4.2 resistive load of 100Ω is connected to the rectifier with a capacitor filter of 500μF. The waveforms (a), (b), (c) and (d) of Fig. 4.1 and Fig. 4.2 show the 3-phase source current (i_a, i_b and i_c), transformed 2–phase currents (i_α and i_β), extracted 2-phase fundamental currents ($i_{\alpha f}$ and $i_{\beta f}$) and three-phase harmonic currents (i_{ah}, i_{bh} and i_{ch}) respectively. The values of source current harmonics and extracted harmonic components, measured using Fast Fourier Transform (FFT) function of the waveforms are given in Table 4.1 and 4.2 for resistive and RC loads respectively.

Table 4.1: Comparison of Measured values of Source Current Harmonics and Extracted Source Current Harmonics for Balanced Resistive Load

Harmonic Order	Source Currents			Extracted Harmonic Components		
	i_a (rms)	i_b (rms)	i_c (rms)	i_{ah} (rms)	i_{bh} (rms)	i_{ch} (rms)
1st (Amp)	4.366	4.355	4.377	----	----	----
5th (Amp)	0.989	0.995	1.02	0.980	0.991	0.995
7th (Amp)	0.495	0.492	0.485	0.492	0.491	0.482
11th (Amp)	0.389	0.390	0.388	0.390	0.390	0.385
13th (Amp)	0.268	0.261	0.265	0.266	0.260	0.264
17th (Amp)	0.233	0.240	0.231	0.231	0.240	0.230
19th (Amp)	0.169	0.171	0.170	0.170	0.169	0.170
23th (Amp)	0.155	0.157	0.152	0.153	0.155	0.152
25th (Amp)	0.134	0.132	0.127	0.132	0.132	0.127

Table 4.2: Comparison of Measured values of Source Current Harmonics and Extracted Source Current Harmonics for Balanced RC Load

Harmonic Order	Source Currents			Extracted Harmonic Components		
	i_a (rms)	i_b (rms)	i_c (rms)	i_{ah} (rms)	i_{bh} (rms)	i_{ch} (rms)
1st (Amp)	4.6	4.6	4.62	----	----	----
5th (Amp)	3.667	3.71	3.53	3.7	3.68	3.52
7th (Amp)	2.91	2.82	2.83	2.915	2.80	2.80
11th (Amp)	1.27	1.414	1.273	1.265	1.405	1.271
13th (Amp)	0.671	0.707	0.671	0.670	0.707	0.668
17th (Amp)	0.281	0.282	0.285	0.280	0.280	0.287
19th (Amp)	0.261	0.263	0.265	0.260	0.263	0.262
23th (Amp)	0.162	0.164	0.148	0.162	0.164	0.148
25th (Amp)	0.142	0.146	0.139	0.142	0.144	0.140

A visual comparison of the extracted values of harmonics using neural networks reveals that their magnitudes are same as that of source current harmonics. From the waveforms of Fig. 4.1 and Fig. 4.2 it is also clear that the proposed neural network controller is performing accurate under steady state condition with nonlinear loads.

4.2.1.2 Dynamic performance with sudden increase in load

Fig. 4.3 demonstrates the performance of the neural network controller under step change in loading condition. In Fig. 4.3, initially a three phases bridge diode rectifier with resistance load (100Ω) is connected to source. Suddenly at time t = 0.08 Sec., the load is increased by 100%. From the waveforms shown in Fig. 4.3(a), (b), (c) and (d) it is clear that the proposed neural network extract the fundamental components from highly distorted waveform under transient (sudden change in load) state. The values of source current harmonics and extracted

harmonic components, measured using Fast Fourier Transform (FFT) function of the waveforms in steady state are given in Table 4.3

Table 4.3: Comparison of Measured values of Source Current Harmonics and Extracted Source Current Harmonics

Harmonic Order	Source Currents			Extracted Harmonic Components		
	i_a (rms)	i_b (rms)	i_c (rms)	i_{ah} (rms)	i_{bh} (rms)	i_{ch} (rms)
1st (Amp)	8.73	8.715	8.754	----	----	----
5th (Amp)	1.978	2.00	2.044	1.974	2.00	1.994
7th (mA)	990	984	970	986	981	974
11th (mA)	780	782	776	780	780	781
13th (mA)	536	522	530	532	524	527
17th (mA)	465	480	463	463	240	460
19th (mA)	340	343	340	343	340	340
23th (mA)	310	313	305	306	309	303
25th (mA)	266	264	254	264	256	254

4.2.1.3 Dynamic Performance with sudden load unbalancing

In Fig. 4.4, at = 0 sec., a three phase bridge rectifier followed by a 100Ω resistance is connected to the source, now at t = 0.08 Sec, an additional single-phase rectifier with resistive load. This sudden insertion of 1-ph rectifier makes the source currents highly distorted and unbalanced. From the waveforms in Fig. 4.4, it is clear that the proposed NN controller is responding fast and accurate to the sudden unbalance in the load in an adaptive way. The comparison of extracted harmonics and source current harmonics (Table 4.4) clearly demonstrates the effectiveness of the proposed NN algorithm under severe unbalanced load condition.

Table 4.4: Comparison of Measured values of Source Current Harmonics and Extracted Source Current Harmonics with Sudden Load Unbalancing

Harmonic Order	Source Currents			Extracted Harmonic Components		
	i_a (rms)	i_b (rms)	i_c (rms)	i_{ah} (rms)	i_{bh} (rms)	i_{ch} (rms)
1st (Amp)	8.202	4.384	8.205	-----	-----	-----
5th (Amp)	0.99	0.975	1.02	0.95	0.975	0.985
7th (mA)	473	487	477	470	482	474
11th (mA)	403	389	400	399	384	399
13th (mA)	290	265	284	290	266	279
17th (mA)	230	231	234	231	231	231
19th (mA)	190	169	193	188	166	191
23th (mA)	159	141	156	157	137	153
25th (mA)	100	86	98	98	84	96.5

4.2.1.4 Performance under unbalance source voltage condition

In Fig. 4.5 the performance of the proposed neural network controller is given under unbalance supply voltage with balanced resistive load of 100Ω is connected to the rectifier. In this case the unbalance supply voltages are 240, 200, and 160Vrms for phases a, b, and c respectively. The waveforms of Fig. 4.5 show that the controller harmonic extraction is independent of source voltage condition. From the comparison of extracted values of harmonics and source harmonic components (Table 4.5) it is clear that the proposed NN algorithm performs accurately under unbalance source condition.

4.2.1.5 Performance under distorted source voltage condition

In Fig 4.6, the source voltage is balanced but contaminated with some harmonics. The source voltage contains 3rd and 5th harmonic of 7% and 5% respectively. The waveforms given in Fig. 4.6 show the performance of neural

network controller is quite satisfactory if the supply source is polluted with harmonics. The comparison of extracted harmonics and source current harmonics (Table 4.6) also demonstrates the effectiveness of the proposed NN algorithm with distorted supply.

Table 4.5: Comparison of Measured values of Source Current Harmonics and Extracted Source Current Harmonics under Unbalanced Source Condition

Harmonic Order	Source Currents			Extracted Harmonic Components		
	i_a (rms)	i_b (rms)	i_c (rms)	i_{ah} (rms)	i_{bh} (rms)	i_{ch} (rms)
1st (Amp)	3.978	3.712	3.252	----	----	----
3rd (Amp)	0.706	0.636	0.523	0.704	0.633	0.520
5th (mA)	473	403	387	470	404	388
7th (mA)	307	267	242	304	268	242
11th (mA)	259	232	206	259	230	204
13th (mA)	172	167	139	173	167	139
17th (mA)	123	104	87	121	102	84
19th (mA)	90	78	59	90	76	56
23th (mA)	54	48	37	54	46	34

Table 4.6: Comparison of Measured values of Source Current Harmonics and Extracted Source Current Harmonics with Distorted Supply

Harmonic Order	Source Currents			Extracted Harmonic Components		
	i_a (rms)	i_b (rms)	i_c (rms)	I_{ah} (rms)	i_{bh} (rms)	i_{ch} (rms)
1st (Amp)	4.454	4.33	4.32	----	----	----
3rd (Amp)	0.813	0.802	0.803	0.810	0.798	0.802
5th (Amp)	0.601	0.596	0.599	0.600	0.597	0.600
7th (mA)	438	432	430	435	430	431
11th (mA)	247	244	244	248	240	240
13th (mA)	159	158	159	159	156	156
17th (mA)	70	73	72	70	72	72
19th (mA)	48	49	46	46	49	47
23th (mA)	27	29	27	27	29	29
25th (mA)	13	15.5	14	13	16	15

These results demonstrate that the proposed neural network controller can extract fundamental component from balanced, unbalanced & distorted signals. Further, it demonstrates excellent performance both in steady state as well as dynamic conditions.

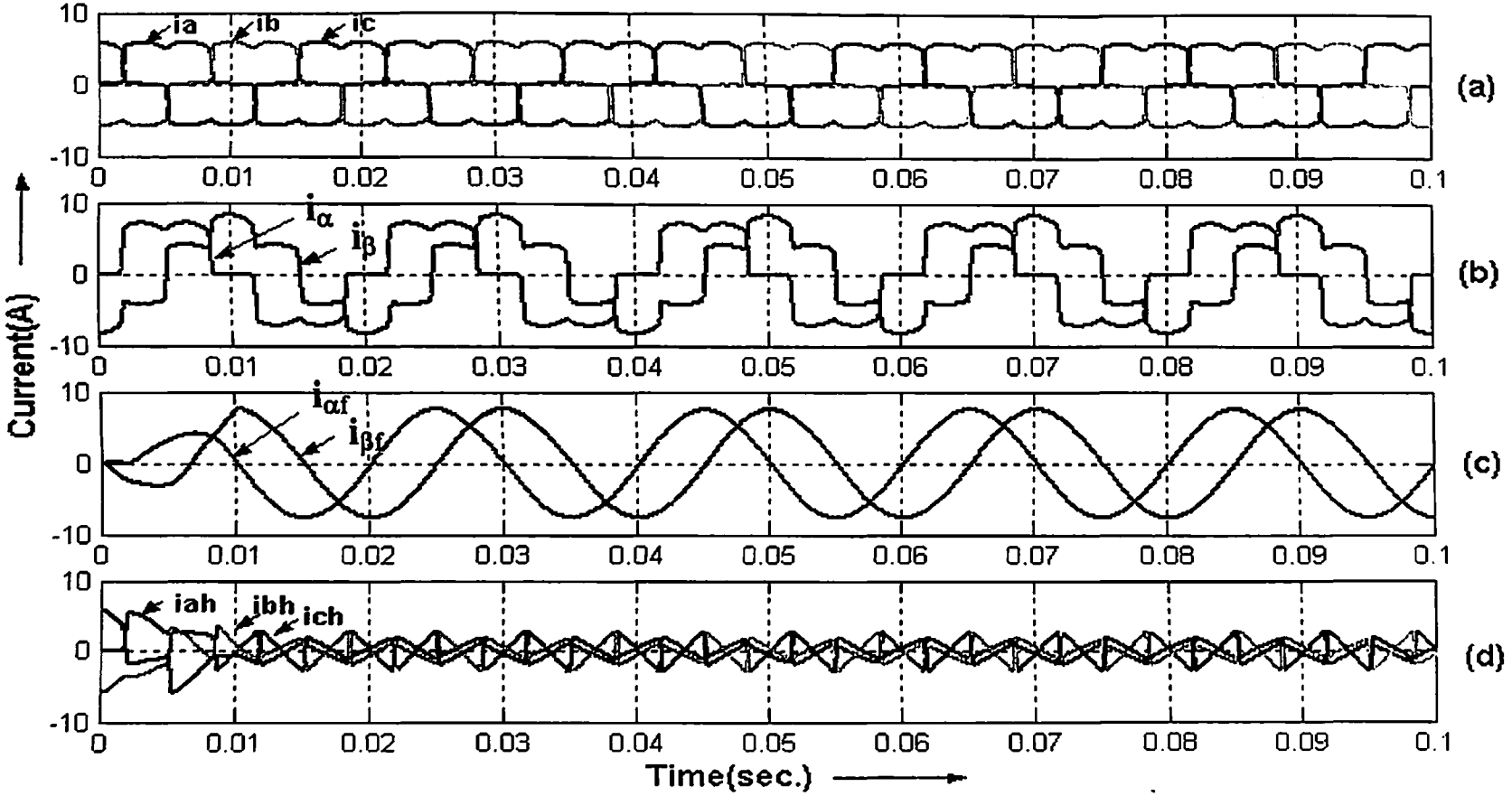

Fig.4.1 Performance of NN controller for (rectifier + resistive) load (a) 3-ph source currents (b) 2-ph transformed currents (c) extracted 2-ph fundamental currents (d) computed 3-ph harmonic currents

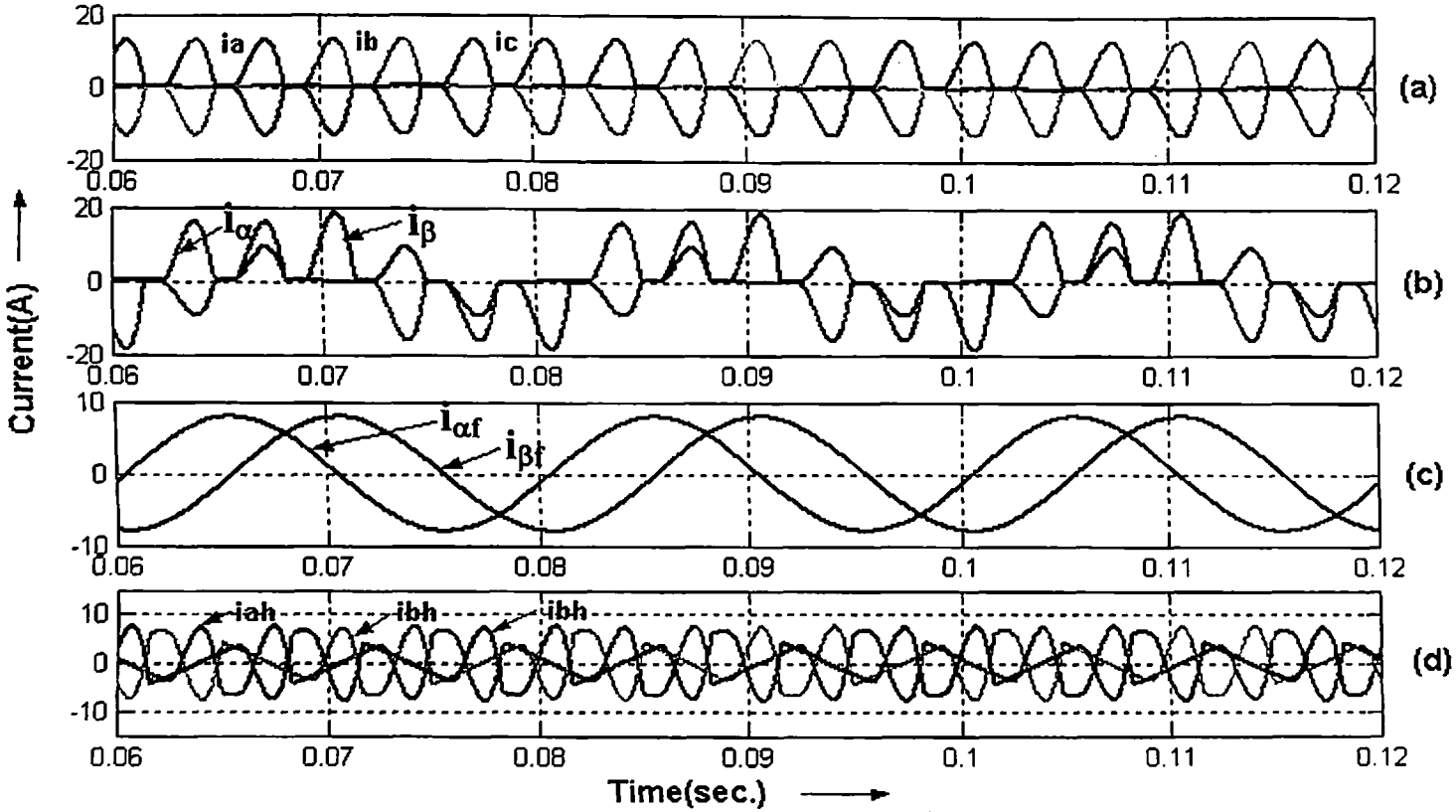

Fig. 4.2 Performance of NN controller for (rectifier + resistive) load with capacitor filter (a) 3-ph source currents (b) 2-ph transformed currents (c) extracted 2-ph fundamental currents (d) computed 3-ph harmonic currents

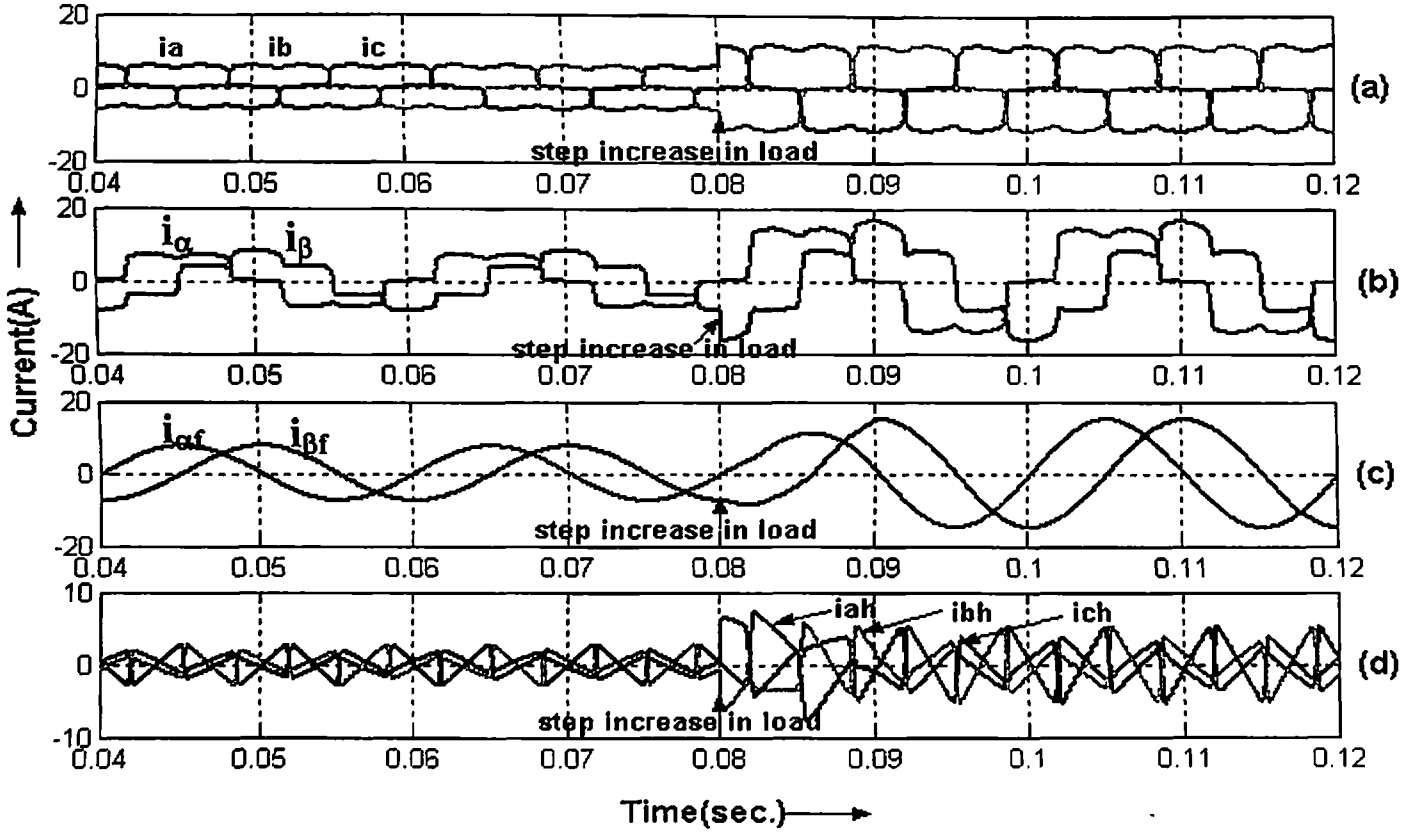

Fig.4.3 Dynamic performance of NN controller with 100% step increase in load (a) 3-ph source currents (b) 2-ph transformed currents (c) extracted 2-ph fundamental currents (d) computed 3-ph harmonic currents

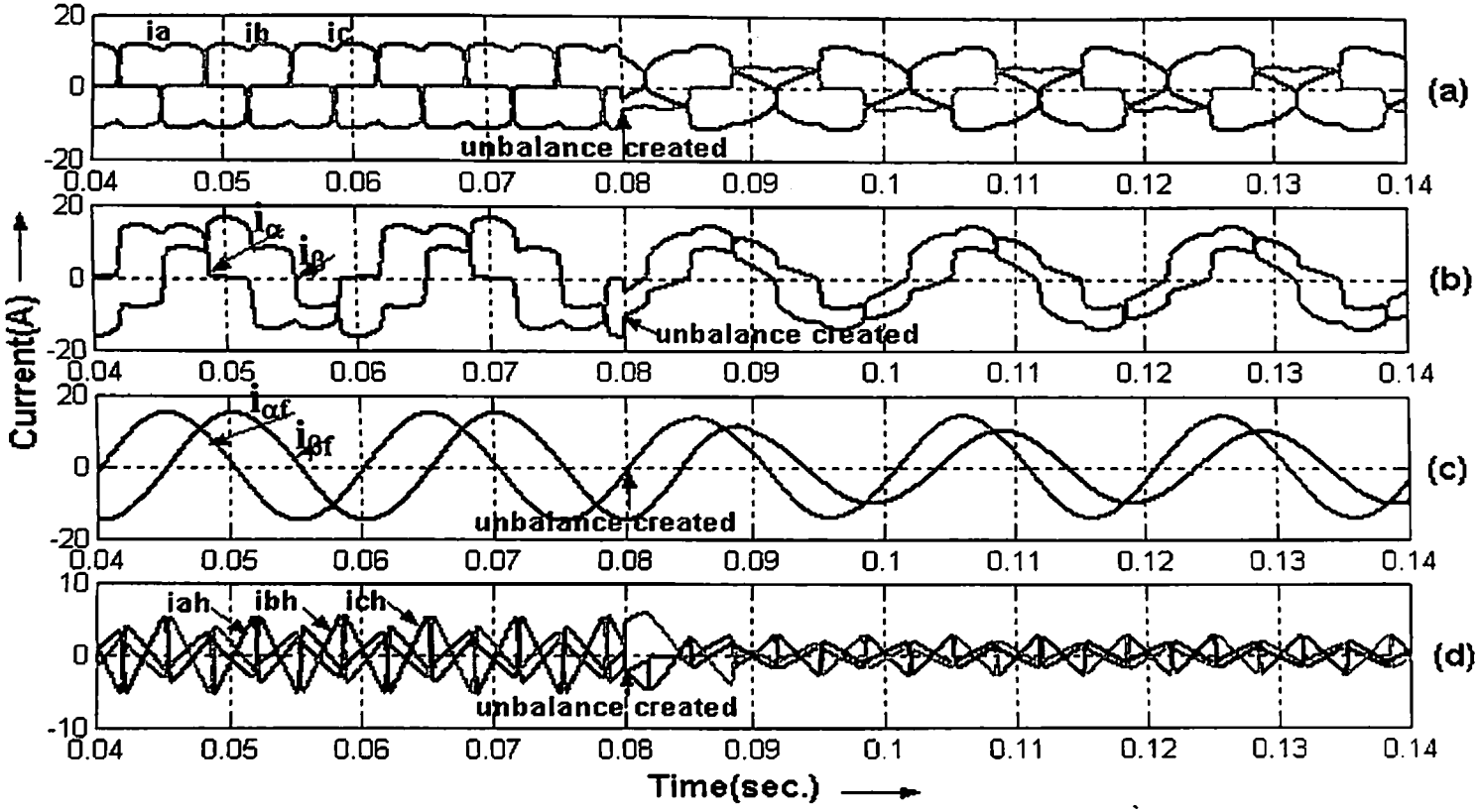

Fig .4.4 Dynamic performance of NN controller under Unbalanced condition (a) 3-ph source currents (b) 2-ph transformed currents (c) extracted 2-ph fundamental currents (d) computed 3-ph harmonic currents

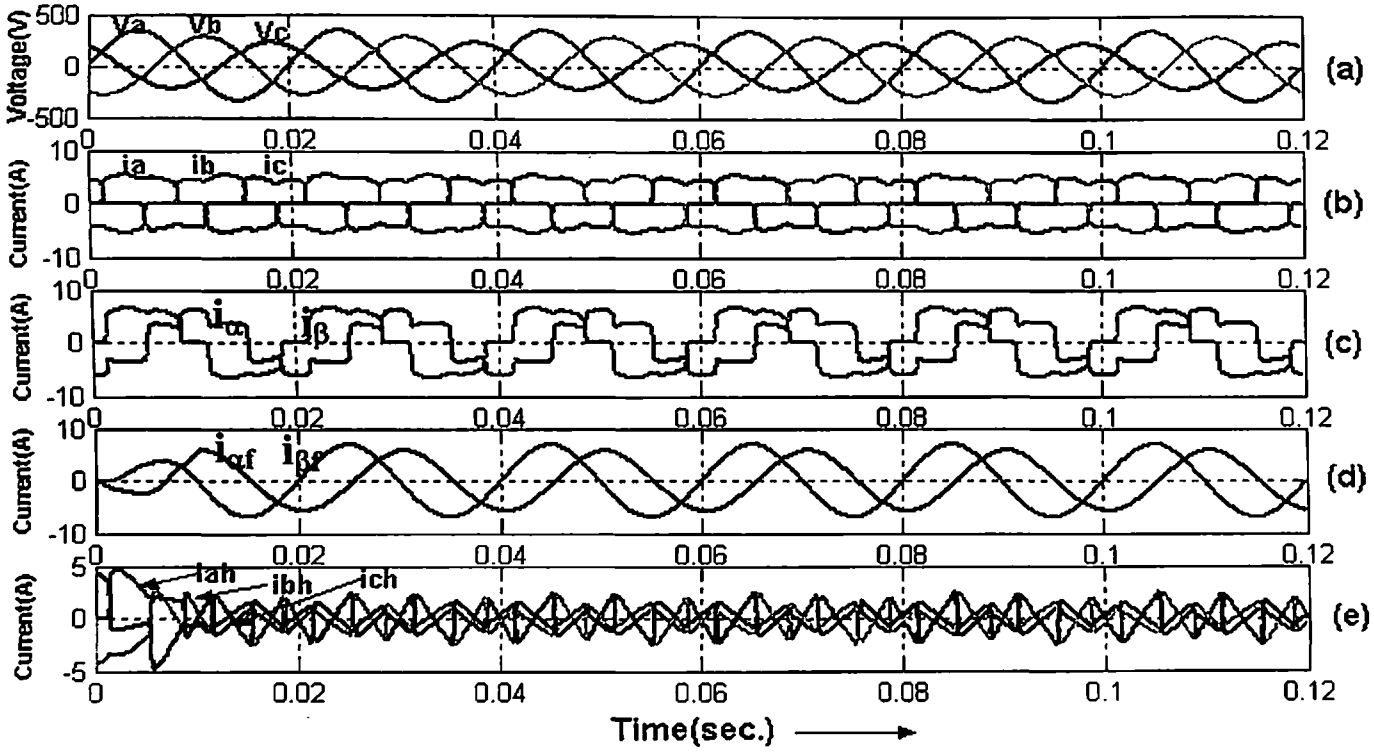

Fig 4.5 Performance of NN controller under unbalanced source voltages (a) 3-ph source voltages (b) 3-ph source currents (c) 2-ph transformed currents (d) extracted 2-ph fundamental currents (e) computed 3-ph harmonic currents

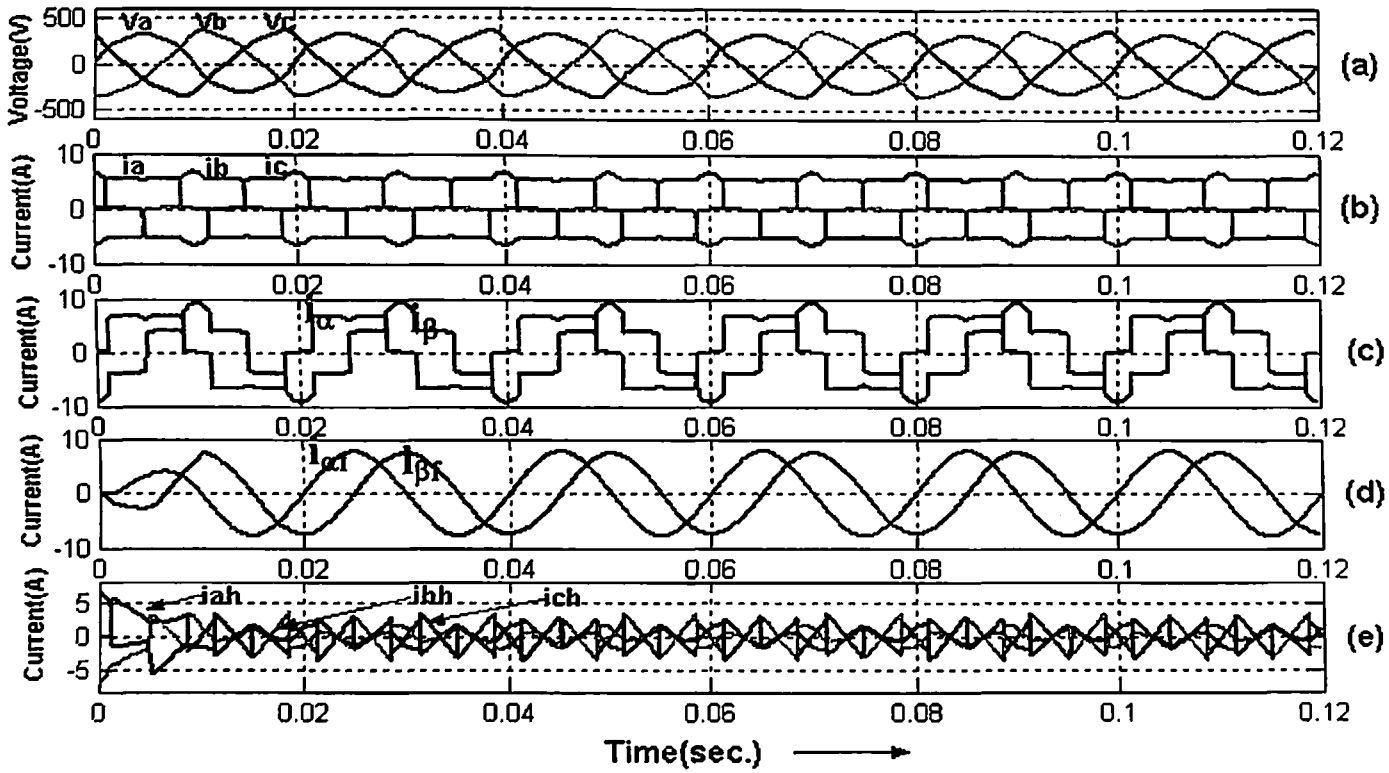

Fig. 4.6 Performance of NN controller under distorted source voltages (a) 3-ph source voltages (b) 3-ph source currents (c) 2-ph transformed currents (d) extracted 2-ph fundamental currents (e) computed 3-ph harmonic current

4.2.2 Three Phase Four Wire System

In this section the performance of neural network controller has also been tested for three-phase system with neutral i.e. three-phase four- wire system. The controller has tested under various loads and source conditions.

4.2.2.1 Steady state performance with balanced load

The neural network controller was first simulated with balanced non-linear load (three single phase full bridge diode rectifier with resistive load followed by capacitive filter) and sinusoidal & balanced source voltages (with source inductance 0.5mH and resistance 0.3Ω) set at 240Vrms (phase voltage) at 50 Hz. The waveforms (a), (b), (c) and (d) of Fig. 4.7 show the 3-phase source current (i_a, i_b and i_c), transformed 2–phase currents (i_α, i_β and i_o), extracted 2-phase fundamental currents ($i_{\alpha f}$, $i_{\beta f}$ and i_{of}) and three-phase harmonic currents (i_{ah}, i_{bh} and i_{ch}) respectively. The comparison table (Table 4.7) and waveforms of Fig. 4.7 demonstrate that the proposed controller performing well in steady state.

Table 4.7: Comparison of Measured values of Source Current Harmonics and Extracted Source Current Harmonics with Balanced RC load

Harmonic Order	Source Currents			Extracted Harmonic Components		
	$i_{a(rms)}$	$i_{b(rms)}$	$i_{c(rms)}$	$i_{ah(rms)}$	$i_{bh(rms)}$	$i_{ch(rms)}$
1st (Amp)	4.6	4.24	4.24	----	----	----
3rd (Amp)	4.24	3.90	3.92	4.236	3.91	3.90
5th (Amp)	3.53	3.36	3.35	3.526	3.36	3.35
7th (Amp)	2.82	2.65	2.65	2.808	2.65	2.65
11th (Amp)	1.27	1.167	1.163	1.262	1.163	1.166
13th (Amp)	0.622	0.566	0.568	0.627	0.562	0.563
17th (Amp)	0.256	0.247	0.245	0.252	0.245	0.245
19th (Amp)	0.176	0.195	0.196	0.173	0.193	0.193
23th(Amp)	0.141	0.141	0.143	0.142	0.141	0.142
25th (Amp)	0.074	0.071	0.0708	0.072	0.072	0.071

4.2.2.2 Steady state performance with unbalanced load

In Fig. 4.8, three single-phase bridge diode rectifiers with unbalanced resistance and capacitance (RC) load is connected to the source. The unbalanced loading is 80% and 60% in "b", and "c" phases respectively of "a" phase loading. In Fig. 4.7(c), the current i_{of} is zero, because in this case loading is balanced, while in Fig. 4.8 (c), where the unbalanced load is applied, the current i_{of} is a nonzero quantity. From the comparison of measured source harmonics and extracted harmonic given in Table 4.8 and the waveforms shown in Fig. 4.8, it is clear that the NN extracts instantaneous fundamental component embedded in the highly distorted waveforms ($i_{\alpha f}$, $i_{\beta f}$ and i_{of}) accurately under unbalance load conditions.

Table 4.8: Comparison of Measured values of Source Current Harmonics and Extracted Source Current Harmonics with Unbalanced RC load

Harmonic Order	Load Currents			Extracted Harmonic Components		
	i_a (rms)	i_b (rms)	i_c (rms)	i_{ah} (rms)	i_{bh} (rms)	i_{ch} (rms)
1st (Amp)	4.95	2.58	1.782	-------	-------	------
3rd (Amp)	4.42	2.386	1.572	4.422	2.380	1.574
5th (Amp)	3.53	2.121	1.396	3.527	2.120	1.396
7th (Amp)	2.19	1.60	1.202	2.188	1.602	1.202
11th (Amp)	0.318	0.636	0.707	0.318	0.635	0.707
13th (Amp)	0.238	0.283	0.460	0.236	0.283	0.460
17th (Amp)	0.176	0.162	0.099	0.179	0.160	0.099
19th (Amp)	0.120	0.134	0.0707	0.123	0.131	0.071
23th (Amp)	0.085	0.053	0.035	0.083	0.053	0.035
25th (Amp)	0.047	0.028	0.021	0.044	0.026	0.023

4.2.2.3 Dynamic performance with sudden increase in load

Fig. 4.9 demonstrates the dynamic performance of the proposed neural network controller under sudden increase in load. In Fig. 4.9, three single-phase bridge diode rectifiers with balance resistance and capacitance (RC) load is connected to the source, but suddenly at time t = 0.1 Sec., the load is stepping up by 100%. The comparison table (Table 4.9) and waveforms given in Fig. 4.9 clearly demonstrate the controller performance is satisfactory under dynamic condition.

Table 4.9: Comparison of Measured values of Source Current Harmonics and Extracted Source Current Harmonics with Sudden Stepping -up of Balanced RC load

Harmonic Order	Source Currents			Extracted Harmonic Components		
	i_a (rms)	i_b (rms)	i_c (rms)	i_{ah} (rms)	i_{bh} (rms)	i_{ch} (rms)
1st (Amp)	9.2	8.48	8.48	----	----	----
3rd (Amp)	8.48	7.8	7.808	8.482	7.8	7.803
5th (Amp)	7.04	6.72	6.717	7.041	6.717	6.714
7th (Amp)	5.64	5.3	5.295	5.644	5.302	5.293
11th (Amp)	2.54	2.334	2.332	2.538	2.332	2.330
13th (Amp)	1.244	1.132	1.132	1.242	1.131	1.134
17th (Amp)	0.512	0.494	0.494	0.510	0.492	0.492
19th (Amp)	0.352	0.39	0.394	0.351	0.39	0.394
23th(Amp)	0.280	0.282	0.280	0.280	0.280	0.295
25th (Amp)	0.152	0.143	0.142	0.151	0.141	0.143

4.2.2.4 Performance under unbalanced source voltage condition

In Fig. 4.10 the performance of the proposed neural network controller is given under unbalanced supply voltages. In Fig. 4.10 the supply voltages are 240, 200, and 160Vrms in Phase a, b, and c respectively. The waveforms given in Fig.

4.10 and comparison table of harmonics (Table 4.10) show that the controller is extracting fundamental current in adaptive way without affecting by supply voltage level condition.

Table 4.10: Comparison of Measured values of Source Current Harmonics and Extracted Source Current Harmonics with Unbalanced Supply

Harmonic Order	Load Currents			Extracted Harmonic Components		
	i_{La} (rms)	i_{Lb} (rms)	i_{Lc} (rms)	i_{ha} (rms)	i_{hb} (rms)	i_{hc} (rms)
1st (Amp)	4.6	3.818	3.11	-------	--------	-------
3rd (Amp)	4.14	3.43	2.83	4.14	3.432	2.826
5th (Amp)	3.53	2.728	2.475	3.528	2.722	2.475
7th (Amp)	2.828	2.321	1.944	2.824	2.320	1.943
11th (Amp)	1.273	1.06	0.848	1.271	1.065	0.843
13th (Amp)	0.60	0.53	0.424	0.606	0.532	0.422
17th (Amp)	0.269	0.24	0.226	0.266	0.237	0.226
19th (Amp)	0.176	0.142	0.133	0.173	0.142	0.132
23th(Amp)	0.141	0.116	0.089	0.141	0.113	0.083
25th (Amp)	0.081	0.068	0.049	0.074	0.066	0.043

4.2.2.5 Performance under distorted source voltage condition

In Fig 4.11, the source voltage is not a pure sinusoidal, it contains 3rd and 5th harmonic of 7% and 5% respectively. The comparison of extracted harmonics and source current harmonics (Table 4.11) and waveforms of Fig.4.11 clearly demonstrates the effectiveness of the proposed NN algorithm under severe distorted source condition.

Table 4.11: Comparison of Measured values of Source Current Harmonics and Extracted Source Current Harmonics with Distorted Supply

Harmonic Order	Load Currents			Extracted Harmonic Components		
	i_{La} (rms)	i_{Lb} (rms)	i_{Lc} (rms)	i_{ha} (rms)	i_{hb} (rms)	i_{hc} (rms)
1st (Amp)	4.505	4.95	4.952	-------	--------	-------
3rd (Amp)	4.107	4.594	4.592	4.104	4.591	4.597
5th (Amp)	3.670	4.14	4.14	3.670	4.142	4.144
7th (Amp)	2.97	3.43	3.43	2.966	3.426	3.431
11th (Amp)	1.46	2.12	2.12	1.457	2.122	2.122
13th (Amp)	0.848	1.41	1.41	0.846	1.411	1.413
17th (Amp)	0.212	0.353	0.352	0.212	0.352	0.352
19th (Amp)	0.176	0.268	0.269	0.174	0.264	0.266
23th (Amp)	0.123	0.194	0.197	0.121	0.192	0.197
25th (Amp)	0.073	0.106	0.103	0.073	0.104	0.106

From the waveforms in Fig. 4.7-4.11, and comparison tables of FFT of source current harmonics and extracted harmonics, it is clear that the proposed neural network controller is responding fast and accurate in steady state, dynamic loading and unbalance & non-sinusoidal source voltages in an adaptive way

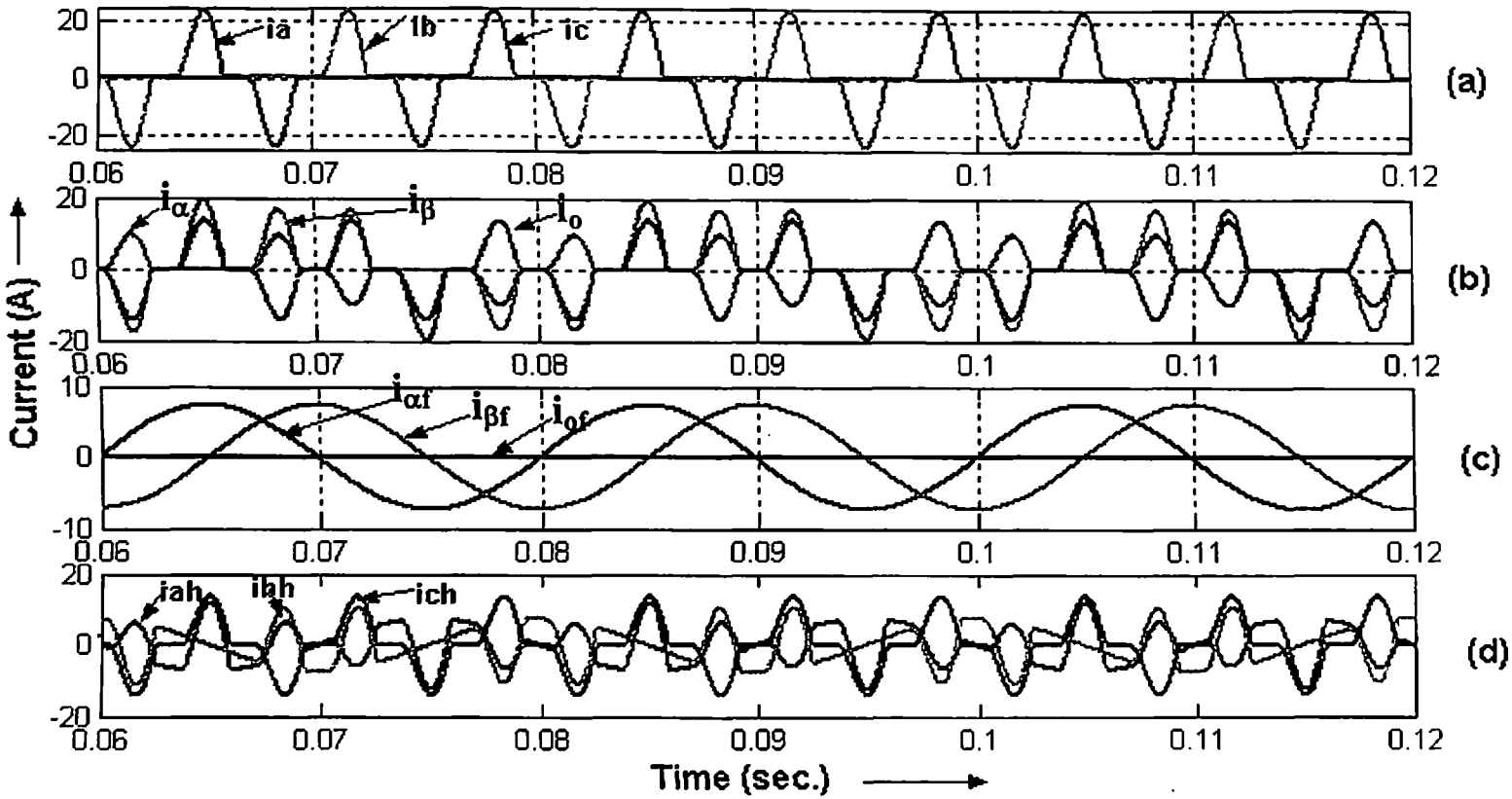

Fig. 4.7 Steady state performance with balanced load (a) 3-ph source currents (b) 2-ph transformed currents (c) extracted 2-ph fundamental currents (d) computed 3-ph harmonic currents

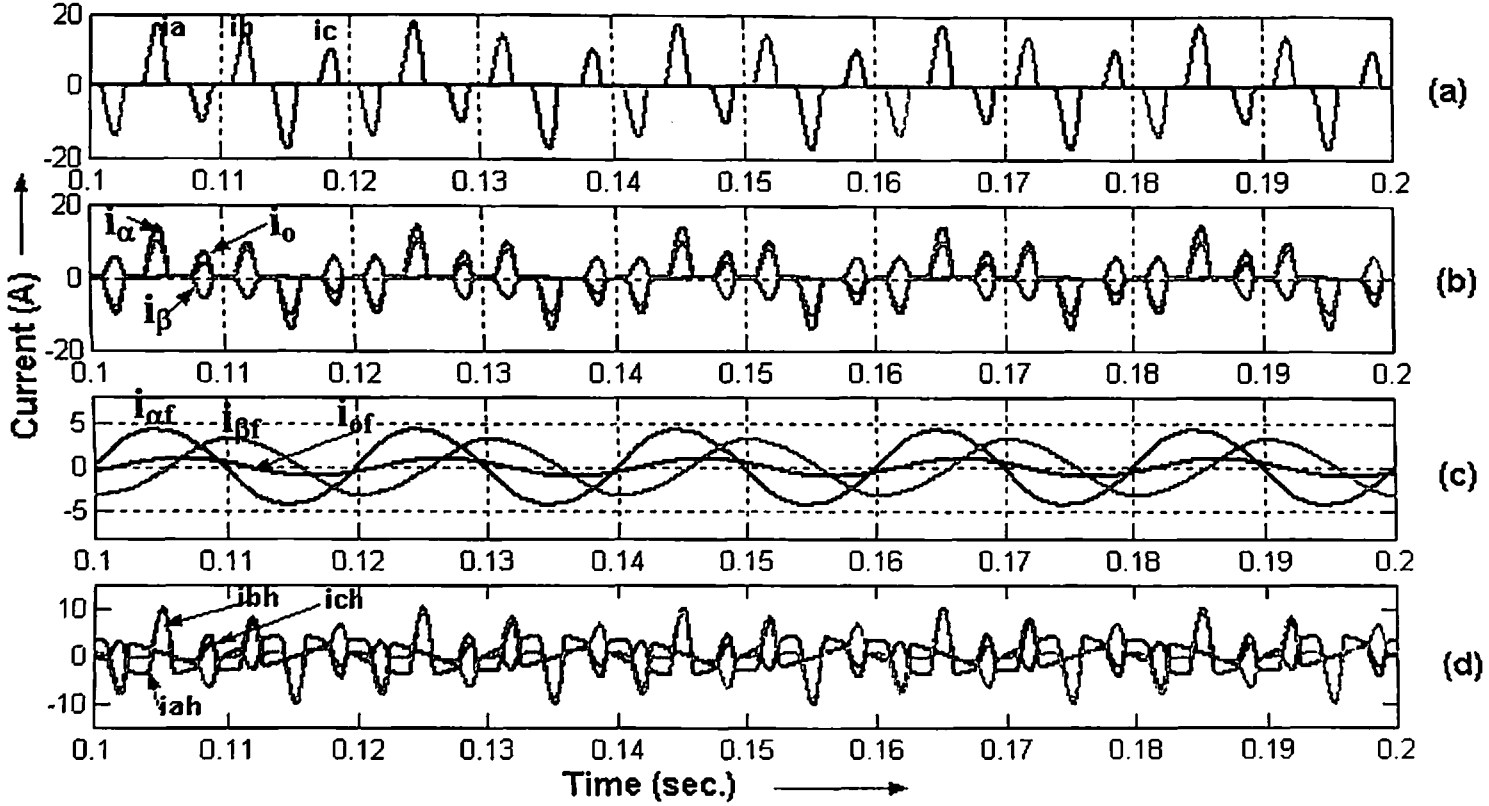

Fig. 4.8 Steady state performance with unbalanced load (a) 3-ph source currents (b) 2-ph transformed currents (c) extracted 2-ph fundamental currents (d) computed 3-ph harmonic currents

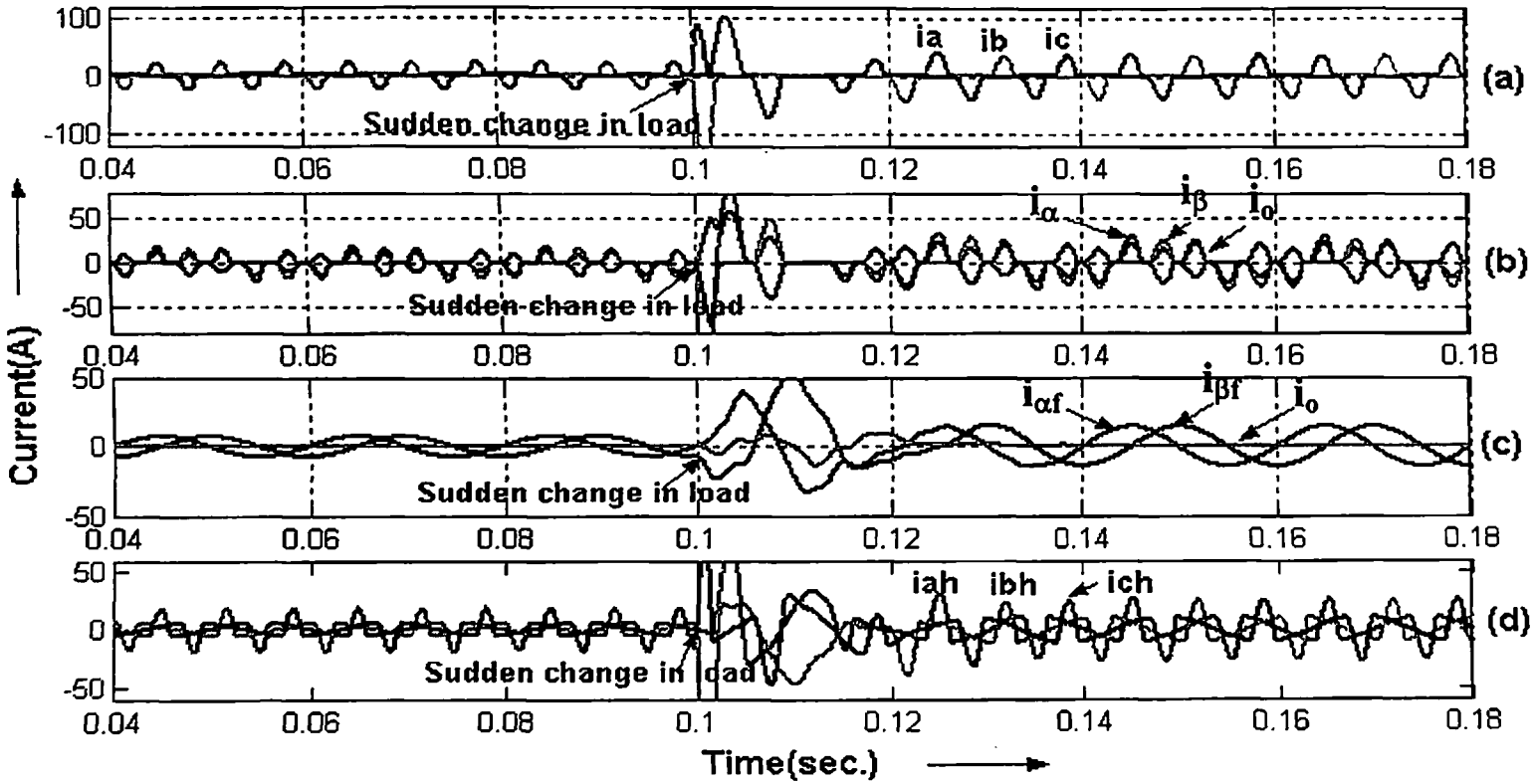

Fig. 4.9 Dynamic performance of NN controller under sudden stepping-up in load by 100% (a) 3-ph source currents (b) 2-ph transformed currents(c) extracted 2-ph fundamental currents (d) computed 3-ph harmonic currents

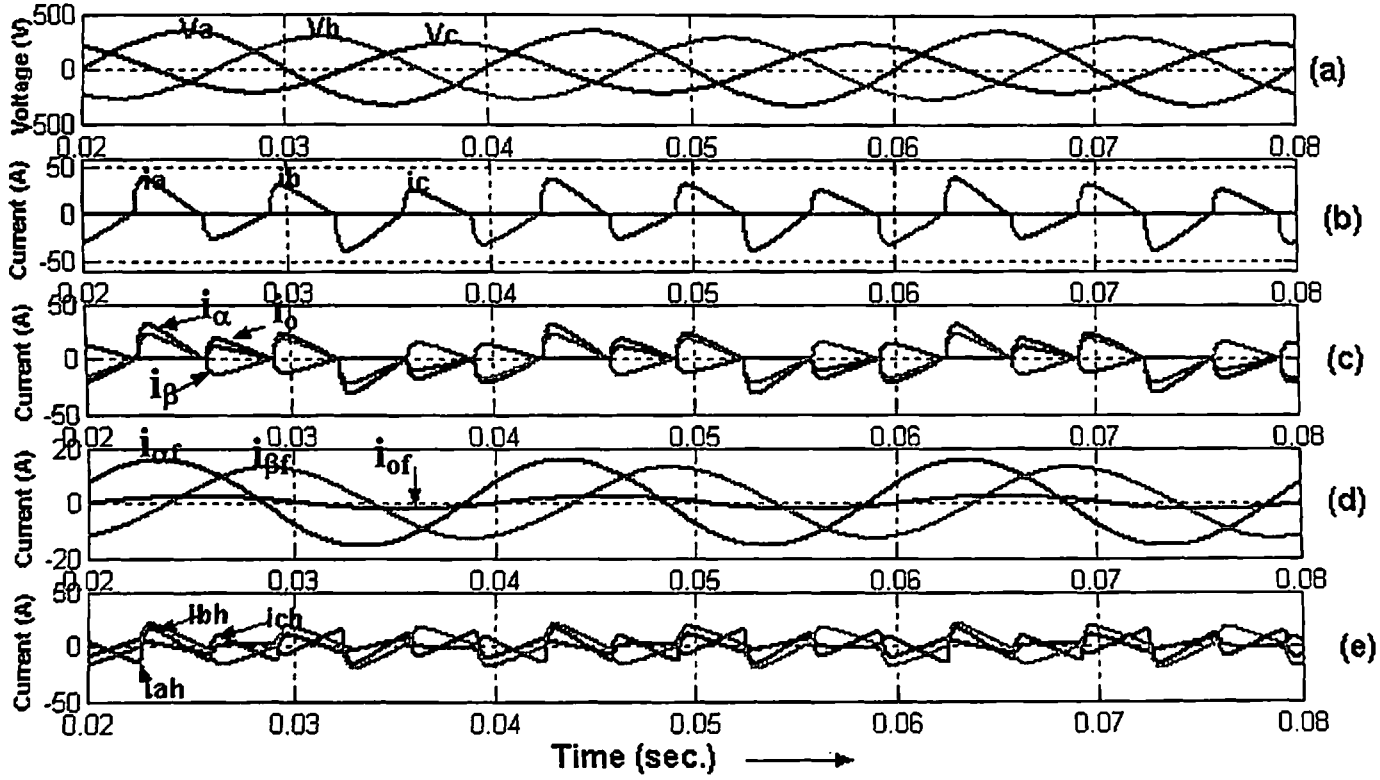

Fig. 4.10 Performance of NN controller under unbalanced source voltages (a) 3-ph source voltages (b) 3-ph source currents (c) 2-ph transformed currents (d) extracted 2-ph fundamental currents (e) computed 3-ph harmonic currents

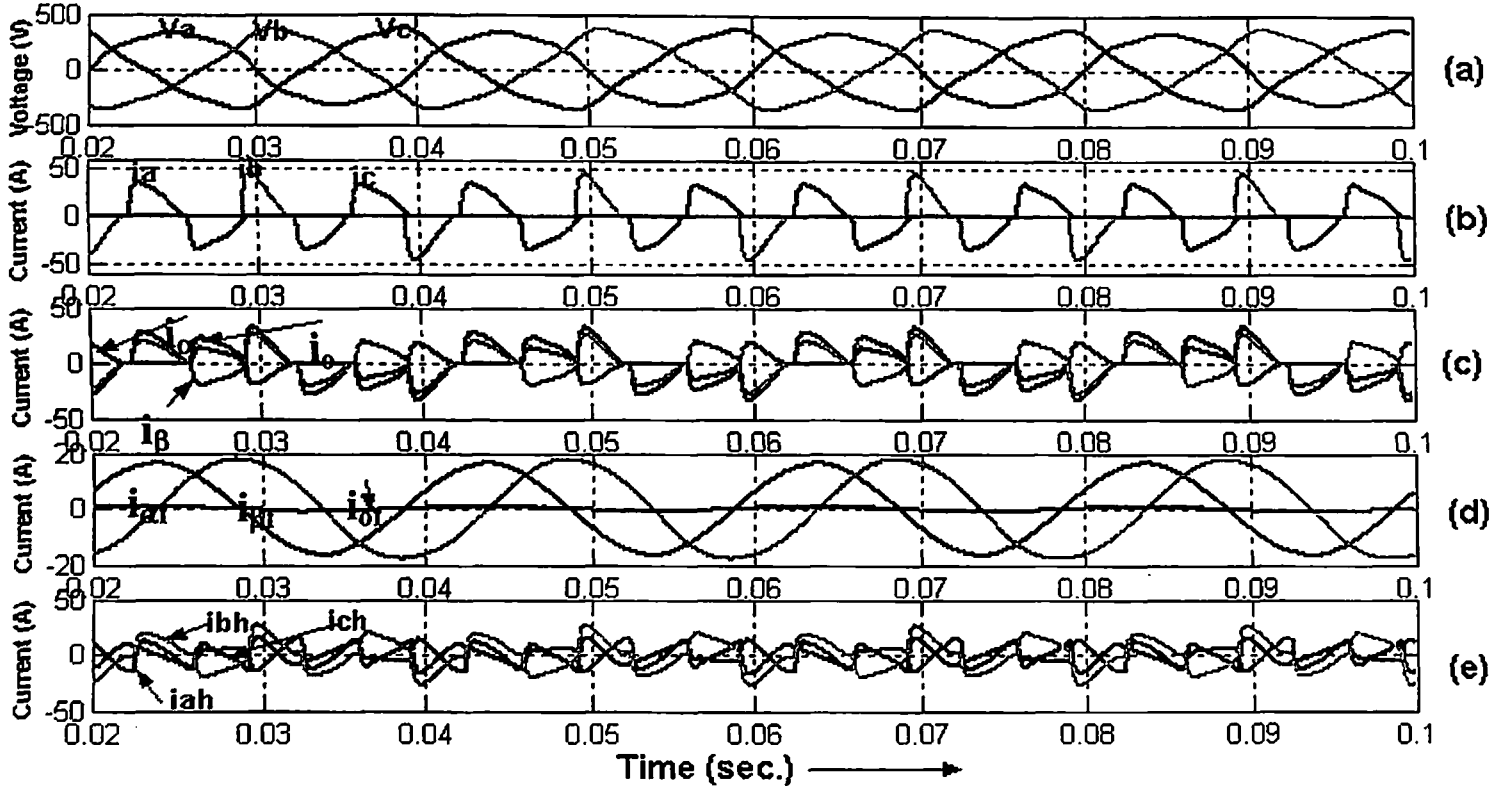

Fig. 4.11 Performance of NN controller under distorted source voltages (a) 3-ph source voltages (b) 3-ph source currents (c) 2-ph transformed currents (d) extracted 2-ph fundamental currents (e) computed 3-ph harmonic currents

4.3 IMPLEMENTATION ON DIGITAL SIGNAL PROCESSOR (DSP)

The ADMC401Digital Signal Processor (DSP) from Analog devices has been selected for the implementation of the proposed control scheme. This is a 16-bit fixed point DSP, with a clock frequency of 26 MHz. It has several peripherals on its core suitable for this application, such as 8-channel 12-bit analog to digital converter with simultaneous sampling capability (conversion time: 2μs for all 8-channels), three phase PWM generation unit, event timer unit for time /frequency measurement, RAM, PIO and two high-speed serial ports. The neural network algorithm (flow chart is given in the following section) has been implemented in real time on this DSP. The source current is measured using in-built ADC. For correct measurement of current under source frequency variation, 120 samples / fundamental period of AC mains are taken while sampling time is calculated and updated every half cycle. The input given to the DSP are the 2-phase transformed currents i_α & i_β and the output are the 2-phase fundamental current $i_{\alpha f}$ & $i_{\beta f}$, which are the outputs of neural network algorithm.

4.4 FLOW CHART FOR NEURAL NETWORK CONTROLLER INPLEMENTATION

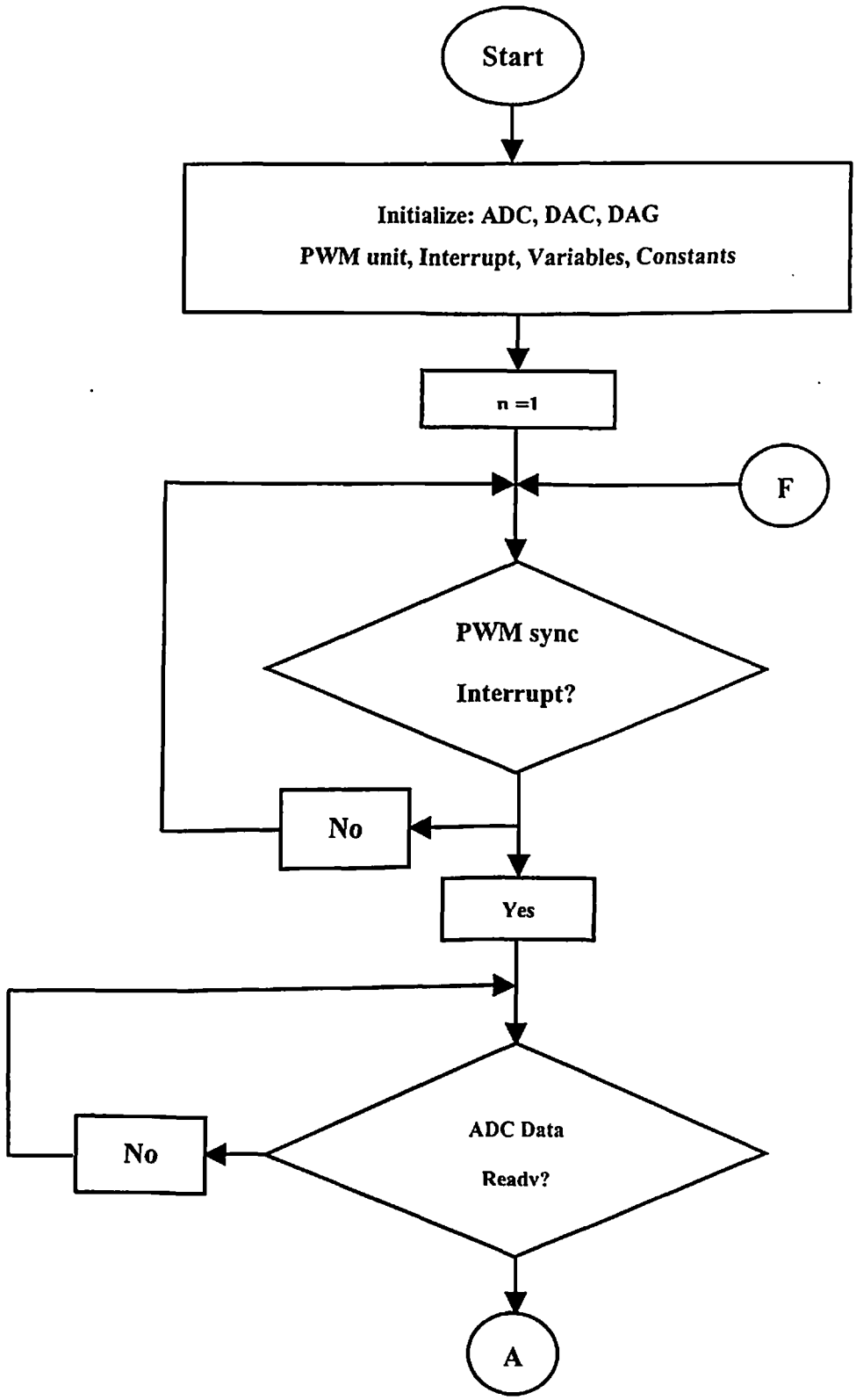

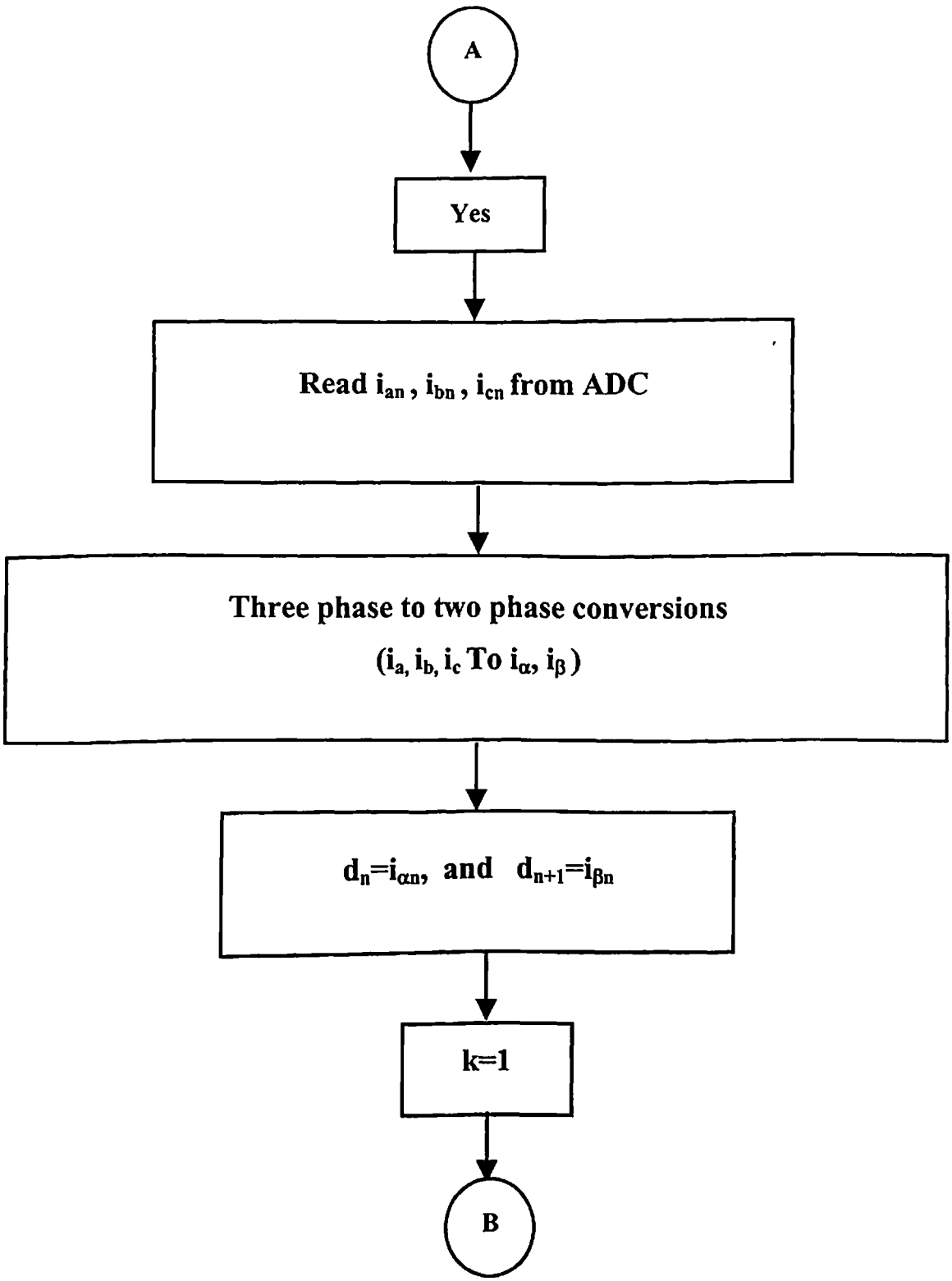
A
Yes
Read i_{an} , i_{bn} , i_{cn} from ADC
Three phase to two phase conversions
(i_a, i_b, i_c To i_α, i_β)
$d_n=i_{\alpha n}$, and $d_{n+1}=i_{\beta n}$
k=1
B

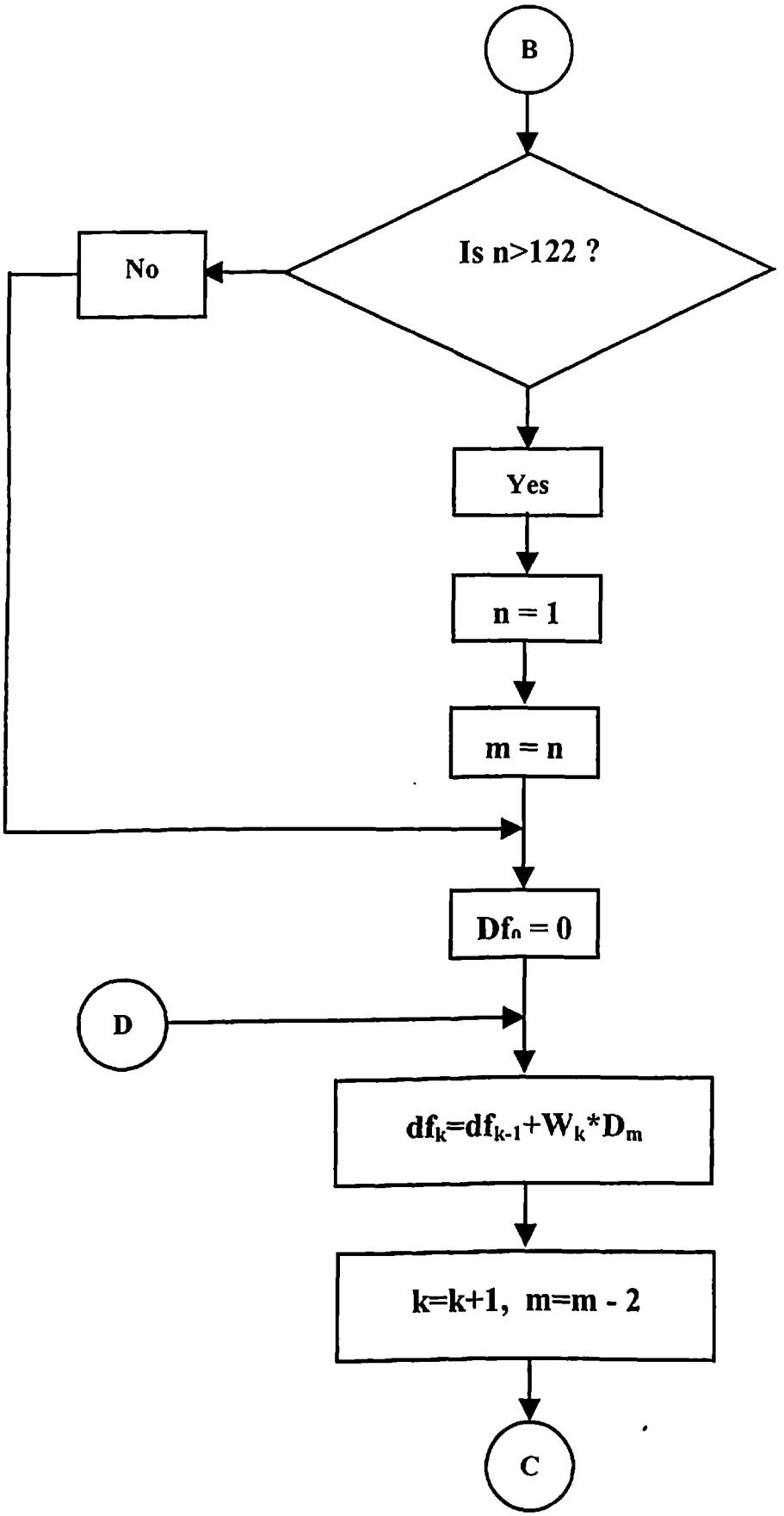
B
Is n>122 ?
No
Yes
n = 1
m = n
Dfn = 0
D
dfk=dfk-1+Wk*Dm
k=k+1, m=m - 2
C

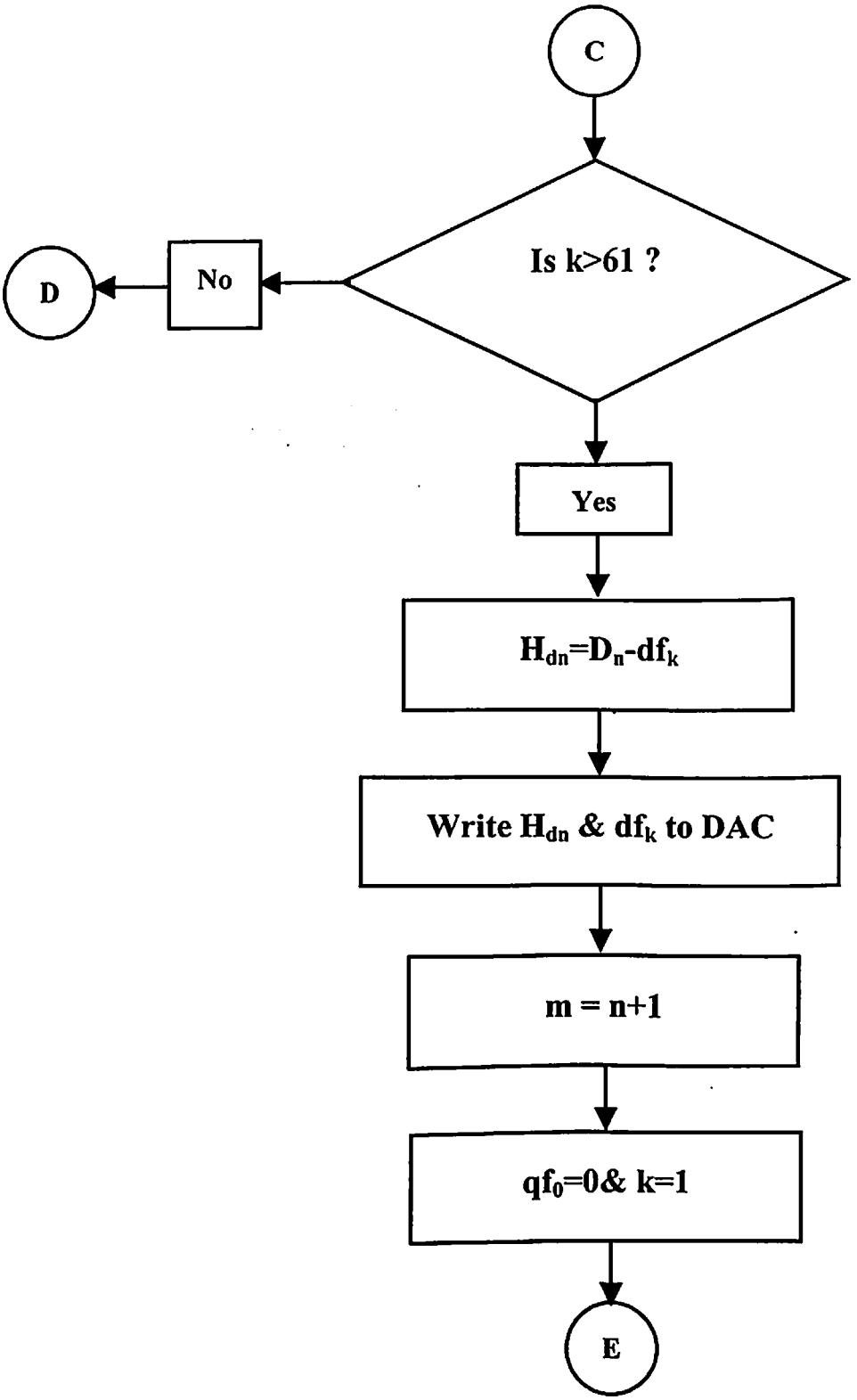
C
Is k>61 ?
No
D
Yes
$H_{dn}=D_n-df_k$
Write H_{dn} & df_k to DAC
m = n+1
$qf_0=0$& k=1
E

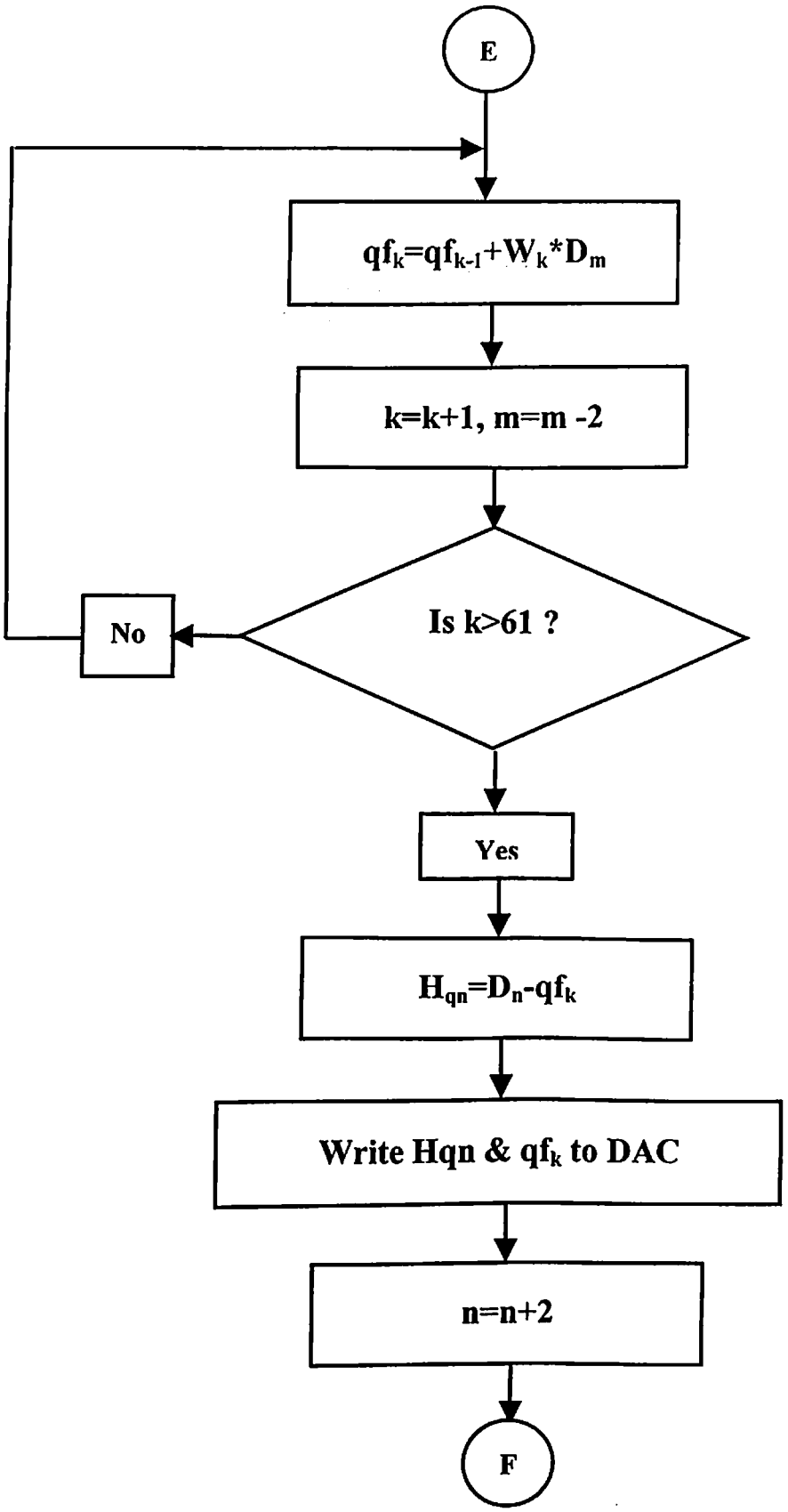

Fig. 4.12 Flow chart for neural network controller implementation

4.5 DIGITAL SIGNAL PROCESSOR RESULTS

To demonstrate the validity of the simulated results and practicability of the proposed neural network algorithm, it is implemented on DSP. This section shows the results of proposed neural network algorithm implemented on DSP (ADMC401).

4.5.1 Steady State Performance with Balanced Load

Fig. 4.13 shows the steady state performance of neural network controller with balance load. The waveforms of Fig. 4.13 shows the transformed 2–phase currents (i_α & i_β) and extracted 2-phase fundamental currents ($i_{\alpha f}$ & $i_{\beta f}$). The results given in the form of waveforms verify the steady state performance of the proposed controller.

4.5.2 Dynamic Performance with Sudden Application of Balanced Load

Waveforms in Fig. 4.14 demonstrate the performance of the proposed neural network controller under no load to balance loading condition. Initially (at t = 0.0 Sec.) there is no load, at t = 0.02 sec. a balance load (rectifier with resistive load) is suddenly applied. The waveforms shown in Fig. 4.14, verify that the controller extracts fundamental current accurately under dynamic condition (under sudden application of load).

4.5.3 Dynamic Performance with sudden application of Unbalanced load

In Fig. 4.15, the controller started without any load but at t = 0.02 sec. a sudden unbalance (rectifier with unbalance resistance) load is applied. This sudden insertion of unbalance load makes the source currents highly distorted and unbalance. The waveforms of Fig. 4.15 validate the simulation results taken under dynamic condition of loading.

From the waveforms given in Fig. 4.13-4.15, it is clear that the response of proposed neural network controller is accurate and fast in real time also, these results verify the simulation results given in previous section (in Fig. 4.1-4.11).

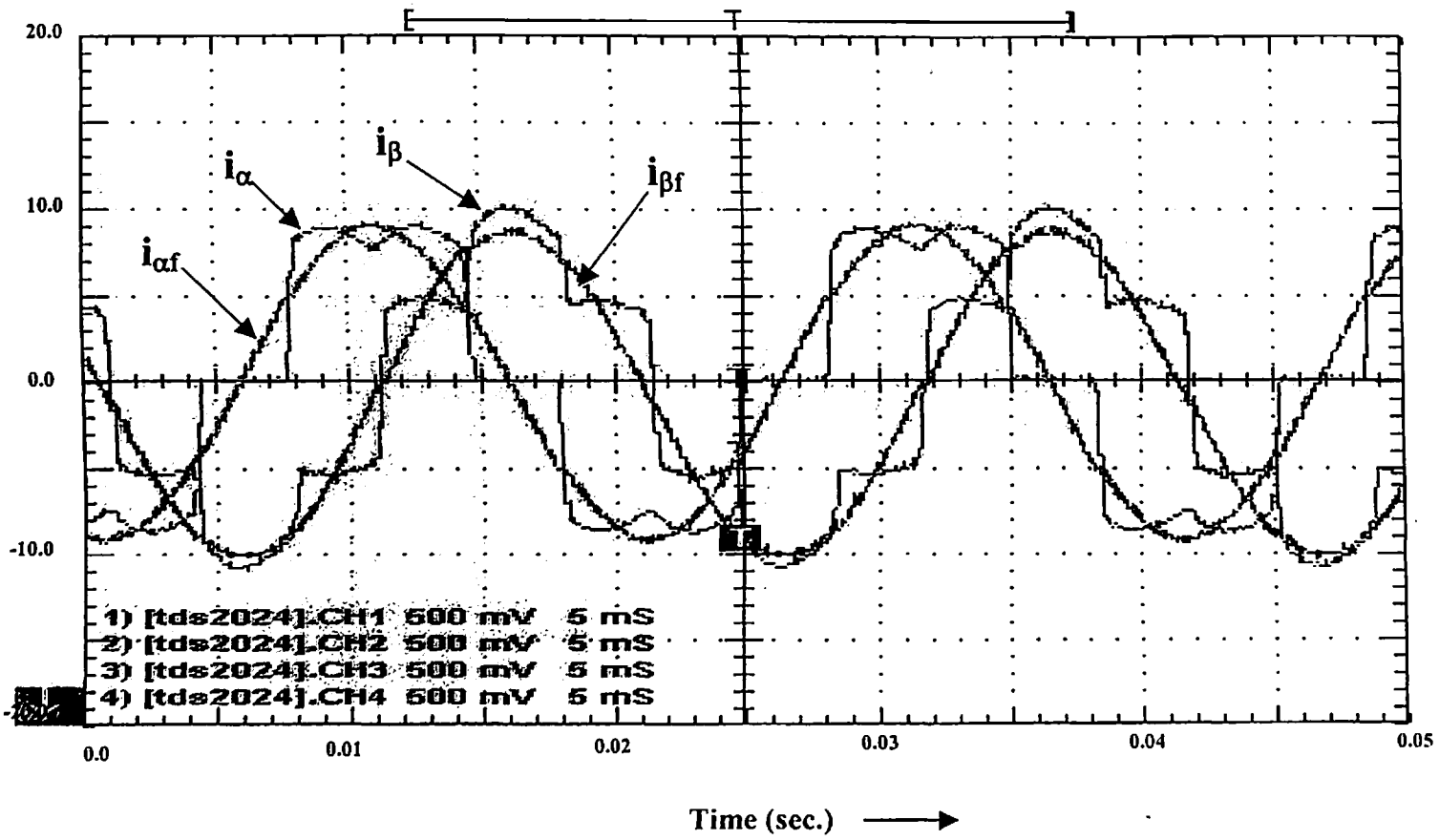

Fig. 4.13 Steady state performance of neural network controller under balance load condition

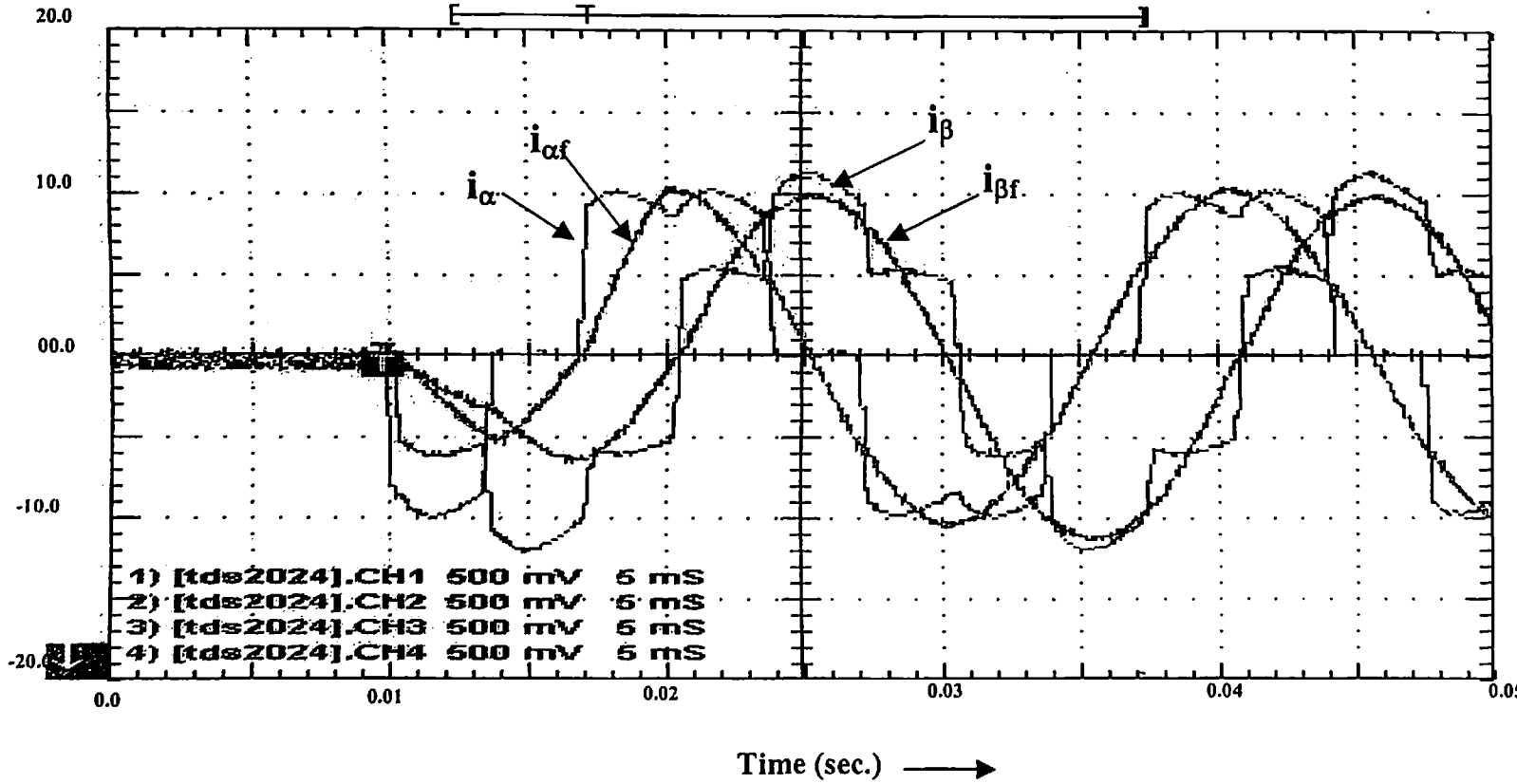

Fig. 4.14: Dynamic performance of neural network controller under no load to sudden application of balance load condition

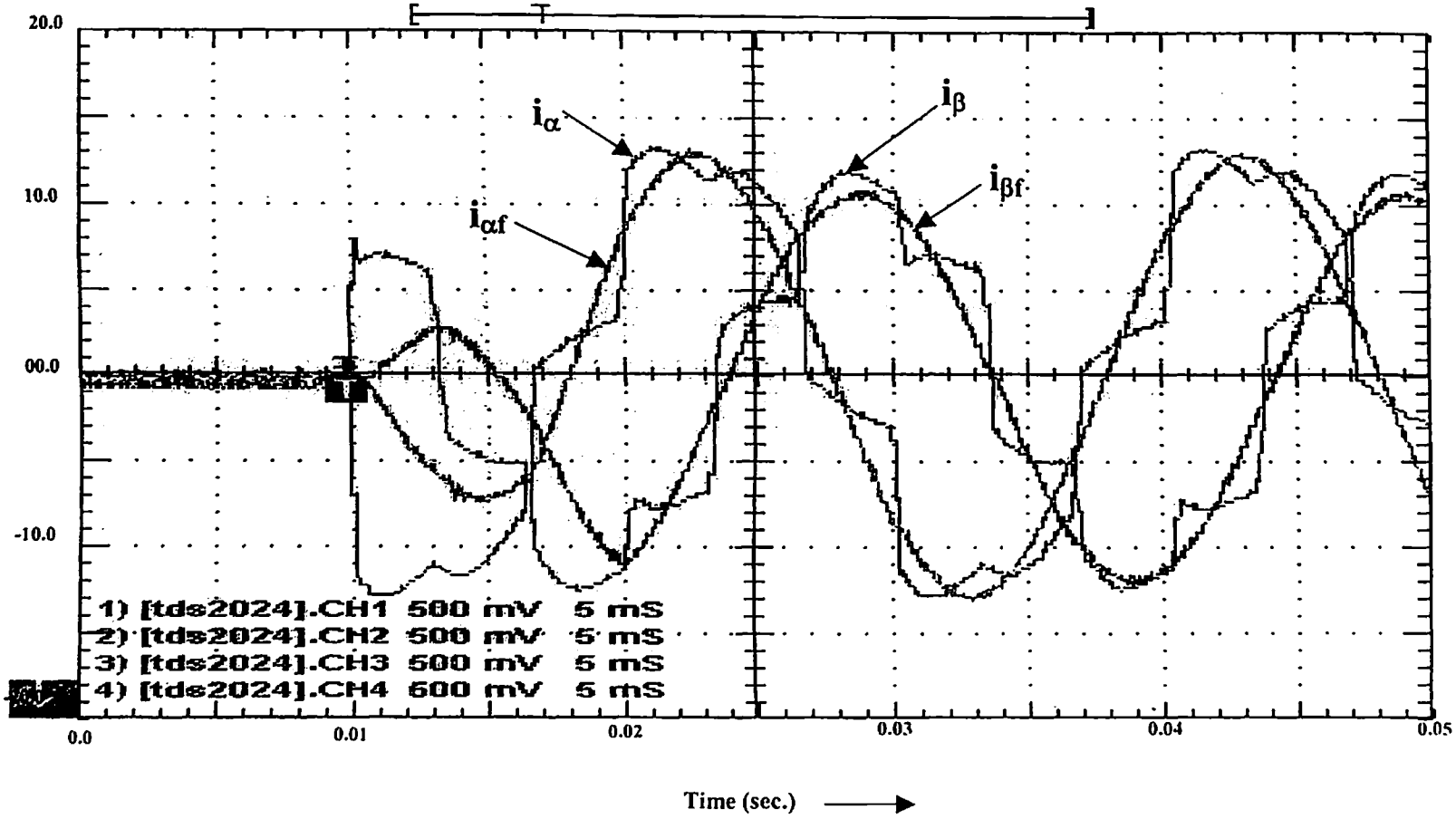

Fig. 4.15 Dynamic performance of controller under no load to sudden application of unbalance load condition

4.6 SUMMARY

In this Chapter the proposed neural network controller has been simulated and implemented in real time for different load conditions. The waveforms given in Fig. 4.1- 4.15 show the performance of neural network controller under various load and source conditions. From the waveforms given in these figures, it is clear that the proposed neural network controller is responding fast and accurate under steady state and dynamic condition. It has also shown that the output of the neural network (fundamental current waveforms) settles to the steady state value in less than half cycle of fundamental frequency. Further, the magnitude of extracted fundamental components in all above-mentioned cases was compared with the magnitude obtained through FFT. This comparison showed negligible error. These results demonstrate that the proposed neural network controller can extract fundamental component from balanced, unbalanced & distorted signals. Further, it demonstrates excellent performance both in steady state as well as dynamic conditions.

CHAPTER 5

SIMULATION STUDY OF HYBRID ACTIVE POWER FILTER

5.1 INTRODUCTION

In previous chapter Neural Network controller has been simulated for three-phase three-wire and three-phase four-wire systems under different load and source conditions. In this chapter, the performance of the hybrid active power filter using neural network controller has been studied by using computer simulation with MATLAB-SIMULINK 6.1. The active power filter has been simulated under various load conditions and the evaluation has been made using the total harmonic distortion (%THD) for the source current for the comparison with IEEE Standard 519.

5.2 SIMULATION RESULTS

This section presents the simulation results of hybrid active power filter for three-phase system under various operating conditions. The results have been presented in waveforms and finally summarized in tabular form, showing the THD before and after compensation.

5.2.1 Three-Phase Three-Wire Hybrid Active Power Filter

The harmonic current compensation through the hybrid active power filter has simulated in a three-phase, three-wire system with the utility power supply of

240V (with inductance of 0.5mH and resistance0.3Ω). A number of simulated results with the different load and source conditions have been developed and studied.

5.2.1.1 Steady state filtering performance

Fig.5.1 shows the filtering performance before and after the starting of active filter. The waveforms (a), (b), (c) and (d) of Fig. 5.1 show the three-phase source voltages, three-phase load currents, three-phase source currents and three-phase source currents THD respectively. At the starting, i.e. t = 0 Sec., the passive tuned filters and rectifier load is connected to AC supply. Initially, the source currents are highly distorted and in transient condition. Active filter is started at time t = 0.16 Sec. It can be seen that source currents become sinusoidal immediately after starting the active filter. The THD in individual source current before filtering is around 7% and after filtering it is found to be less than 3%.

5.2.1.2 Dynamic performance (50% step increase in load)

The waveforms in Fig. 5.2 show the filtering performance of active filter when a load is suddenly increased by 50%. At starting the passive tuned filters and rectifier load is connected to AC supply, at the time t = 0.04 Sec. active filtering started and the source current THD becomes 3%, under this condition at time t = 0.12 Sec. the is load increased by 50%. The Fig. 5.2 shows that the waveforms are maintained sinusoidal and source currents THD become approximately 3% in spite of such large variation in load.

5.2.1.3 Filtering performance under unbalanced loading

Fig. 5.3 shows the filtering performance under unbalanced load condition. In this simulation study, a 1-phase rectifier load is connected between phase 'a' & 'c' in addition to 3-phase rectifier. This creates an unbalance of 60% in line currents. The APF is starting at t = 0.06 Sec. It can be seen that the proposed neural network controller keeps source currents in each phase nearly sinusoidal and THD maintained around 4%.

5.2.1.4 Filtering performance under unbalanced source voltage condition

Fig. 5.4 shows the performance of hybrid filter when source voltage is unbalance. Here, the three-phase unbalanced source voltages are 240, 200, and 160Vrms. From the waveforms shown in Fig. 5.4, it is clear that they are highly distorted (THD=17%) before compensation, at t=0.16 Sec., active power filter starts, it can be seen that source current become sinusoidal immediately after starting the active filter and the THD in individual source is found to be less than 4%.

5.2.1.5 Filtering performance under distorted voltage source condition

The Fig. 5.5 demonstrates the performance of active power filter when source is also distorted. In this case a balanced load is connected to the distorted source, the source is not a pure sinusoidal, it is contaminated with 3^{rd}, 5^{th} and 7^{th}

harmonics of 7%, 5% and 3% respectively. The waveforms given in Fig. 5.5 show that of source current become sinusoidal after starting the active filter. After filtering the source current THD in each phase is found to be less than 5%.

In the case of distorted source voltage higher value of gain (K_h) is required to achieve the desired 5% THD in source current. The Fig. 5.6 shows the required value of gain (K_h) for the higher distortions in source voltage to achieve the desired value of THD in source current.

The results shown in Fig.5.1-5.5 demonstrate the excellent steady state and dynamic performance of the hybrid active power filter using neural network controller under nonlinear, balance/unbalance, load and source conditions.

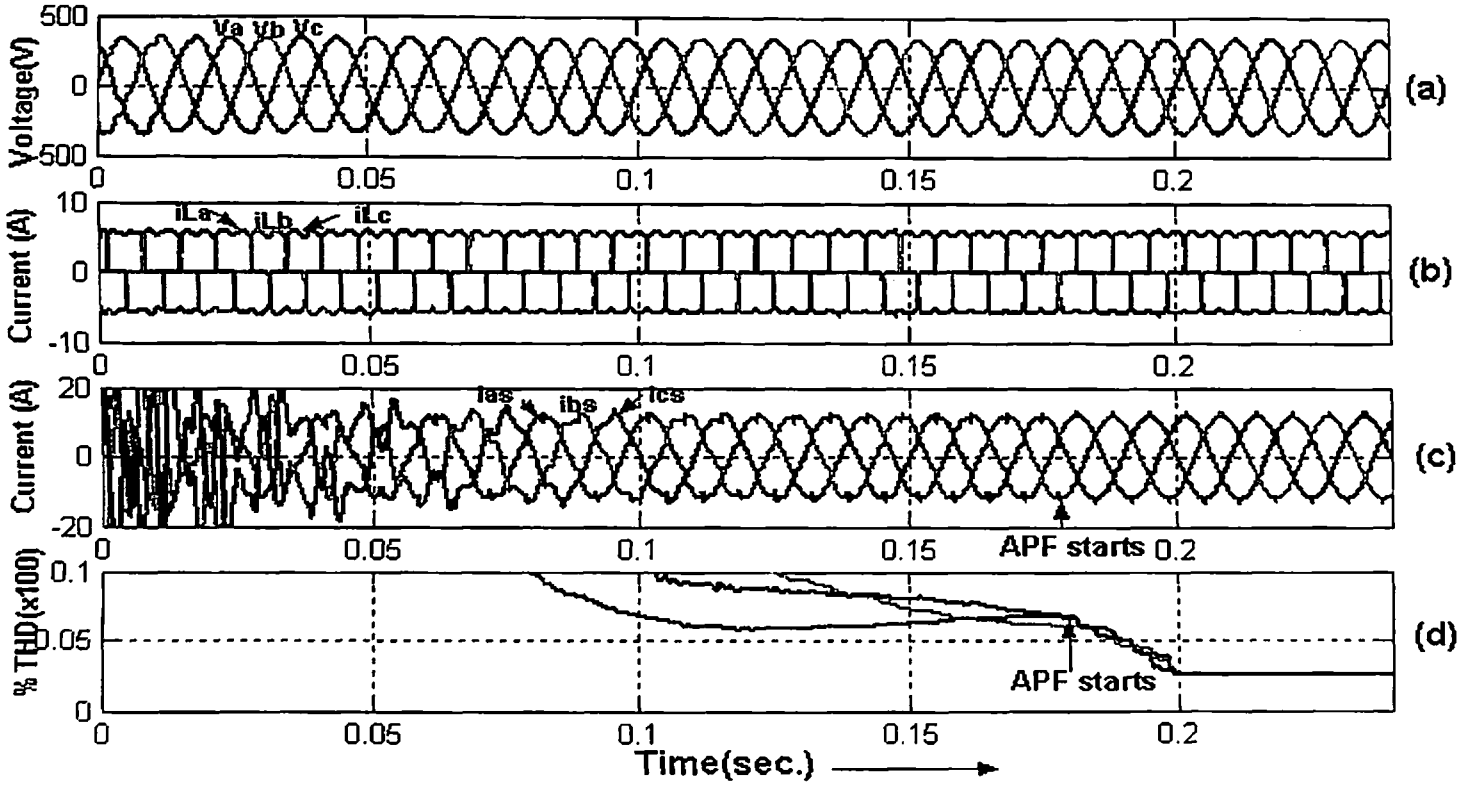

Fig.5.1 Steady state filtering performance: (a) 3-ph source voltages (b) 3-ph load currents (c) 3-ph source currents (d) 3-ph source currents THD

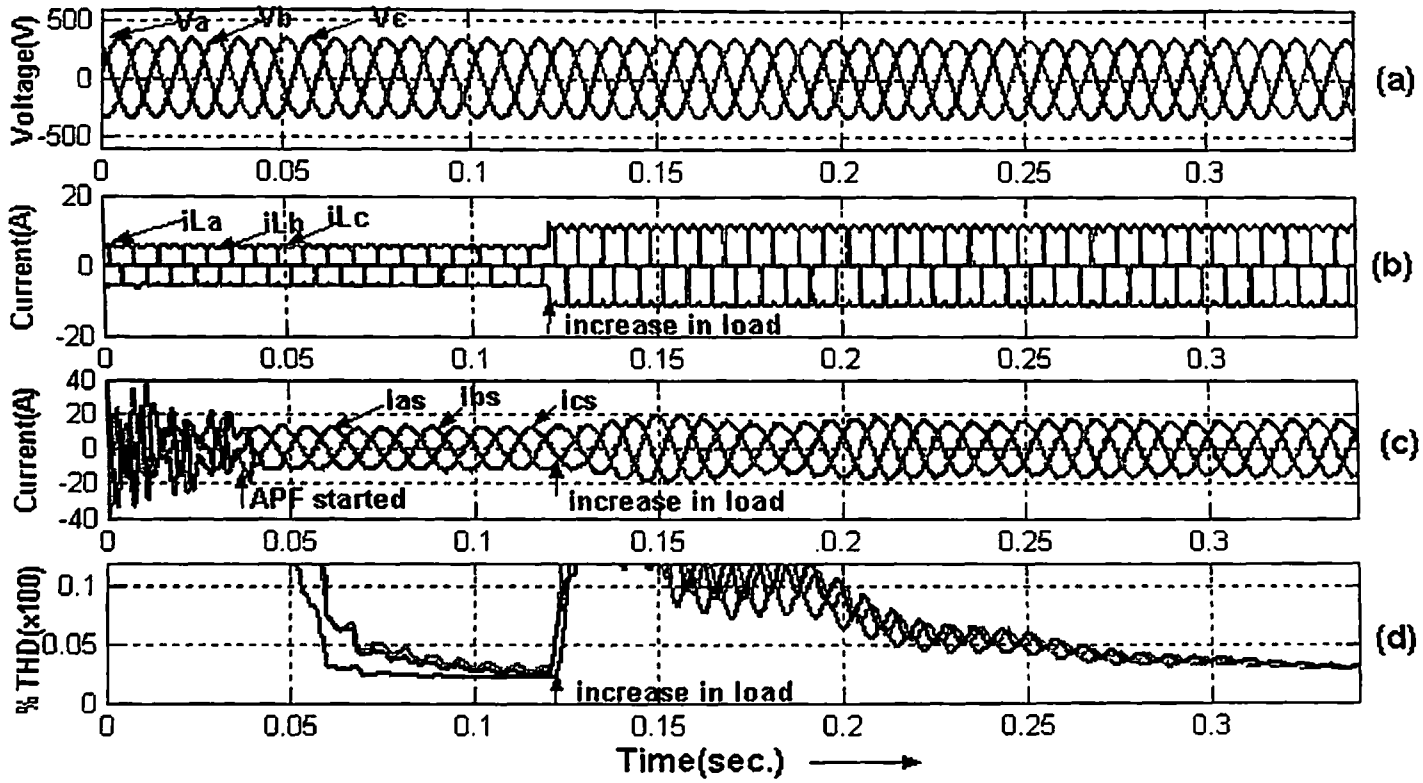

Fig.5.2 Dynamic performance with 50% step increase in resistive load (a) 3-ph source voltages (b) 3-ph load currents (c) 3-ph source currents (d) 3-ph source currents THD

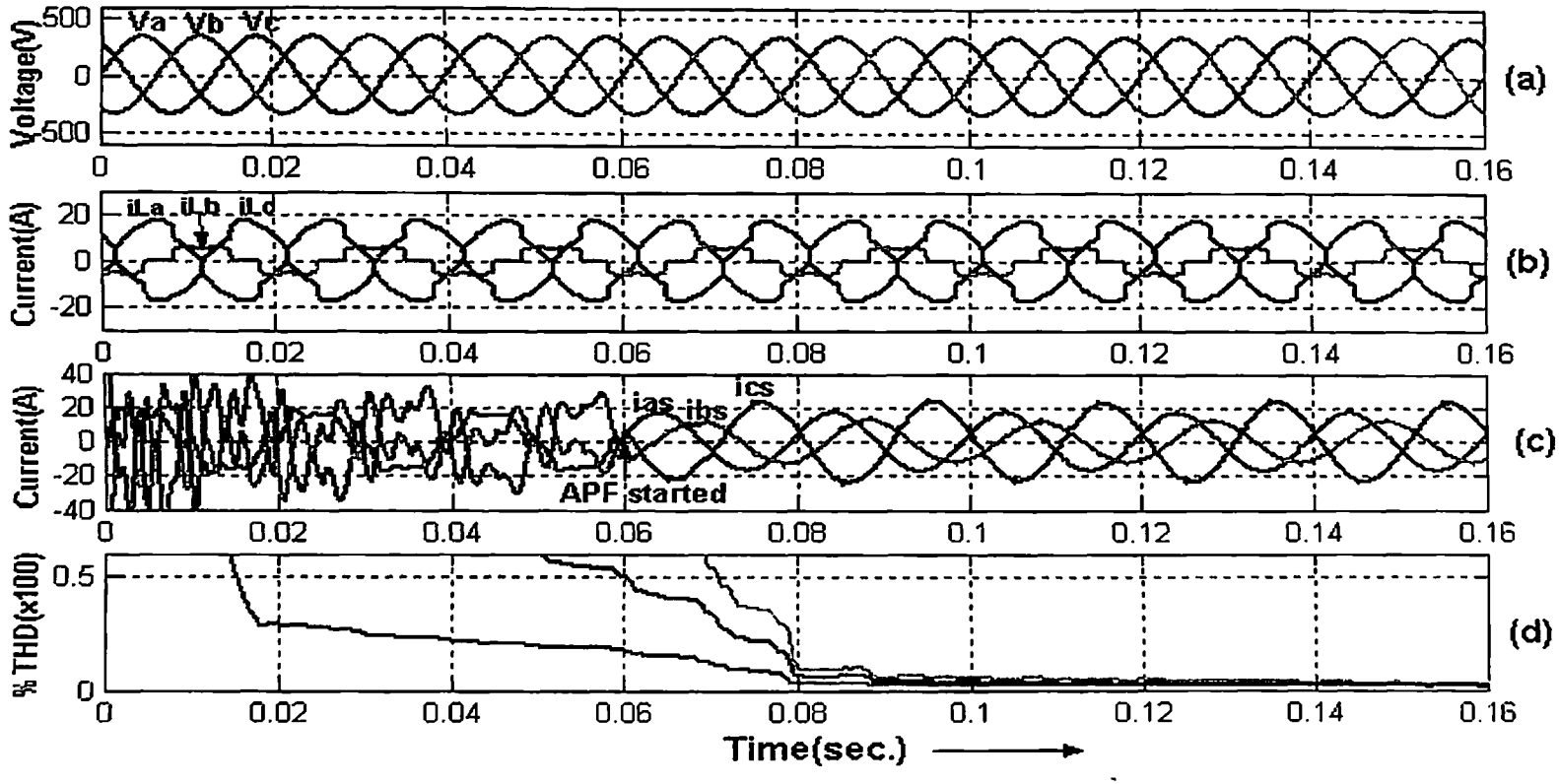

Fig. 5.3 Filtering performance under unbalanced loading (a) 3-ph source voltages (b) 3-ph load currents (c) 3-ph source currents (d) 3-ph source currents THD

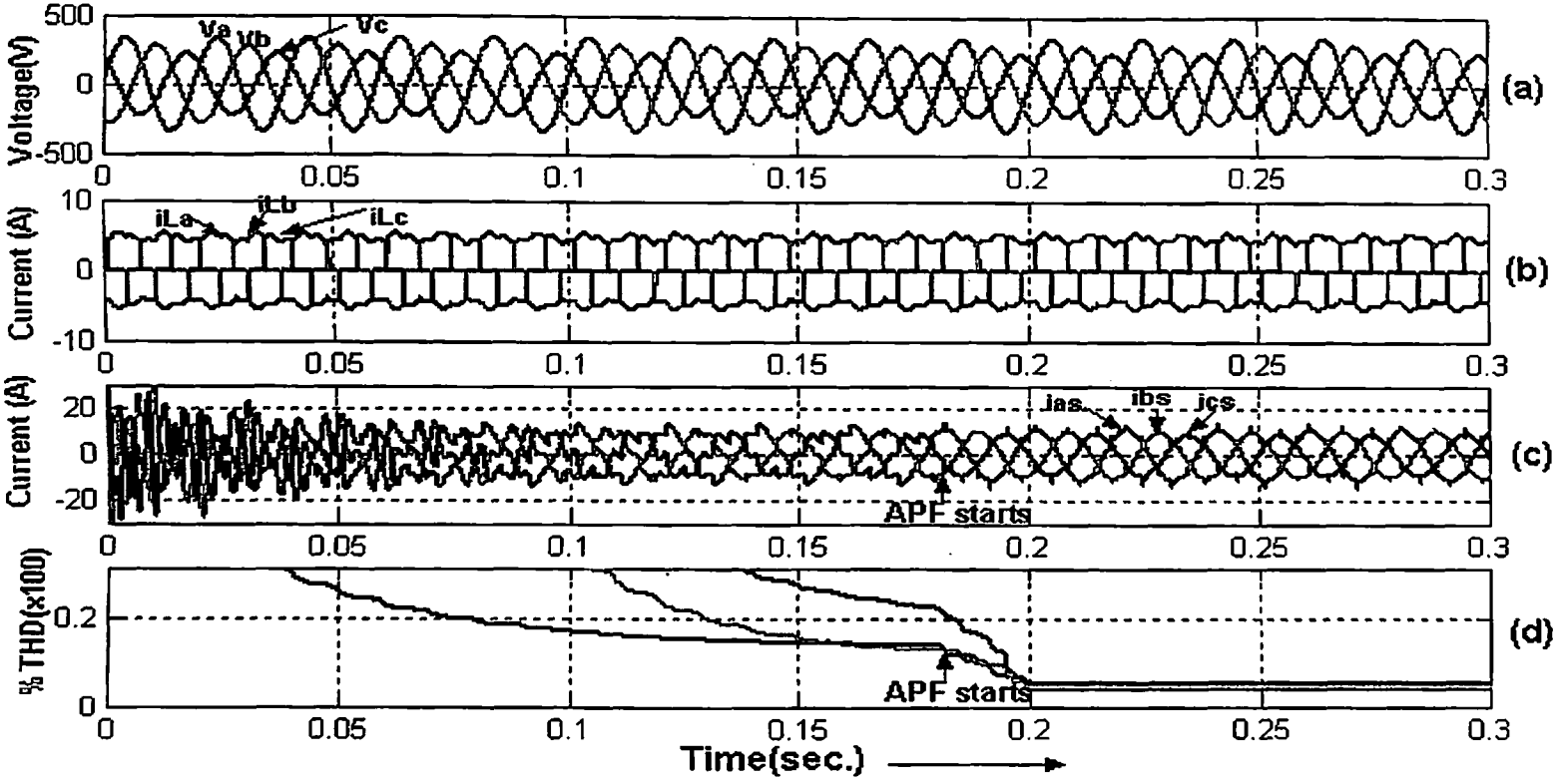

Fig.5.4 Filtering performance under unbalanced source voltages: (a) 3-ph source voltages (b) 3-ph load currents (c) 3-ph source currents (d) 3-ph source currents THD

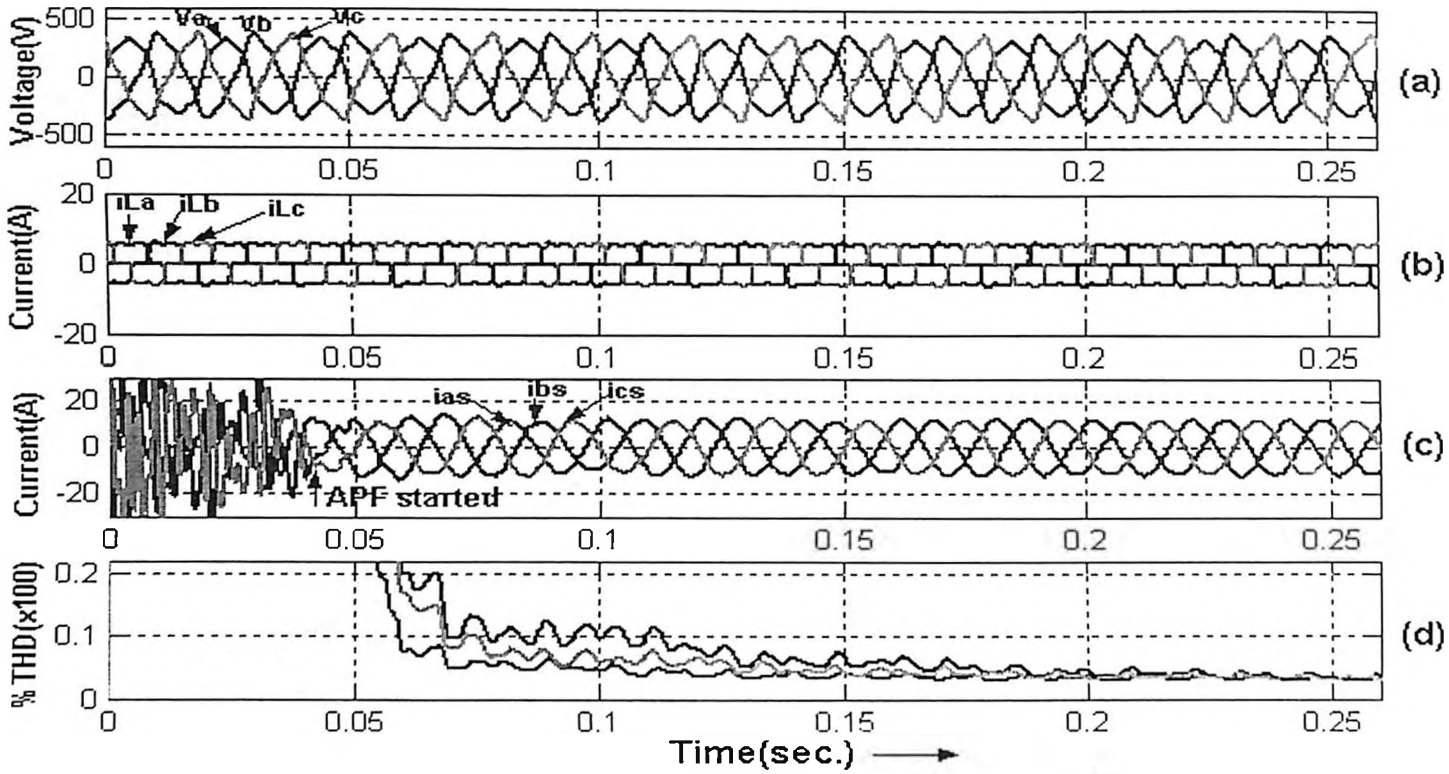

Fig.5.5 Filtering performance under distorted source voltages: (a) 3-ph source voltages (b) 3-ph load currents (c) 3-ph source currents (d) 3-ph source currents THD

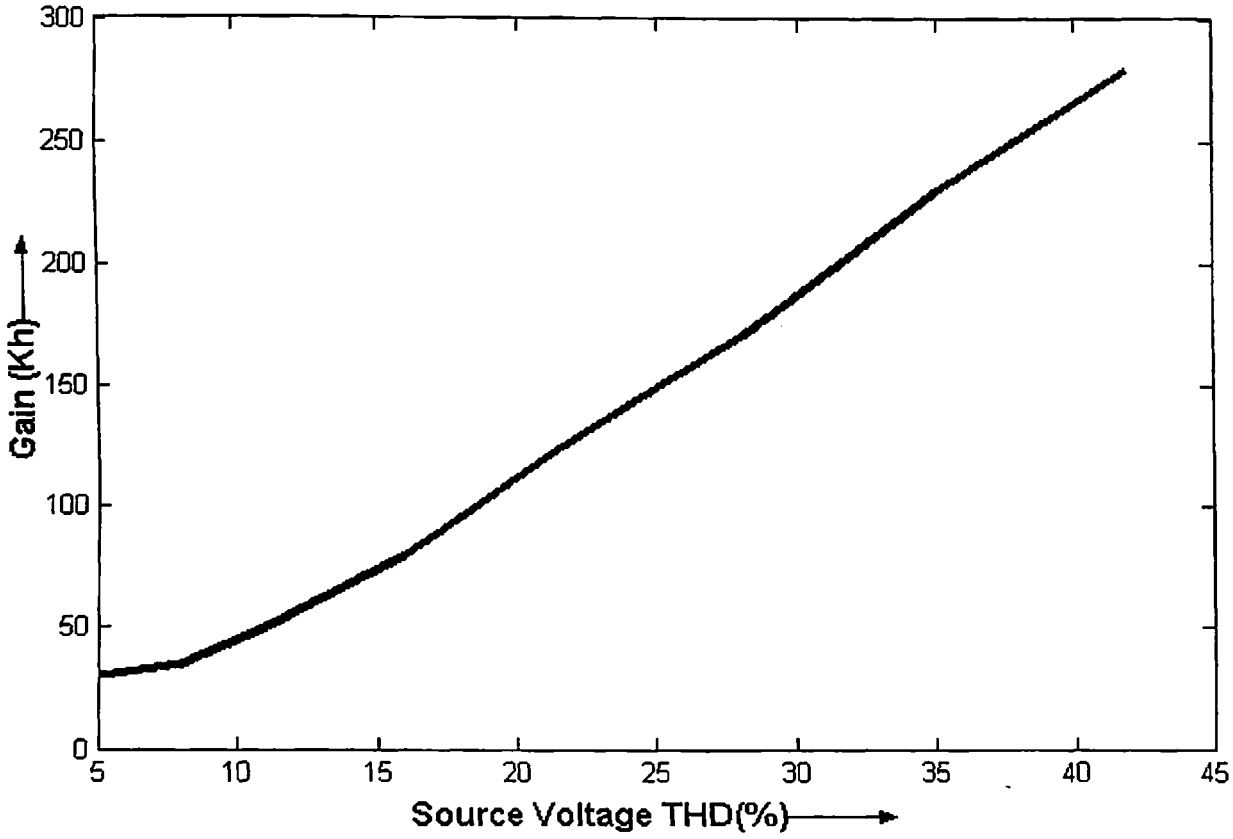

Fig. 5.6 Gain (K_h) vs Source Voltage THD

Table 5.1: Comparison of Source Current %THD in Three-Phase, Three-Wire System

Load and Source Conditions	**Source Current THD (%)**	
	Before Compensation	After Compensation
Balance load with balance supply voltages	7%	3 %
Sudden increases in load (by 50%) with balanced supply voltages	7%	3%
Unbalanced load (30% unbalance) with balanced supply voltages	20-40%	4%
Balance load with unbalanced supply voltage	17%	4. 5%
Balanced load with distorted supply voltage (12% THD)	40%	5%

5.2.2 Three-Phase Four-Wire Hybrid Active Power Filter

In previous section the simulation results of three-phase three-wire hybrid active power filter have been shown and discussed. Present section carried out the simulation results of three-phase four-wire hybrid active power filter system. Fig. 5.7-5.11 shows the performance of hybrid active power filter under various load and source conditions.

5.2.2.1 Steady state filtering performance with balanced loading

Fig 5.7 shows the source current neutral current and total harmonic distortion (THD) waveforms before and after the starting of active filter. At t = 0 Sec., the passive tuned filters and rectifier load is connected to AC supply. Initially, the source currents are highly distorted and in transient condition. Active filter is started at time t = 0.1 Sec. It can be seen that source current become sinusoidal immediate after starting the active filter. Before starting of filter the THD in individual source current was 10% and after filtering is found to be 4% and the neutral current also decreases significantly.

5.2.2.2 Steady state filtering performance with unbalanced loading

Fig.5.8 shows the filtering performance under unbalance load condition. The unbalance created in the line current is 30%. Before compensation the THD was very high i.e. 10-25% in three different phases and neutral current was also very high that is because of unbalance and distortions. The active filtering in

given condition decreases the THD in all the three phases between 4 - 5%, that is as per IEEE standard, and it also reduces the demand of neutral current.

5.2.2.3 Dynamic performance (40% step increase in load)

Fig.5.9 shows the three phase source currents when a load is suddenly increased by 40% at the time t = 0.1 Sec. The waveforms are maintained sinusoidal in spite of such large variation in load. It can be seen that the proposed NN controller keeps currents in each phase nearly sinusoidal and THD less than 5%.

5.2.2.4 Filtering performance under unbalanced source

In Fig.5.10 the three-phase unbalanced source voltages are 240, 200, and 160Vrms. At t=0.06 APF starts and THD of source current in each phase reduced to 4%. Without active filtering, with this unbalance in supply voltages the THD in source current is around 17%, after compensation it decreases to 4.5% that is in the line of IEEE standard.

5.2.2.5 Filtering performance under distorted source voltages

In Fig.5.11 the source voltage is contaminated with 3^{rd} and 5^{th} harmonics with THD of source current was very high, After filtering the THD of source current in each phase becomes around 5%. Under distorted source condition the neutral current was also very high, which is undesirable. After filtering neutral current decreases by a significant value. In the case of distorted source voltage higher value of gain (K_h) is required to achieve the desired 4% THD in source current. As given in previous section in Fig. 5.12, it required higher value of gain

(K_h) for the higher distortions in source voltage to achieve the desired value of THD in source current.

The results shown in Fig.5.7-5.11 demonstrate the excellent performance of the proposed system to compensate the harmonics present in source current. The results obtained from Fig. 5.7-5.11 have given in tabular form in Table 5.2, that the proposed compensate the harmonics to a satisfactory neural network controller and hybrid active power filter are giving equally excellent performance for both the three-phase, three-wire and three-phase-four wire systems under steady state and dynamic conditions with balance/unbalance, nonlinear load and source conditions.

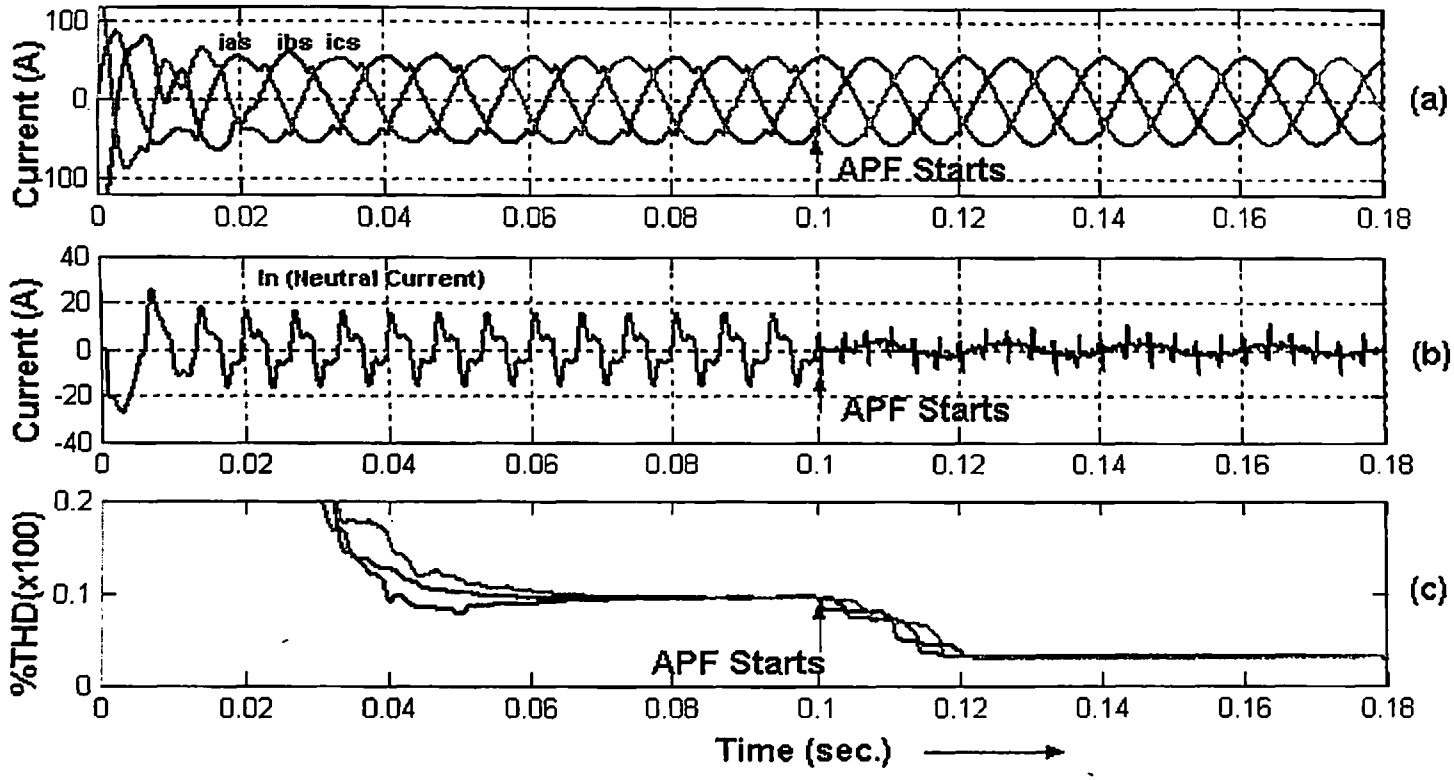

Fig. 5.7. Steady state filtering performance: (a) 3-ph source currents (b) Neutral current (c) 3-ph THD

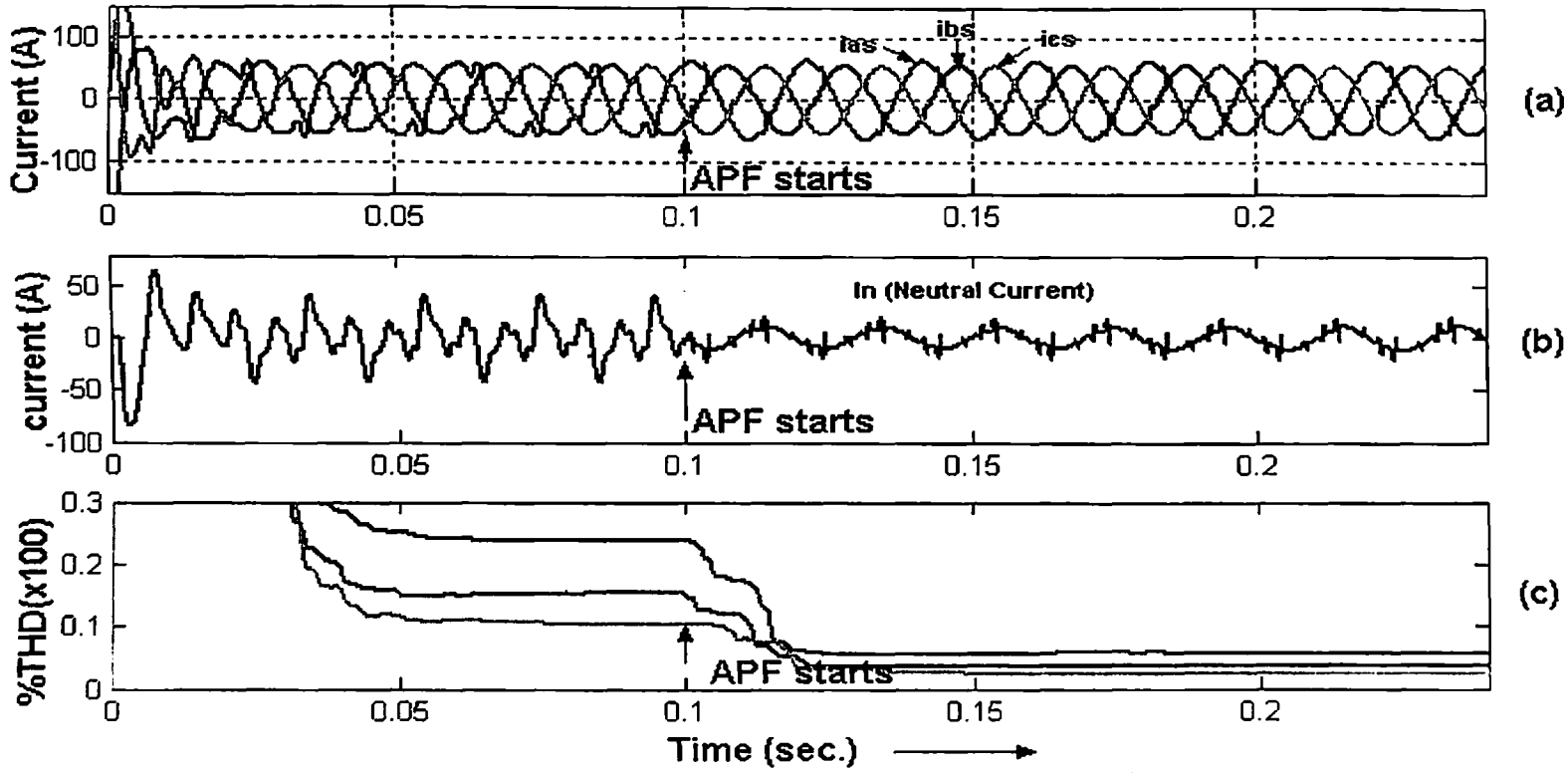

Fig. 5.8. Filtering performance under unbalanced loading: (a) 3-ph source currents (b) Neutral current (c) 3-ph THD

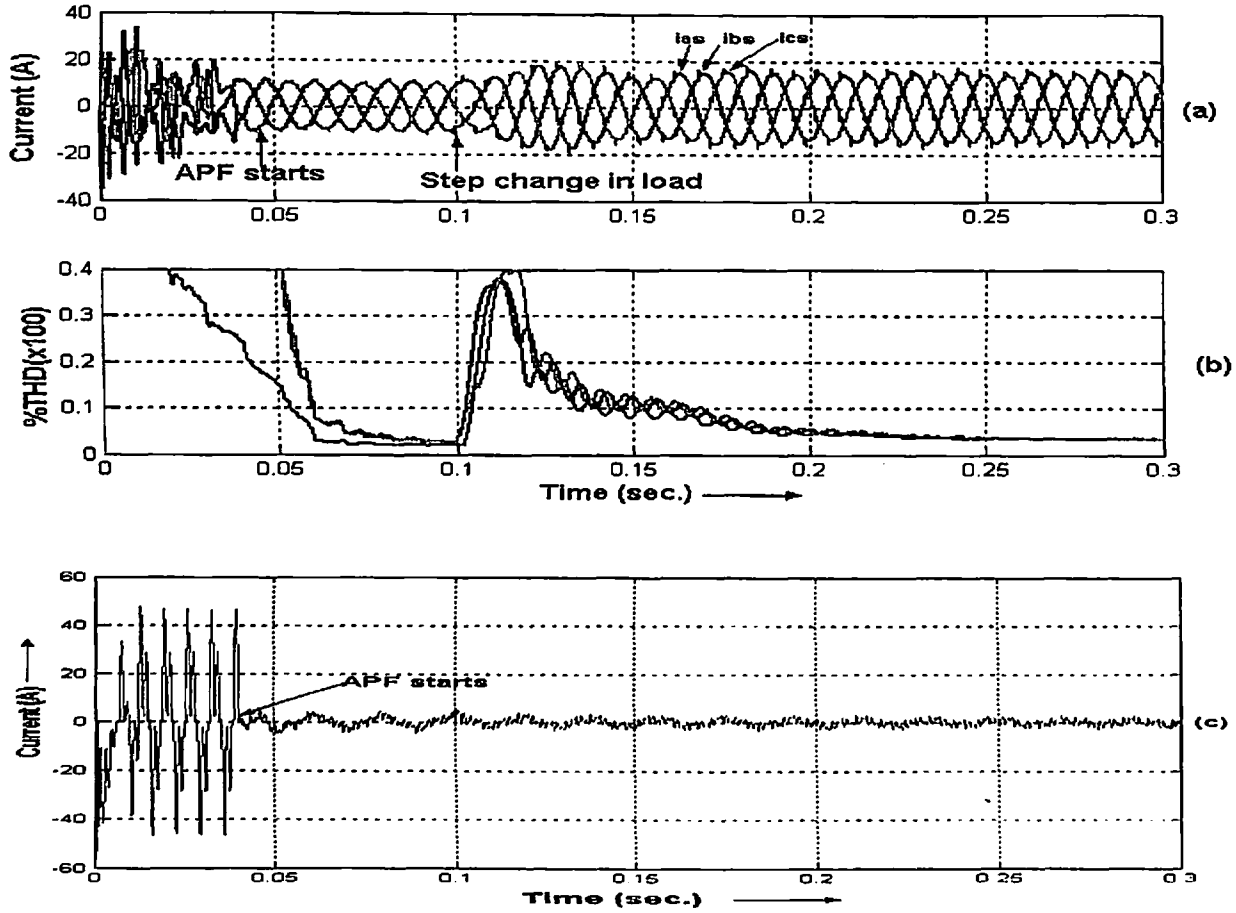

Fig. 5.9. Dynamic performance: 40% Step change in load: (a) 3-ph source currents (b) 3-ph THD (c) Neutral current

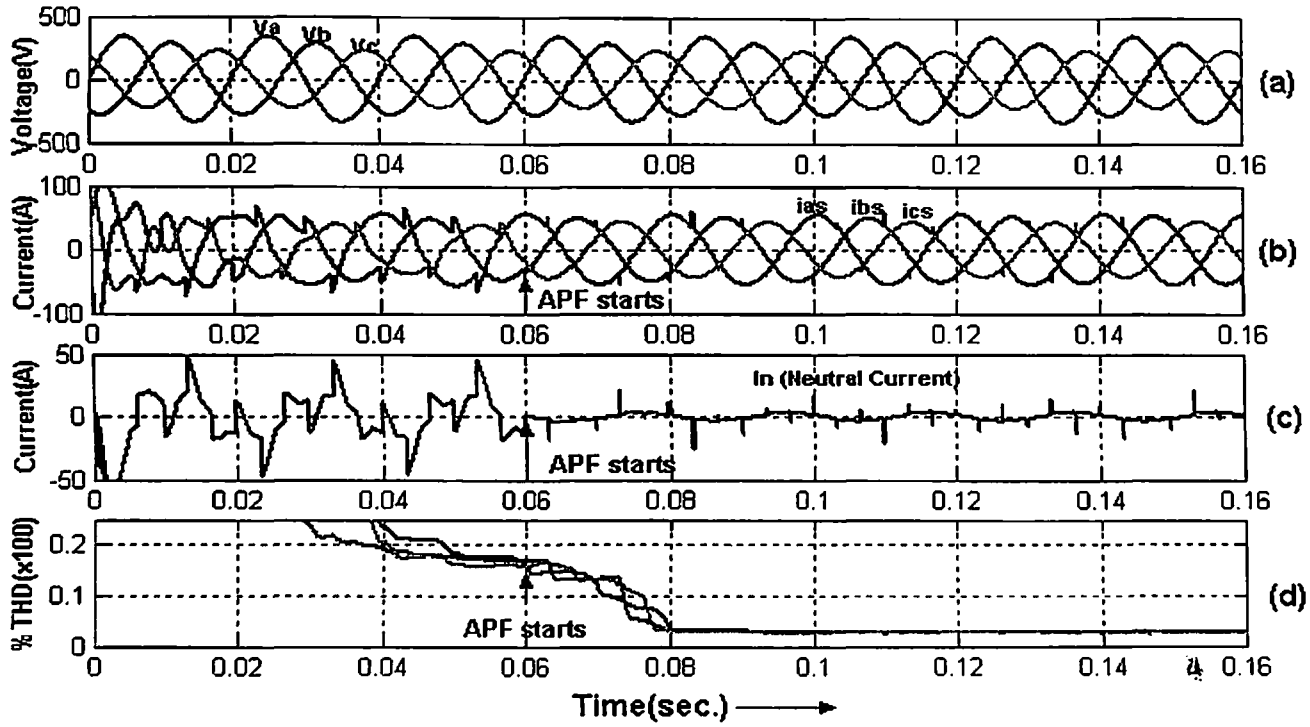

Fig. 5.10. Filtering performance under unbalanced source voltages: (a) 3-ph source voltages (b) 3-ph source currents (c) neutral current (d) 3-ph THD

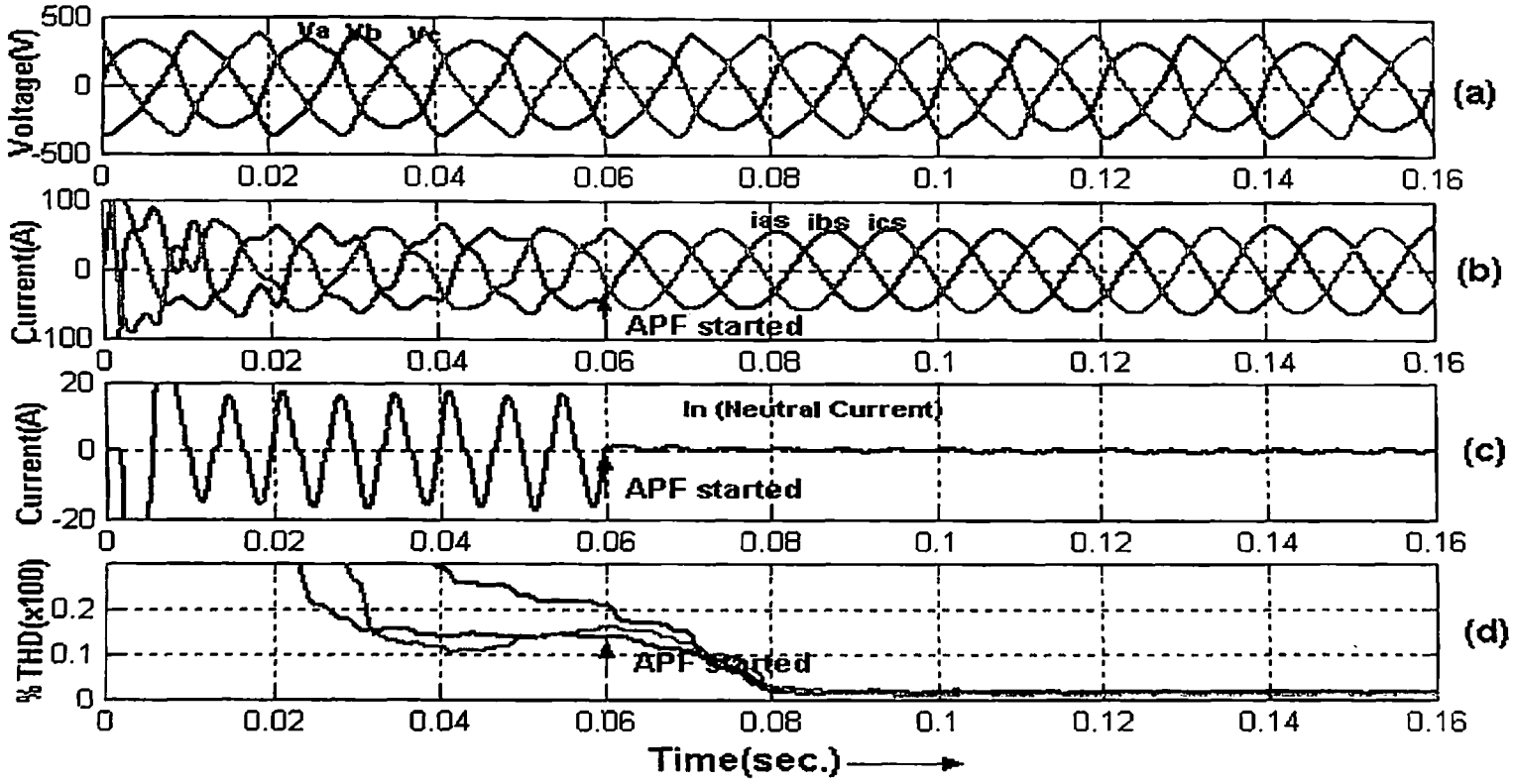

Fig. 5.11. Filtering performance under distorted source voltages: (a) 3-ph source voltages (b) 3-ph source currents (c) neutral currents (d) 3-ph THD

Table 5.2: Comparison of Source Current %THD in Three-Phase, Four-Wire System

Load and Source Conditions	**Source Current THD (%)**	
	Before Compensation	After Compensation
Balanced RC Load with balanced supply voltages	10%	4 %
Unbalanced RC load (30% unbalanced) with balanced supply voltages	10-25%%	4-5%
Sudden increases in load (by 40%) with balanced supply voltages	10%	4.7%
Balanced RC load with unbalanced supply voltage	18%	4.5%
Balanced load with distorted supply voltage (12% THD)	14-18%	5%

5.3 SUMMARY

In this Chapter the proposed hybrid active filter using neural network based controller has been simulated using SIMULINK for three-phase, three-wire and three-phase, four-wire systems under various load and source conditions. The proposed system satisfactorily compensates the harmonic currents present in source current due to nonlinear load. The proposed neural network controller and hybrid active power filter are giving equally excellent performance for both the three-phase, three-wire and three-phase-four wire systems under steady state and dynamic conditions with balanced/unbalanced, nonlinear load and source conditions.

CHAPTER 6

CONCLUSIONS

6.1 GENERAL

The proliferation of nonlinear loads such as static power converters and arc furnaces results in a variety of undesirable phenomena in the operation of power systems. The most important among these are harmonic contamination, increased reactive power demand and power system voltage fluctuations. Harmonic contamination has become a major concern for power system specialists due to its effects on sensitive loads and on the power distribution system. Harmonic current components increase power system losses, cause excessive heating in rotating machinery, can cause significant interference with communication circuits that shared common right-of-ways with ac power lines, and can generate noise on regulating and control circuits causing erroneous operation of such equipment.

Various compensation methods using conventional techniques have proved insufficient for mitigation and control of power quality problems. Harmonic distortion, for example, has traditionally been dealt with at the source end by the use of passive tuned filters. However, their application for harmonic reduction in the present scenario has been limited due to their inherent limitations. The use of active power filtering technique has although been in practice for the last about one decade, there are still many problems which have not been able to be handled.

The research work carried out and reported in this thesis has concentrated on some of the less focused problems of Active Filters, which have been extensively researched within the scope of this investigation. A novel control scheme for hybrid active power filter has been proposed, modeled and investigated in order to overcome the limitations of earlier reported work, on active as well as passive filters. It is demonstrated that the application of proposed hybrid active filters can eliminate most of the problems created by non-linear, unbalanced loads. Furthermore, these novel techniques offer flexibility in control of harmonic power, with good steady state and dynamic performance. However, there are still several issues associated with the proposed active filters, which are beyond the scope of this investigation, and need to be addressed and solved to make these more effective and economical. These issues have been listed under further scope of investigations.

This section presents some salient and significant contributions and conclusions of the research work carried out and reported during the course of this Ph.D. thesis. The objectives laid at the time of start of this research activity have been successfully realized through mathematical model and simulation investigations. The significant achievements are listed as under:

- Investigation on the existing approaches of harmonic power compensation as available in the published literature has been carried out and some significant suggestions have been made.
- A simplified neural network algorithm for the decomposition of non-sinusoidal current in three-phase system under asymmetrical

and non-sinusoidal conditions has also been carried out through the following research achievements:

- ❖ Development of mathematical model.
- ❖ Implementation of the developed algorithm using Digital Signal Processor (DSP).
- ❖ Evaluation of the performance of the algorithm by means of digital simulation using MATLAB and SIMULINK under balanced as well as unbalanced conditions.

- Development of a hybrid active power circuit topology having low power rated active filters for compensation of load current harmonics.
  - ❖ Complete computational model of the proposed control and power circuit topology has been developed in MATLAB/SIMULINK.
  - ❖ Evaluation of performance under different power system conditions (balanced as well as unbalanced conditions) by means of simulation investigations.

This research work has brought out some very significant contributions in the methodologies of simulation, as well as in the design and development of some efficient and relatively low cost active power filter. In this direction, a novel power circuit configurations of active power filter having low power rated PWM converters, and simplified control schemes have been successfully designed,

developed and simulated. The results thus obtained in the steady state as well as in dynamic conditions have been validated successfully, through digital simulation. The salient points of novel approaches proposed in this research work are described in the following sub-sections.

6.2 NEURAL NETWORK BASED CONTROL ALGORITHM

A simple, comprehensive and flexible neural network algorithm has been developed and proposed for obtaining the harmonics of three-phase currents and/or voltages, under non-sinusoidal and unbalanced conditions with minimal computational efforts. Mathematical model and training details of the proposed algorithm have been developed and presented. This algorithm has been efficiently implemented in real time using 16-bit Digital Signal Processor (DSP) and it has been demonstrated that it can perform decomposition of currents in less than half cycle. Further, it can be effectively used without modifications to control most of the Active Filter topologies reported so far in the published literature. The algorithm has been evaluated by simulation study performed under balanced, unbalanced and non-sinusoidal conditions. The simulation results demonstrated its effectiveness under various operating conditions. Some advantageous features of the proposed controller are:

1. It is independent of source voltage distortion and unbalance.
2. Fast and accurate training of fundamental component under balanced/unbalanced and nonlinear conditions.
3. Simple architecture and easy for implementation.

6.3 HYBRID ACTIVE POWER FILTER

A novel power circuit configuration named Hybrid Active Power Filter suitable for the compensation of high power non-linear loads in three-phase system has been presented and analyzed. The following capabilities of hybrid active power filter have been demonstrated by means of simulation, with very impressive results, under balanced as well a unbalanced source and load conditions:

1. Total Harmonic Distortion (THD) below 5% of fundamental have been measured and reported. These figures are in line with the IEEE 519-1992 harmonic standards.
2. Low power rated active filters.
3. It can maintain sinusoidal current and also meet harmonic standards even under the failure of some of its components.
4. Excellent dynamic response under sudden connection (step change/unbalancing) of non-linear loads.
5. Simple and fast control scheme.

6.4 SCOPE FOR FUTURE RESEARCH WORK

There are several important points, which need to be investigated but could not be covered in this research work due to its limited scope and time frame. Some of these significant points, which need an immediate investigation

for future works in order to take maximum advantage of this research work, are mentioned below:

(i) Implementation of the proposed hybrid active power filter using neural network controller can be done to verify the simulation results.

(ii) The performance and protection schemes of the proposed configurations of hybrid active power filter under power system faults need to be studied, developed and investigated.

(iii) Another very important aspect that needs to be investigated is the possibility of application of PWM control, which reduces the switching frequency of SAF in the proposed topological configurations. This aspect of design is expected to reduce substantially the losses and variable frequency related problems.

(iv) Filtering capabilities of the hybrid active filter under poor power quality of AC source such as large harmonic distortion, notching etc., also need to be thoroughly investigated.

It is hoped that the simulation investigations as reported in this thesis will help in establishing new topological designs and control schemes for active power compensators in an attempt to filter out the harmonics.

REFERENCES

1. IEEE Working Group in Power System Harmonics, "Power System Harmonics: An Overview," IEEE Trans. Power App. Syst., vol. PAS-102, pp. 2455-2460, Aug. 1983.
2. IEEE Std. 519-1992, "IEEE Recommended Practices and Requirements for Harmonic Control in Electric Power Systems".
3. A report by load characteristics task force and effects of harmonic task force, " The Effects of Power System Harmonics on Power System Equipment and Loads," IEEE Trans. PAS, vol. PAS-104, no.9, pp. 2555-2563, Sept. 1985.
4. P. Indrajit and P. J. Savoie, "Effect of Harmonics on Power Measurement," IEEE Trans. IA, vol.26, no.5, pp. 944-946, Sep/Oct 1990.
5. IEEE Recommended Practice for Monitoring Electric Power Quality, IEEE Std., pp. 1159-1995, Jun. 1995.
6. J. S. Subjak Jr. and J. S. Mcquilkin, "Harmonics-Causes, Effects, Measurements, Analysis: An Update," IEEE Trans. Ind. Applicat., vol. 26, pp. 1034-1042, Nov./Dec. 1990.
7. H. M. Ryan and M. Osborne, "Power Quality: A Perspective of System Problems and Solution Considerations," IEE Colloquium on Issues in Power Quality, pp.1/1-1/9, 1995.

8. H. M. Beides and G. T. Heydt, "Power System Harmonics Estimation, Monitoring," Elect. Mach. Power Syst., vol. 20, pp. 93-102, 1992.

9. A. E. Emanuel, J. A. Orr, D. Cyganski and E. M. Gulchenski, "A Survey of Harmonics Voltages, Currents at the Customer's Bus," IEEE Trans. Power Delivery, vol. 8, pp. 411-421, Jan. 1993.

10. Ching-Yin Lee, Wei-Jen Lee, Yen-Nien Wang and Jyh-Cherng Gu, " Effects of Voltage Harmonics on the Electrical and Mechanical Performance of a Three-Phase Induction Motor," IEEE Industrial and Commercial Power Systems Technical Conference, pp. 88-94, 1998.

11. T. C. Shuter, H. T. Vollkommer and J. L. Kirkpatrick. "Survey of Harmonic Levels on the American Electric Power Distribution System," IEEE Trans. Power Delivery, vol. 4, pp. 2204-2213, Oct. 1989.

12. IEEE Working Group on Nonsinusoidal Situations, "Practical Definitions for Powers in Systems with Nonsinusoidal Waveforms, Unbalanced Loads: A Discussion," IEEE Trans. Power Delivery, vol. 11, pp. 79 – 101, Jan. 1996.

13. P. J. A. Ling and C. J. Eldridge, "Designing Modern Electrical Systems with Transformers that Inherently Reduce Harmonic Distortion in a PC-rich Environment," in Proc. Power Quality Conf., pp. 166-178, Sept. 1994.

14. IEEE Working Group on Nonsinusoidal Situations, "A survey of North American Electric Utility Concerns Regarding Nonsinusoidal Waveforms," IEEE Trans. Power Delivery, vol. 11, pp. 73-78, Jan. 1996.

15. H. Akagi, "New Trends in Active Filters for Improving Power Quality," IEEE Conf. on PEDES, New Delhi, pp. 417-425,1996.

16. K. Chattergee, B. G. Fernandes and G. K. Dubey, "An Instantaneous Reactive Volt-Ampere Compensator and Harmonic Suppressor System," IEEE Trans. Power Electronics, vol. 14, no. 2, pp. 381-392, 1999.

17. P. Lynch, "An Active Approach to Harmonic Filtering," IEE Review, vol. 45, Issue: 3, pp. 128 – 130, May 1999.

18. C. Hochgraf and R. H. Lasseter, "Statcom Controls for Operation with Unbalanced Voltages," IEEE Trans. Power Delivery, vol. 13, Issue: 2, pp. 538 – 544, April 1998.

19. H. Sasaki and T. Machinda, "A New Method to Eliminate AC Harmonic Currents by Magnetic Compensation – Considerations on Basic Design," IEEE Trans, PAS, vol. 90, no. 5, pp. 2009-2019, 1971.

20. B. Singh, Al-Haddad and A. Chandra, "A Review of Active Filters for Power Quality Improvement," IEEE Trans. Industrial Electronics, vol. 46, Issue: 5, pp. 960-971, Oct. 1999.

21. H. Akagi, "Trends in Active Power Line Conditioners," IEEE Trans. Power Electronics, vol.9, no.3, pp. 263-268, May 1994.

22. W. M. Grady, M. J. Samotyj and A. H. Noyola, " Survey of Active Power Line Conditioning Methodologies," IEEE Trans. Power Delivery, vol.5, no.3, pp. 1536-1541, July 1990.

23. A. Mansoor, et. al, " Predicting the Net Harmonic Currents Produced by Large Numbers of Distributed Single-Phase Computer Loads," IEEE Trans. Power Delivery, vol.10, pp.2001-2006, Oct. 1994.

24. S. L. Clark, P. Famouri and W. L. Cooley, "Elimination of Supply Harmonics: an Evolution of Current Compensation and Active Filtering Methods," IEEE, IAS 94, Denver, Colorado, USA, pp. 1699-1704, Oct.1994.

25. B. M. Bird, J. F. Marsch and P. R. McLellan, "Harmonic Reduction in Multiplex Converters by Triple-Frequency Current Injection," Proc. IEE, 116(10), pp. 1730 – 1734, Oct. 1969.

26. A. Ametani, "Generalized Method of Harmonic Reduction in AC-DC Converters by Harmonic Current Injection," Proc. IEE, vol. 119, no. 7, pp. 857-864, July 1972.

27. A. Ametani, "Harmonic Reduction in Thyristor Converters by Harmonic Current Injection," IEEE Trans. on Power Apparatus and Systems, PAS-95 (2), pp. 441-449, Mar./Apr., 1976.

28. H. Sasaki and T. Machida, "A New Method to Eliminate AC Harmonic Currents by Magnetic Flux Compensation," IEEE Trans. on Power Apparatus and Systems, vol. PAS-90, pp. 2009-2019, 1971.

29. L. Gyugyi and E. Strycula, "Active AC power filters," IEEE IAS Annual Meeting, pp. 529-535, 1976.

30. L. Benchaita and S. Saadate, "A Comparison of Voltage Source and Current Source Shunt Active Filter by Simulation and Experimentation," IEEE Trans. Power Systems, vol. 14, Issue: 2, pp. 642 – 647, May 1999.

31. A. Chandra, B. Singh, B. N. Singh and K. Al-Haddad, "An Improved Control Algorithm of Shunt Active Filter for Voltage Regulation, Harmonic Elimination, Power-Factor Correction, and Balancing of Nonlinear Loads," IEEE Trans. Power Electronics, vol. 15, Issue: 3, pp. 495-507, May 2000.

32. Jih-Sheng Lai and T.S.Key, "Effectiveness of Harmonic Mitigation Equipment for Commercial Office Building," IEEE Trans. Industry Applications, vol. 33, no. 4, pp. 1104-1110, July/Aug. 1997.

33. J. Nastran, R. Cajhen, M. Seliger and P. Jereb, " Active Power Filter for Nonlinear AC loads," IEEE Trans. Power Electronics, Vol. 9, pp. 92-96, Jan. 1994.

34. H. Akagi, Y. Tsukamoto and A. Nabae, "Analysis and Design of an Active Power Filter using Quad-Series Voltage Source PWM

converters," IEEE Trans. Industry Applications, vol. 20, no.1, pp. 93-98, Jan/Feb. 1990.

35. G. Ledwich and P. Doulai, "Multiple Converter Performance and Active Filtering," IEEE Trans. Power Electronics, vol. 10, no. 3, pp. 273-279, May 1995.

36. H. Akagi, A. Nabae and S. Atoh, "Control Strategy of Active Power Filters using Multiple Voltage Source PWM converters," IEEE Trans. Industry Applications, IA-22, pp. 460-465, 1986.

37. F. Z. Peng, H. Akagi and A. Nabae, "A New Approach to Harmonic Compensation in Power Systems – A Combined System of Shunt and Series Active Filters," IEEE Trans. Industry Applications, vol. 26, no. 6, pp. 983-990, Nov./Dec. 1990.

38. H. Fujita and H. Akagi, "A Practical Approach to Harmonic Compensation in Power Systems-Series Connection of Passive and Active Filters," IEEE Trans. Industry Applications, vol. 27, no. 6, pp. 1020-1025, Nov./Dec. 1991.

39. M. Rastogi, R. Naik and N. Mohan, "A Comparative Evaluation of Harmonic Reduction Techniques in Three-Phase Utility Interface of Power Electronic Loads," IEEE Trans. Industry Applications, vol. 30, Issue: 5, pp. 1149-1155, Sept-Oct. 1994.

40. D. Rivas, L. Moran, J. W. Dixon and J. R. Espionoza, "Improving Passive Filter Compensation Performance with Active Techniques," IEEE Trans. Industrial Electro., vol. 50, no. 1, pp. 161-170, Feb. 2003.

41. M. Rastogi, N. Mohan and Adbel-Aty Edris, "Hybrid-Active Filtering of Harmonic Currents in Power Systems," IEEE Trans. Power Delivery, vol. 10, no. 4, pp. 1994-2000, Oct. 1995.

42. A. Van Zyl, J. H .R. Enslin and R. Spee, "A New Unified Approach to Power Quality Management," IEEE Trans. Power Electronics, vol. 11, no. 5, pp. 691-697, Sep. 1996.

43. S. Park, J.H. Sung and K. Nam, "A New Parallel Hybrid Filter Configuration Minimizing Active Filter Size," Power Electronics Specialists Conference 99, vol. 1, pp. 400-405, 1999.

44. J. Hafner, M. Aredes and K. Heumann, "A Shunt Active Power Filter Applied to High Voltage Distribution Lines," IEEE Trans. on Power Delivery, no. 1, pp. 266-272, Jan. 1997.

45. M. Aredes, K. Heumann and E. H. Watanabe, "An Universal Active Power Conditioner," IEEE Trans. on Power Delivery, Vol. 13, no. 2, pp. 545-551, April 1998.

46. S. Fryze, "Active, Reactive and Apparent Power in Circuits with Non-sinusoidal Voltage and Current," ETZ, Vol. 53, No. 25,1932.

47. M. Depenbrock, "The EBD-Method, Generally Applicable Tool for Analyzing Power Relations," IEEE Trans. on Power System, Vol. 8, no. 2, pp. 381-387, May 1993.

48. H. P. Chester, "Reactive Power in Non-sinusoidal Situations," IEEE Trans. Instrumentation and Measurement, vol. I M-29, no. 4, pp. 420-426, Dec. 1980.

49. P. Flipski, "The Measurement of Distortion Current and Distortion Power," IEEE Trans. Instrumentation and Measurement, vol. IM-33, no. 1, pp. 36-40, March 1984.

50. L. S. Czarnechi, "Orthogonal Decomposition of the Currents in a 3-Phase Nonlinear Asymmetrical Circuit with a Non-sinusoidal Voltage Source," IEEE Trans. I & M, vol. 37, no. 1, pp. 30-34, March 1988.

51. L. S. Czarnechi, "Active, Reactive and Scattered Currents in Circuits with Non-periodic Voltage of a Finite Energy," IEEE Trans. I & M, vol. 37, no. 3, Sep.1988.

52. J. H. R. Enslin, J. D.DVan wyk and M. Naude, "Adaptive, Closed-Loop Control of Dynamic Power Filters in Supplies with High Contamination," IEEE Trans. on Industrial Electronics, vol. 37, no. 3, pp. 203-211, June 1990.

53. H. Akagi, Y. Kanazawa and A. Nabae, "Instantaneous Reactive Power Compensations Comprising Switching Devices without Energy Storage Components," IEEE Trans. Ind. Appl., vol. 20, pp. 625 – 630, 1984.

54. V. Kaura and V. Blasko, "Operation of Phase Locked Loop System under Distorted Utility Conditions," IEEE Trans. Ind. Applicat., vol. 33, no.1, pp. 58-63, Jan./Feb. 1997.

55. S. Bhattacharya and D. M. Divan, "Hybrid Series Active/Parallel Passive Power Line Conditioner with Controlled Harmonic Injection," US Patent 5-465 203, 1995.

56. E. H. Watanabe, R. M. Stephan and M. Aredes, "New Concepts of Instantaneous Active and Reactive Powers in Electrical Systems with Generic Loads," IEEE Trans. Power Delivery, vol. 8, Issue: 2, pp. 697-703, April 1993.

57. Y. Komatsu and T. Kawabata, "A Control Method of Active Power Filter in Unsymmetrical and Distorted Voltage System," Proceedings of Power Conversion Conference – Nagaoka 1997, vol. 1, pp. 161-168, 1997.

58. Ruben Inzunza and H. Akagi, " A 6.6kV Transformerless Shunt Hybrid Active Power Filter for Installation on a Power Distribution System," 35th Annual IEEE Power Electronics Specialists Conference, Germany, 2004, pp. 4630-4636.

59. S. Senini, and P. Wolf, " Analysis and Design of a Multiple-Loop Control System for a Hybrid Active Filter," IEEE Trans. on Industrial Electronics, vol. 49, no. 6, pp. 1283-1292, Dec. 2002.

60. P. Jintakosonwit, H. Fujita, H. Akagi and S. Ogasawara, " Implementation and Performance of Automatic Gain Adjustment in a

Shunt Active Filters for Harmonic Damping Throughout a Power Distribution System," IEEE Trans. on Power Electronics, vol. 17, no.3, pp. 438-447, May 2002.

61. H. Akagi, S. Srianthumrong and Y. Tamai, " Comparisons in Circuit Configurations and Filtering Performance between Hybrid and Pure Shunt Active Filter," Proc. IEEE/IAS Conf., pp. 1195-1202, 2003.

62. P. Jintakosonwit, H. Fujita, H. Akagi and S. Ogasawara, " Implementation and Performance of Cooperative Control of Shunt Active Filters for Harmonic Damping Throughout a Power Distribution System," IEEE Trans. on Industrial Application, vol. 39, no.2, pp. 556-564, Mar./Apr. 2003.

63. M. Depenbrock, V. Staudt and H. Wrede, " A Theoretical Investigation of Original and Modified Instantaneous Reactive Power Theory Applied for Four- Wire System," IEEE Trans. on IA, vol. IA-39, no. 4, pp. 1160-1167, Jul./Aug. 2003.

64. S. Bhattacharya, D. M. Divan and S. Banergee, "Synchronous Frame Harmonics Isolator using Active Series Filter," EPE 91, pp. 3-030-3-035, Italy.

65. E. H. Watanabe, R.M. Stephan and M. Aredes, "New Concepts of Instantaneous Active and Reactive Powers in Electrical Systems with Generic Loads," IEEE Trans. on Power Delivery, vol. 8, no. 2, pp. 697-703, April 1993.

66. M. Aredes and Edson H. Watanabe, "New Control Algorithms for Series and Shunt Three Phase Four Wire Active Power Filters," IEEE Trans. on Power Delivery, vol. 10, no. 3, pp. 1649-1656, July 1995.

67. E. H. Song and B. H. Kwon, "A Novel Digital Control for Active Power Filter," IECON 1992, pp. 1168-1173, 1992.

68. M. Matsui and T. Fukao, "A Detecting Method for Active-Reactive-Negative Sequence Powers and its Application," IEEE Trans. on Industry Applications, vol. 26, no. 1, pp. 99-106, Jan./Feb. 1990.

69. Y. Komatsu and T. Kawabata, "A Control Method of Active Power Filter in Unsymmetrical and Distorted Voltage System." Proceedings of Power Conversion Conference – Nagaoka 1997, vol. 1, pp. 161-168, 1997.

70. A. Ferrero and G. Superti-Furga, "A New Approach to the Definition of Power Components in Three-Phase Systems under Nonsinusoidal Conditions," IEEE Trans. Instrum. Meas., vol. 40, no.3, pp. 568-577, Jun. 1991.

71. M. J. Newman, D. N. Zmooed and D. G. Holmes, "Stationary Frame Harmonic Reference Generation for Active Filters," IEEE Trans. Ind. Appl., vol. 38, no. 6, pp. 1591-1599.

72. Hong-Seok Song and Kwanghee Nam, "Dual Current Control Scheme for PWM Converter under Unbalanced Input Voltage Conditions," IEEE Trans. Industrial Electronics, vol. 46, no. 5, pp. 953-959, Oct. 1999.

73. Shyh-Jier Huang and Jinn-Chang Wu, "A Control Algorithm for Three-Phase Three-Wired Active Power Filters under Non-ideal Mains Voltages," IEEE Trans. Power Electronics, vol. 14, no. 4, pp. 753 – 760, July 1999.

74. N. Bruyant and M. Machmoum, "Simplified Digital-Analogical Control for Shunt Active Power Filters under Unbalanced Conditions," International Conference on (Conf. Publ. No. 456) Power Electronics and Variable Speed Drives, pp. 11-16, 1998.

75. Pukhraj Singh, "Compensation of reactive and harmonic power in three phase power system," Ph.D. thesis, IIT Delhi 2001.

76. M. A. Perales, J. L. Mora, J. M. Carrasco and L. G. Franquelo, "A Novel Control Method for Active Filters based on Filtered Current," in Proc. IEEE Power Electronics Specialists Conf., vol. 3, pp. 1408-1413, 2001.

77. B. Lin. and R. G. Hoft, "Power Electronics Inverter Control with Neural Networks," IEEE Technology Update Series, Neural Networks Applications, pp. 211 – 217,1996.

78. M. Mohaddes, A. M. Gole and P. G. Mclaren, "Hardware Implementation of Neural Network Controlled Optimal PWM Inverter using TMS320C30 board," Conference on Communications, power and computing WESCANEX '97, 22 – 23 May 1997, Winnipeg, MB, pp. 168 – 173.

79. B. Widrow and M. A. Lahr, "30-Years of Adaptive Neural Networks: Perceptron, Madaline, and Backpropagation," Proc. IEEE, vol. 78, no.9, pp. 1415-1442, 1990.

80. P. K. Simpson, "Foundation of Neural Networks," IEEE Technology Update Series, Neural Networks Theory, Technologies and Applications, pp. 1 – 22, 1996.

81. A. Cichocki and T. Lobos, "Artificial Neural Networks for Real Time Estimation of Basic Waveforms of Voltages and Currents," IEEE Trans. Power Syst. vol. 9, no. 2, pp. 612 – 618, 1994.

82. B. R. Lin, "Analysis of Neural and Fuzzy-Power Electronic Control," IEE Proc.-Sci. Meas. Technology, vol. 144, no. 1, january 1997.

83. P. K. Dahs, S. K. Panda, S. K., A. C Liew, B. Mishra and R. K. Jena, "A New Approach to Monitoring Electric Power Quality," Electr. Power Syst. Res., vol. 46, pp. 11-20,1998.

84. N. Pecharanin, H. Mitsui and M. Sone, "Harmonic Detection by using Neural Network," Proc. IEEE International conf. On neural networks, vol. 2, pp. 923-926, 1995.

85. J. R. Vazquez and P. Salmeron, "Active Power Filter Control using Neural Network Technologies," IEE Proc-Electr. Power Appl., vol. 150, no.2, pp.139-145, March 2003.

86. M. Rukonuzzaman and M. Nakaoka, "Single-Phase Shunt Active Power Filter with Harmonic Detection," IEE Proc-Electr. Power Appl., vol. 149, no.5, pp.343-350, Sept.2002.

87. P. K. Dash, D. P. Swain, A. C. Liew and S. Rahman, "An Adaptive Linear Combiner for On-Line Tracking of Power System Harmonics," IEEE Trans. power systems, vol. 11, no. 4, pp.1730-1735, NOV. 1996.

88. J. R. Vazquez and P. R. Salmeron, " Three-Phase Active Power Filter using Neural Networks," 10th Mediterranean Electrotechnical Conference, MeleCon 2000, vol. III, pp. 924-927.

89. J. H. Marks and T. C. Green, "Predictive Transient-Following Control of Shunt and Series Active Power Filters," IEEE Trans. on Power Electro., vol. 17, no. 4, July 2002.

90. P. Enjeti, W. Shireen and I. Pitel, " Analysis, Design of an Active Power Filter to Cancel Harmonic Currents in Low Voltage Electric Power Distribution Systems," in Proc. IEEE IECON'92, pp. 368-373, 1992.

91. G. H. Rim, Y. Kang, W. H. Kim and J. S. Kim, " Performance Improvement of a Voltage Source Active Filter," in Proc. IEEEAPEC'95, pp. 613-619, 1995.

92. P. Singh, J. M. Pacas and C. M. Bhatia, " An Improved Unified Power Quality Conditioner," International Conference on Power Electronics and Electrical Drives (EPE 2001), Austria, Aug. 2001.

93. Jost Allmeling, "A Control Structure for Fast Harmonic Compensation in Active Filters," IEEE Trans. on Power Electronics, vol. 19, no. 2, pp. 508-514, March 2004.

94. Shyh-Jier Huang, Jinn-Chang Wu, "A Control Algorithm for Three-Phase Three-Wired Active Power Filters under Non-ideal Mains Voltages," IEEE Trans. Power Electronics, vol. 14, no. 4, pp. 753 – 760, July 1999.

95. N. Bruyant and M. Machmoum, "Simplified Digital-Analogical Control for Shunt Active Power Filters under Unbalanced Conditions," International Conference on (Conf. Publ. No. 456) Power Electronics and Variable Speed Drives, pp. 11-16, 1998.

96. X. Yuan, J. Allmeling, W. Merk and H. Stemmler, " Stationary Frame Generalized Integrators for Current Control of Active Power Filters with Zero Steady-State Error for Current Harmonics of Concern Under Unbalanced and Distorted Operation Conditions," IEEE Trans. on Industry Application, vol. 38, pp. 523-532, Mar/ Apr. 2002.

97. John N. Chiassion, L. M. Tolbert, K. J. McKenzie and Zhong Du, " A Complete Solution to the Harmonic Elimination Problem," IEEE Trans. on Power Electronics, vol. 19, no. 2, pp. 491-499, March 2004.

98. J. Jacobs, Dirk Detjen, C. U. Karipidis and Rik W. DeDoncker, " Rapid Prototype Tools for Power Electronic System Demonstration with Shunt Active Power Filter," IEEE Trans. on Power Electronics, vol. 19, no. 2, pp. 500-507, March 2004.

99. M. H. Hassoum, "Fundamental of Artificial Neural Networks," Prentice-Hall of India Private Limited, New Delhi, 1998.

100. N. P. Padhy, "Artificial Intelligence and Intelligent Systems," Oxford University Press 2005.

101. J. S. R. Jang, C. T. Sun and E. Mizutani, "Neuro-Fuzzy and Soft Computing," Pearson Education (Singapore) Pte. Ltd., Indian Branch, Delhi, India.

102. K. S. Narendra and K. Parthasarathy, "Identification and Control of Dynamical Systems using Neural Networks," IEEE Trans. Neural Networks, vol. 1, pp. 4 – 27, 1990.

103. D. Hammestrom, "Neural networks at work," IEEE Spectrum, vol. 30. pp. 26 – 32, 1993.

104. R. P. Lippmann, "An Introduction to Computing with Neural Nets," IEEE ASSP Mag., vol. 4, no. 4, pp. 4 – 22, Apr. 1987

105. P. Antognetti and V. Milutinovic, "Neural Networks: Concepts, Applications and Implementations," (Eds.) Volumes I-IV, Prentice Hall, Englewood Cliffs, NJ., 1991.

106. D. DeSieno, "Adding a Conscience to Competitive Learning," Proc. of the Second Annual IEEE International Conference on Neural Networks, vol. 1, pp. I-117 to I-124, 1988.

107. J. Wang, "Analysis and Design of a Recurrent Neural Network for Linear Programming," IEEE Trans. on Neural Networks, vol. 7, no. 4. pp. 629-641, 1994.

108. D. Psaltis, A. Sideris and A. A. Yamamura, "A Multilayered Neural Network Controller," IEEE Contr. Syst. Mag., pp. 17-21, Apr. 1988.

109. Fu-Chuang Chen, "Back-Propagation Neural Networks for Nonlinear Self-Tuning Adaptive Control," IEEE control System Magazine, pp. 44-48, 1990.

110. R. Hecht-Nielsen, "Theory of the Back-Propagation Neural Network," Proc. IEEE 1989 Intl. Conf. Neural Networks, pp. I-593-605.

111. M. P. Kennedy and L. O. Chua, "Neural Netowrks for Nonlinear Programming," IEEE Trans. Circuits Syst., vol. CAS-35, no. 5, pp. 554 – 562, 1988.

112. L. K. Hansen and P. Salamon, "Neural Network Ensembles," IEEE Trans. on Pattern Analysis and Machine intelligence, vol. 12, no. 10, pp. 993-1001, Oct. 1990.

113. D. E. Rumelhart, G. E. Hinton and R. J. Williams, "Learning Internal Representations by Error Propagation in Parallel Distributed Processing: Explorations in the Microstructure of Cognition," Vol. 1: Foundations, D.E. Rumelhart and J.L. McClelland, Eds. Cambridge, MA: MIT Press, 1986.

114. M. Hassoun, Fundamentals of Artificial Neural Networks. Cambridge, MA: MIT Press, 1995.

115. Haykin, Neural Netowrks: A Comprehensive Foundation, New York: Macmillan, 1994.

116. J. Zurada, "Introduction to Artificial Neural Systems," St. Paul, MN: West Publishing, 1992.

117. J. R. Noriega and H. Wang, " A Direct Adaptive Neural-Network Control for Unknown Nonlinear System and its Application," IEEE Trans. on Neural Networks, vol. 9, no. 1, pp. 27-34, Jan. 1998.

118. D. W. Tank and J. J. Hopfield, "Simple Neural Optimization Networks, an A/D Converter, Signal Decision Circuit, and a Linear Programming Circuit," IEEE Trans. Circuits Syst., vol. 33, pp. 533 – 541, May 1986.

119. C. Y. Mas and M. A. Shanblatt, "Linear and Quadratic Programming Neural Network Analysis," IEEE Trans. Neural Netowrks, vol. NN-3, pp. 580 – 594, 1992.

120. J. M. Zurada, "Gradient-type Neural Systems for Computation and Decision-making," Progress in Neural Netowrks. Vol. II, O.M. Omidvar, Ed. Norwood, NJ: Ablex, 1991.

121. W. H. Schiffmann and H. W. Geffers, "Adaptive Control of Dynamic Systems by Backpropagation Networks," Neural Networks, vol. 6, pp. 517 – 524, 1993.

122. Y. Tan and R. D. Keyser, "Neural Network based Adaptive Predictive Control," Advances in MBPC, pp. 77-78, 1993.

123. F. C. Chen and C. C. Liu, "Adaptively Controlling Nonlinear Continuous Time Systems using Multilayer Neural Networks," IEEE Trans. Automat. Contr., vol. 39, pp. 1306 – 1310, 1994.

116. J. Zurada, "Introduction to Artificial Neural Systems," St. Paul, MN: West Publishing, 1992.

117. J. R. Noriega and H. Wang, " A Direct Adaptive Neural-Network Control for Unknown Nonlinear System and its Application," IEEE Trans. on Neural Networks, vol. 9, no. 1, pp. 27-34, Jan. 1998.

118. D. W. Tank and J. J. Hopfield, "Simple Neural Optimization Networks, an A/D Converter, Signal Decision Circuit, and a Linear Programming Circuit," IEEE Trans. Circuits Syst., vol. 33, pp. 533 – 541, May 1986.

119. C. Y. Mas and M. A. Shanblatt, "Linear and Quadratic Programming Neural Network Analysis," IEEE Trans. Neural Netowrks, vol. NN-3, pp. 580 – 594, 1992.

120. J. M. Zurada, "Gradient-type Neural Systems for Computation and Decision-making," Progress in Neural Netowrks. Vol. II, O.M. Omidvar, Ed. Norwood, NJ: Ablex, 1991.

121. W. H. Schiffmann and H. W. Geffers, "Adaptive Control of Dynamic Systems by Backpropagation Networks," Neural Networks, vol. 6, pp. 517 – 524, 1993.

122. Y. Tan and R. D. Keyser, "Neural Network based Adaptive Predictive Control," Advances in MBPC, pp. 77-78, 1993.

123. F. C. Chen and C. C. Liu, "Adaptively Controlling Nonlinear Continuous Time Systems using Multilayer Neural Networks," IEEE Trans. Automat. Contr., vol. 39, pp. 1306 – 1310, 1994.

124. M. M. Polycarpou and P. A. Ioannou, "Modeling, Identification and Stable Adaptive Control of Continous Time Nonlinear Dynamical Systems using Neural Networks," in Proc. Amer. Contr. Conf., 1992, pp. 36-40.

125. Dawei Gao and Xiaorui Sun, " A Shunt Active Power Filter with Control Method based on Neural Network," International Conference on Power System Technology, 2000, PowerCon 2000, vol. 3, pp. 1619-1624, 2000.

126. K. W. E. Cheng, H. Y. Wang and d. Sutanto, " Adaptive Directive Neural Network Control for Three-Phase AC/DC PWM Converter," IEE Proc.-Electro. Power Appl., vol. 148, no. 5, Sept. 2001.

127. M. Rukonuzzaman and M. Nakoka, " Single –Phase Shunt Active Power Filter with Adaptive Neural Network Method for Determining Compensating Current," The 27th Annual Conference of the IEEE Industrial Electronics Society, IECON'01, pp. 2032-2037, 2001.

128. J. R. Vazquez, P. Salemeron, J. Prieto and A. Perez, " Practical Implementation of a Three-Phase Active Power Line Conditioner with ANNs Technology," 28th Annual Conference of the IEEE Industrial Electronics pp. 739-744, 2002.

129. F. B. Libano, R. A. M. Barga, G. Willmann and S. L. Miller, " Application of Neural Networks for the Control Strategy for Series Active Power Filters," 10th International Conference on Harmonics and Quality of Power 2002, pp. 519-523, 2002.

130. C. Madtharad and P. Suttichai, " Active Power Filter for Three-Phase Four-Wire Electric System using Neural Networks," Electric Power System Research, vol. 60, pp.179-192, 2002.

131. G. V. Schoor, J. D. V. Wyk and I. S. Shaw, " Training and Optimization of an Artificial Neural Network Controlling a Hybrid Power Filter," IEEE Trans. on Indust. Electro., vol. 50, no. 3, June 2003.

APPENDIX -A

DESIGN OF COMPONENTS

A-1: COUPLING TRANSFORMER

In order to obtain expression of VA rating of coupling transformer, first of all, we need to analyze current and voltage rating of the transformer. The control target for hybrid active filter is to eliminate dominative source harmonic current, forced into the passive filter. The secondary side current of the transformer depends the configuration passive filter. Assuming passive filter be tuned 3^{rd} and 5^{th} by way of reasonable configuration and proper control for the active filter, the 3^{rd} and 5^{th} load harmonic current will flow into filter branch. As result, the current flowing into secondary side comprises the fundamental current and 3^{rd}, 5^{th} load harmonic current. Secondly, we need to analyze the secondary side voltage of the transformer. At 3^{rd} or 5^{th} frequency, the secondary side voltage of the transformer is the product of load harmonic current and the harmonic impedance of the passive filter at same order harmonic frequency.

Because there is not passive filter branch but 3^{rd} and 5^{th} in the hybrid filter, i.e. the harmonic impedance of the passive filter is large at other order harmonic frequency aside from 3^{rd} and 5^{th}, thus, the other order harmonic current is small in filter branch, it can be neglected. The VA rating of the coupling transformer can be obtained as

$$S = VI = \sqrt{\sum_{n=1}^{\infty} V_n^2}$$

Where S, V, I are apparent power, effective value of secondary side voltage and current of the transformer. V_n, I_n are voltage and current effective value at n order harmonic frequency.

According above conclusion,

$$S = \sqrt{V_{TS3}^2 + V_{TS5}^2 + \cdots + V_{TSn}^2}\sqrt{I_{T1}^2 + I_{T3}^2 + \cdots + I_{Tv}^2}$$

$$= \sqrt{(I_{L3}Z_{F3})^2 + (I_{L5}Z_{F5})^2 + \cdots + (I_{Ln}Z_{Fn})^2} \times$$

$$\sqrt{(V_{S1}/Z_{F1})^2 + I_{L3}^2 + I_{L5}^2 + I_{L7}^2 + \cdots + I_{Ln}^2}$$

The transformer must be ensured to work in the linear region and not in magnetic saturation state in order to achieve little voltage distortion between the primary and secondary side.

A-2: PASSIVE FILTER

The design characteristics of the passive filters have and important influence on the compensation performance of the hybrid topology. The tuned frequency and quality factor of the passive filter directly influence the compensation characteristics of the hybrid topology. If these two factors are not properly selected, the rated power of the active filter must be increased in order to get the required compensation performance. The tuned factor, δ, in per unit with respect to the resonant frequency is defined as

$$\delta = \frac{\omega - \omega_r}{\omega_r}$$

δ, defines the magnitude in which the passive filter resonant frequency changes due to the variations in the power system frequency and modifications in the values of the passive filter parameters L and C. The quality factor, Q, of the passive filter is defined as

$$Q = \frac{X_0}{R}$$

where X_0 is

$$X_0 = \omega_r L = \frac{1}{\omega_r C} = \sqrt{\frac{L}{C}}$$

The passive filter quality factor, Q, defines the ratio between the passive filter reactance with respect to its resistance. In order to have a passive filter low impedance value in a limited frequency band width, defined by the maximum expected changes of the rated power system frequency, it is necessary to reduce X_0 or increase the passive filter resistance R, reducing the value of Q. however, if R increases, the equivalent impedance of the passive filter at the resonant frequency will increase, with the associated power losses, increasing the overall passive filter operational cost. On the other hand, the larger the value of Q, the lower is the passive filter equivalent impedance at the resonant frequency, increasing the currents harmonic components across the filter, at the resonant operation point.

The quality factor, Q, defines the passive filter bandwidth. A passive filter with a high quality factor, Q, presents a larger bandwidth and better compensation characteristics. Equation given below defines the quality factor value in terms of the passive filter parameters. L, R and C. This equation shows that if R or C decreases, Q increases, and the filter bandwidth becomes larger improving the hybrid scheme compensation characteristics.

$$Q = \frac{1}{R}\sqrt{\frac{L}{C}}$$

Although decreasing R or C the passive filter quality factor is improved, each element produces a different effect in the hybrid filtering behavior. For example, by increasing R, the filter equivalent impedance at the resonant frequency becomes bigger, affecting the current harmonic compensation characteristics at this specific frequency.

A-3: LINK REACTOR

The design of the synchronous link reactor is performed with the constraint that for a given switching frequency the minimum slope of the inductor current is smaller than the slope of the triangular waveform that defines the switching frequency. In this way, current error signal is forced to remain between the maximum and minimum of the triangular waveform and as a result the inverter line current follows the reference signal closely. The slope of the triangular waveform is defined by:

$$\lambda = 4\xi f_s$$

Where ξ is the amplitude of the triangular waveform, which has to be equal to the maximum amplitude permitted in the high frequency ripple current, and f_t is the frequency of the inverter switching frequency (i.e. the frequency of the triangular waveform). The maximum slope of the inverter line current is equal to:

$$\frac{di}{dt} = \frac{V_a + 0.5V_{dc}}{L}$$

In order to ensure that the intersection between the current error signal and the triangular waveform exists, the slope of the inductor current has to be smaller than the slope of the triangular waveform.

$$L = \frac{V_a + 0.5V_{dc}}{4\xi f_t}$$

A-4: DC CAPACITOR

Transient changes in the instantaneous power absorbed by the load generate voltage fluctuations in the dc voltage. The amplitude of these voltage fluctuations can be controlled effectively with an appropriate dc capacitor value. It must be notice that the dc voltage control loop stabilizes the capacitor voltage after few cycles, but is not fast enough to limit the first voltage variations. The capacitor value obtained with this criterion is bigger than the value obtained based on maximum dc voltage ripple constraint. For this reason, the voltage across the dc capacitor presents a smaller harmonic distortion factor.

The maximum over voltage generated across the dc capacitor is given by:

$$V_{c\max} = \frac{1}{C}\int_{t_1}^{t_2} i_c(t)dt + V_{dc}$$

where V_{cmax} is the maximum voltage across the dc capacitor. V_{dc} is the steady state average dc voltage. $i_c(t)$ is the instantaneous dc bus current.

From above expression

$$C = \frac{1}{\Delta V}\int_{t_1}^{t_2} i_c(t)dt$$

The above equation defines the value of the dc capacitor that will keep the transient voltage fluctuations across the dc bus below ΔV. The product of the inverter line currents with the respective switching functions defines the instantaneous value of the dc current. The average value of the dc current that generates the maximum over voltage can be estimated by

$$\int_{t_1}^{t_2} i_c(t)dt = I_{inv}\int_{t_1}^{t_2}\left[\{\sin(\omega t) + \sin(\omega t + 120^0)\}\right]$$

In this expression the inverter line current is assumed to be sinusoidal. This operating condition represents the worst case.

APPENDIX –B

RATINGS OF COMPONENTS

AC SOURCE

Phase voltage (V_s)	240 V_{rms}
Frequency (f)	50 Hz
Source Resistance (R_s)	0.3 Ω
Source Inductance (L_s)	0.5 mH

PASSIVE TUNED FILTER

Tuned filter	R (Ω)	L (mH)	C (μF)
5^{th} tuned filter	0.33	10.44	39
7^{th} tuned filter	0.33	7.15	29
11^{th} tuned filter	0.50	3.24	25.8

PWM INVERTER

Switching Frequency	6kHz
C_{dc}	5000 uF
$V_{dc(ref.)}$	300 Volts
Switching filter	12mH
Coupling Transformer ratio	10:1
K_p	0.1
K_I	20

LIST OF PUBLICATIONS

(1) Satya Prakash Dubey, Pukhraj Singh and H.V. Manjunath, " DSP based Neural Network Controlled Hybrid Active Power Filter," Accepted for Publication in International Journal of Emerging Electric Power System.

(2) Satya Prakash Dubey, Pukhraj Singh and H.V. Manjunath, "A Neural Network based Harmonic Suppression Scheme for Three-Phase Four-Wire System," Journal of the Energy and Fuel User's Association of India, vol. LV, Book 2, pp. 22-30, July/Sept. 2005.

(3) Satya Prakash Dubey, Pukhraj Singh , H.V. Manjunath and Rahul Verma, "Neural Network Controlled Parallel Hybrid Active Power Filter," International Conference on Power System, ICPS 2004, Kathmandu, Nepal, P (122), pp. 635-639.

(4) S.P. Dubey et. al, " Neural Network Based Controller for Active Power Filter for Three Phase Four Wire System," IEEE Annual Symposium on Power Systems, Nov. 26-27, 2004, Indian Institute of Science Banglore, Banglore.

(5) Rajneesh Kumar, Satya Prakash Dubey, Dheerendra Singh and H.V. Manjunath, "Output Voltage Distortion in a High Switching Frequency PWM Inverter," International Conference on Energy Automation and Information Technology, Indian Institute of Technology Kharagpur, EAIT-2001, pp.581-586.

(6) Satya Prakash Dubey, Pukhraj Singh and H.V. Manjunath, "Three Phase Four Wire Neural Network based Parallel Hybrid Active Power Filter,"

Accepted Paper in National Power Electronics Conference NPEC-2005, Indian Institute of Technology Kharagpur, Dec.22-24, 2005.

(7) Satya Prakash Dubey, Pukhraj Singh and H.V. Manjunath, "Neural Network based Hybrid Active Power Filter under Non-Ideal Conditions," Accepted Paper in 2nd Control Instrumentation System Conference, CISCON-2005, MIT, Manipal, Nov. 11-12, 2005.

BIOGRAPHY

Biography of Candidate

Satya Prakash Dubey received the B.E. (Electrical) degree from the Pt. Ravishankar University Raipur, Raipur, in 1995 and M.E. degree (Power Apparatus & Electrical Drives) from University of Roorkee, Roorkee, in 2000. He is currently working as a lecturer in Electrical and Electronic Engineering Group of Birla Institute of Technology & Science, Pilani, having five year teaching and research experience in the same Institute.

Biography of Supervisor

H.V. Manjunath received the B.E. (E&C) degree from the University of Mysore, Mysore, in 1977, M.Sc. (Engg.) in Power Electronics & Drives, and Ph. D. (Engg.) from Indian Institute of Science Banglore, Banglore, in 1983 and 1987 respectively. His Professional experience includes Project Assistant, E.E., I.I.Sc. Banglore, Scientific Officer, CEDT, I.I.Sc. Banglore, Design Engineer, Semiconductor Circuits & APC, USA, and Scientist, Central Electronics Engineering Research Institute, Pilani. He is currently an Associate Professor in Electrical and Electronic Engineering Group of Birla Institute of Technology & Science, Pilani. He has authored and coauthored 11 publications in various international and national journals.